MODELLING SHEAR RATE AND HEAT TRANSFER IN A TWIN SCREW CO-ROTATING FOOD EXTRUDER

BY

Ibrahim Omer Mohamed

A DISSERTATION

Submitted to
Michigan State University
in partial fulfillment of the requirements
for the degree of

DOCTOR OF PHILOSOPHY

In

Agricultural Engineering

Department of Agricultural Engineering

1988

ABSTRACT

MODELLING SHEAR RATE AND HEAT TRANSFER IN A TWIN SCREW CO-ROTATING FOOD EXTRUDER

BY

Ibrahim Omer Mohamed

A systematic approach analogous to mixer analysis has been used to estimate an average shear rate for three screw configurations of a Baker Perkins (MPF-50D) twin screw co-rotating extruder. A Newtonian standard (Polybutene) and a non-Newtonian standard (mixture of 93% honey and 7% soy polysaccharide) were used to generate the data needed for estimation of the average shear rate. Following the estimation procedure, the average shear rate was found to correlate well with screw speed.

From a macroscopic energy balance on the filled zone of the extruder, a one-dimensional heat transfer equation has been developed, with viscous dissipation effects incorporated. The heat transfer differential equation was solved numerically for the average heat flux, using an experimentally determined temperature profile. Soy polysaccharide at 70 % moisture content was used as the test material. From the estimated value of the average heat flux, an average heat transfer coefficient was estimated for different extrusion conditions. The average heat transfer coefficient was found to correlate well with the Graetz number and Brinkman number ($R^2 = 0.96$).

The model of the average shear rate and average heat transfer coefficient were used in the one-dimensional energy equation to obtain the temperature profile for single flighted screw (single lead), double

flighted screw (feed screw) and kneading discs staggered at 30 degree forwarding (30 F). An experiment was conducted to determine the temperature profile and to provide the inlet temperature to the model. SPS at 70 % moisture content was used as the test material. For the 30 F paddles and the feed screws, good agreement was obtained between the predicted and observed temperature profiles over a wide range of operating conditions. The predictions of the single lead screws were very poor. This can be attributed to the poor mixing characteristics of these types of screws, in violation of the major assumption of uniform temperature in the direction perpendicular to the screw shafts.

The approach used in this study for modelling the average shear rate and heat transfer provides a good foundation for modelling twin screw extruders. The results obtained could be used for modelling heat transfer in food materials, including the effects of reaction kinetics if adequate rheological models are available.

Approved by

Robert Y. Ofoli 12/2/88

Major Professor Date

Donald G. Edwards 12/6/88

Department Chairperson Date

Dedicated to the memory of my
parents, to my wife Anwar, our
daughter Mihad and son Omer

ACKNOWLEDGEMENTS

I would like to express my gratitude to Dr. Ronnie G. Morgan for serving as my advisor before leaving the university for Kraft, Inc. I appreciated his remarkable input to this research. I would like also to extend my appreciation to Dr. Robert Y. Ofoli for his willingness to carry on the responsibility as my advisor after Dr. Morgan's departure. I greatly appreciated his guidance, encouragement and his valuable input to this research. Special thanks to the members of my committee, Dr. Fred W. Bakker-Arkema, Department of Agricultural Engineering, Dr. James F. Steffe, Department of Agricultural Engineering, Dr. James V. Beck, Department of Mechanical Engineering and Dr. Jack R. Giacin, School of Packaging, for their valuable contributions throughout my graduate study.

Many thanks are due to the University of Gezira, Sudan and to the Sudan goverment for their financial support that made this work possible. Special thanks to the Food Extrusion Group for their help, especially John Keenan and Drew Van-Norman for their help in the extrusion runs. The help and support of my friends and colleagues at the Department of Agriculutral Engineering are greatly appreciated.

In addition, I want to thank my entire family in the Sudan for their prayers, encouragement and sacrifice, specially my brothers Awad-elseed and Dr. Hassabelrasoul for their continuous support. Special thanks to my wife Anwar, my daughter Mihad and son Omer for their understanding, continuous support, and patience during my graduate study.

TABLE OF CONTENTS

LIST OF TABLES

LIST OF FIGURES

CHAPTER 1

INTRODUCTION

Extrusion of food dates back to around 1797 when piston-driven devices were used for production of macaroni (Linko et al., 1981). In 1869 the first twin screw extruder (based on the ancient principle of Archimedes' screw to transport water) was introduced for sausage manufacture (Janssen, 1978). Around 1900 the hydraulically operated batch cylindrical ram macaroni presses came into existence (Harper, 1981). Continuous extrusion was first introduced in 1935 when single screw extruders were used for pasta production. Since then the use of single-screw extrusion has found greater application in the food and feed industries (Rossen and Miller, 1973).

General Mills, Inc. was the first to use an extruder in the manufacture of ready-to-eat (RTE) cereals in the late 1930s (Harper, 1981). RTE cereals were produced by using the extruder to form precooked cereal doughs into a variety of shapes which were then puffed or flaked. Collet extruders were introduced in 1946 for producing expanded corn curls or collets and other variety of expanded snacks from corn grits as the main ingredient (Hess, 1973). The important feature of collet extruders is the grooved barrel and the specially designed flight which generates high shear to cause high viscous dissipation of mechanical energy, the primary source of heat energy. This type of extruder is often classified thermodynamically as autogeneous.

Cooking extruders with barrel heating and cooling were developed in the 1940s for continuous precooking of cereals and oilseed blend for animal feed to improve digestibility and palatability (Anonymous, 1966). In the 1960s, RTE breakfast cereals were produced with cooking extruders, where both cooking and forming were performed in a single step in the extruder. Recently cooking extruders have been developed with greater sophistication to achieve wider processing capabilities.

Food extrusion is growing steadily as the processing technology of the future, especially after recent developments in twin screw extruders overcame most of the limitations of single screw extruders. The list of food products now being produced with cooking extruders includes snacks, chips, RTE cereals of different colors and shapes, breading substitute, beverage and seasoning bases, soft moist and dry pet foods, animal feed, textured vegetable proteins, and confections. One of the important characteristics of the cooking extruder is the possibility of high temperature short time (HTST) cooking. HTST cooking achieves the goal of maintainnig a sterile product with a low microorganism count, inactivating anti-nutritional factors such as trypsin inhibitors in soy beans (Harper, 1978) and maximizing retention of nutrients which degrade with long exposure to temperature.

Cooking extruders have also found application in the biotechnology area, where they are used as reactors for producing high dextrose equivalent (DE) glucose syrup by enzymatic hydrolysis of gelatinized starches by thermostable α-amylase to initiate liquefaction and amyloglucosidase to initiate saccharification (Hakulin et al., 1983).

Mathematical modelling of twin screw extruders is still in the early stages of development. This is due to the geometric complexity of the extruder and the difficulty of adequately modelling the rheological behavior of the extruded food materials that undergo physiochemical changes, such as starch gelatinization and protein denaturation. Most of the information available is developed for polymers where the simplified assumptions of Newtonian and isothermal flow were used (Janssen, 1978; Booy, 1980; Denson and Hwang, 1980; and Riedler, 1981). Much of the published work on modelling twin screw food extruders used response surface methodology (RSM) developed by Box and Wilson (1951) to quantitatively study the effect of various parameters on the extrusion process (Olku et al., 1980). Yacu (1985) developed a mathematical model for twin screw co-rotating food extruders using one dimensional flow to predict temperature and pressure profiles within the extruder using a non-Newtonian non-isothermal viscosity model.

In most food extrusion, process heat transfer phenomena are of great importance and provide the key finger printing mechanism for extrusion modelling. However, lack of progress in modelling heat transfer stems from the difficulty in assessing the shear rates for twin screw extruders, and quantifying the viscous dissipation, which is of great importance in extrusion processing.

1.1 Objectives

The primary objectives of this study are:

(1) To model the average shear rate for three screw configurations: single flighted screw (single lobe), double flighted screw (double lobe) and kneading disks staggered at 30 degrees forwarding.

(2) To develop a model for correlating the average heat transfer coefficents to extruder geometry, operating conditions and material properties.

(3) To predict the temperature profile along the extruder, incorporating the effect of viscous dissipation.

(4) To conduct experimental tests for model verification.

1.2 Literature Cited

Anonymous. 1966. Grain Expansion Data Presented. Feed Stuffs. 38(10):76

Booy, M. L. 1980. Isothermal Flow of Viscous Liquid in Co-Rotating Twin Screw Devices. Polym. Eng. and Sci. 20(18):1220-1228

Box, G. E. P. and Wilson, K. B. 1951. On The Experimental Attainment of Optimum Conditions. J. R. Stat. Ser. E. 13(1):1-35

Denson, C. D. and Hwang Jr., B. K. 1980. The Influence of The Axial Pressure Gradient on Flow Rate For Newtonian Liquids in Self Wiping, Co-Rotating Twin Screw extruder. Polym. and Eng. Sci. 20(14):965-971

Hakulin, S., Linko, Y. Y., Linko, P., Seiler, K. and Seibal, W. 1983. Enzymatic Conversion of Starch in Twin-Screw HTST-Extruder. Starch/ Stårke. 35:411

Harper, J. M. 1978. Extrusion Processing of Foods. Food Technol. 32(7):67

Harper, J. M. 1981. Extrusion of Foods, Volumes 1 and 2. CRC Press, Boca Raton, Fl.

Hess, J. 1973. Puffed The Magic Snack. Snack Foods. 62(4):35

Janssen, L. P. B. M. 1978. Twin Screw Extrusion. Elsevier Scientific Publ. Co. Amsterdam.

Linko, P., Colonna, P. and Mercier, C. 1981. High-Temperature Short-time Extrusion Cooking. In: Advances in Cereal Science and Technology. Pomeranz, Y. Ed., Vol. 4. American Association of Cereal Chemists. St. Paul. PP. 145-235

Olkku, J. , Hagquist, A. and Linko, P. 1982. Steady State Modelling of Extrusion Cooking Employing Response Surface Methodology. Paper presented at the Extrusion Cooking Symposium, World Cereal and Bread Congress, Prague, June/July.

Riedler, J. 1981. Quasi Three- Dimensional Finite Element Solution For a Twin Screw Extruder. In: Numerical Methods in Laminar and Turbulent Flow. Conference Proc. Swansea, UK., PP. 191-202

Rossen, J. L. and Miller, R. C. 1973. Food Extrusion. Food Technol. 27:46-53

Yacu, W. 1985. Modelling a Twin Screw Co-Rotating Extruder. J. Food Proc. Eng. 8:1-21

CHAPTER 2

LITERATURE REVIEW

2.1 Uniqueness of Extrusion Cooking

Extrusion cooking has become one of the most popular processing technologies in the food industry because of many advantages (Harper, 1978 and Mans, 1982):

(1) **Versatility**: With the same extruder, various kinds of products can be made with appropriate changes in die geometry and operating conditions.

(2) **High productivity**: Extruders operate in a continuous mode with high throughput rates.

(3) **Low cost**: Among large volume processing equipments, the extrusion process cost per unit mass of finished products is lower than any industrial cooking process, because of savings in labor, energy, processing and investment cost and floor space.

(4) **Improved functional characteristics**: Extruders are used to alter food product characteristics to improve functionality, such as modification of starches and proteins, uniform mixing of ingredients including items such as vitamins, color, flavors and others; extruders also improve the textural characteristics of foods.

(5) **Product shape**: Food extruders have the capability of producing foods with a wide range of shapes, depending on die design.

(6) High product quality: The high-temperature short-time operating characteristics of the extruder minimize nutrient degradation while destroying most micro-organisms that cause degradation.

(7) Production of new products: Extruders are efficient processing tools for new product development because of the ability to modify product functional characteristics under a wide range of operating conditions.

(8) No effluents: Due to the relatively low level of processing moisture, most extrusion processes contribute very little to the waste stream.

(9) Energy efficiency: Most extrusion processes are performed at lower moisture in contrastto conventional cooking systems; therefore the cost of drying the extrudate is lower, in addition to lower energy requirements for cooking.

2.2 Single Screw Extruders

This type of extruder consists of a single screw that fits tightly inside a barrel. Figure 2.1 shows the screw barrel assembly with the major geometric dimensions labeled. The screw consists of a helical flight. The helix angle (Φ) is the angle that the helical flight makes with the vertical, the flight height (H) is the distance from the barrel to the screw root, the flight clerance is δ , the flight thickness in the axial direction is b, the flight thickness perpendicular to the flight is e, the axial distance between fligths is B and the distance between flights is W. The lead (Le) is the axial distance the material advances in one revolution, and is given by

$$Le = \pi D \tan(\Phi) \tag{2-1}$$

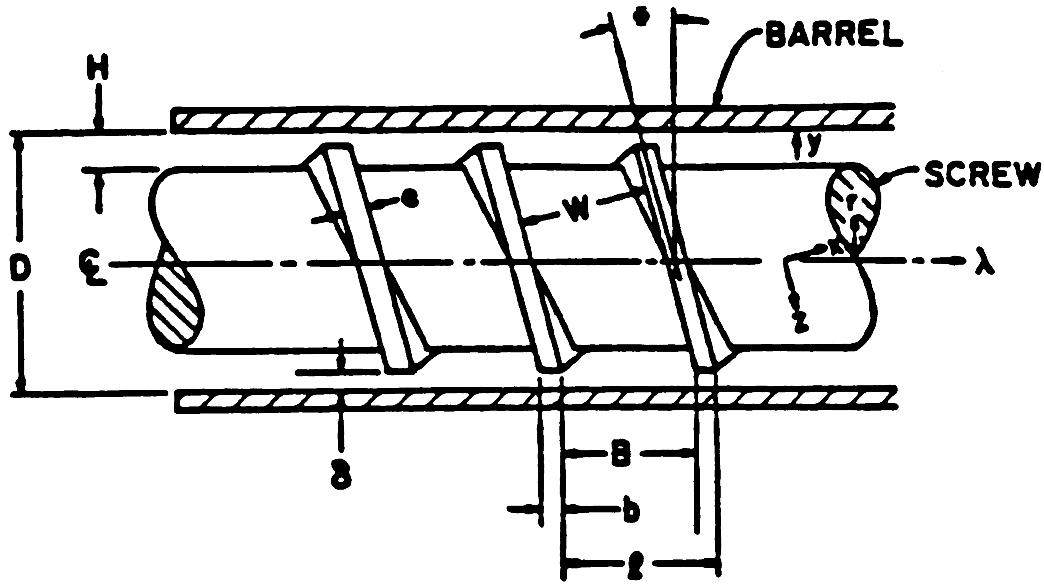

Figure 2.1 Metering Section of Single Screw Extruders (Harper, 1979)

Different screw and barrel designs are available (Harper, 1979) featuring increasing and decreasing root diameter, and decreasing or constant pitch (Figure 2.2). The typical single screw extruder is shown in Figure 2.3. It consists of three main sections: the feed section usually has deep flights to facilitate easy conveyance of the raw materials; the transition section or the compression section converts the raw material to a continuous dough due to the relatively high shear rate and compression maintained by either decreasing pitch or gradual decrease in flight depth towards the exit; the metering section is characterized by very shallow flights which generate high shear rate, thus enhancing cooking and mixing.

2.2.1 Classification of Single Screw Extruders

There are many criteria for classifying food extruders. Rossen and Miller (1973) classified extruders thermodynamically as:

Autogenous: the only source of heat energy for this type is generated from viscous dissipation of mechanical energy. These type of extruders generate high shear rate and operate at low moisture contents. A Collet extruder is one example of this type.

Isothermal: These are generally forming extruders. The isothermal condition is maintained by heating or cooling the barrel through jackets surrounding the barrel. The operating moisture content is relatively high.

Polytropic: Most food extruders are of this kind. They operate between autogenous and isothermal. Temperature control is maintained by heating and cooling through jacketed barrels, as well as control of screw speed. Tribelhorn and Harper (1980) presented a general classification of

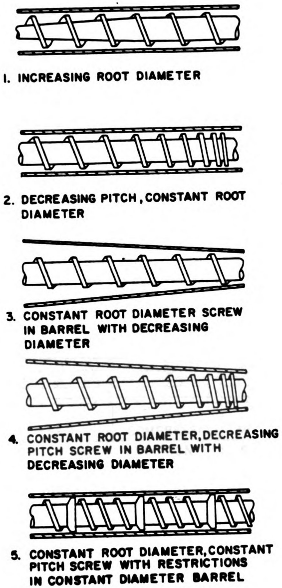

Figure 2.2 Barrel and Screw Designs of Single Screw Extruders

(Harper, 1981)

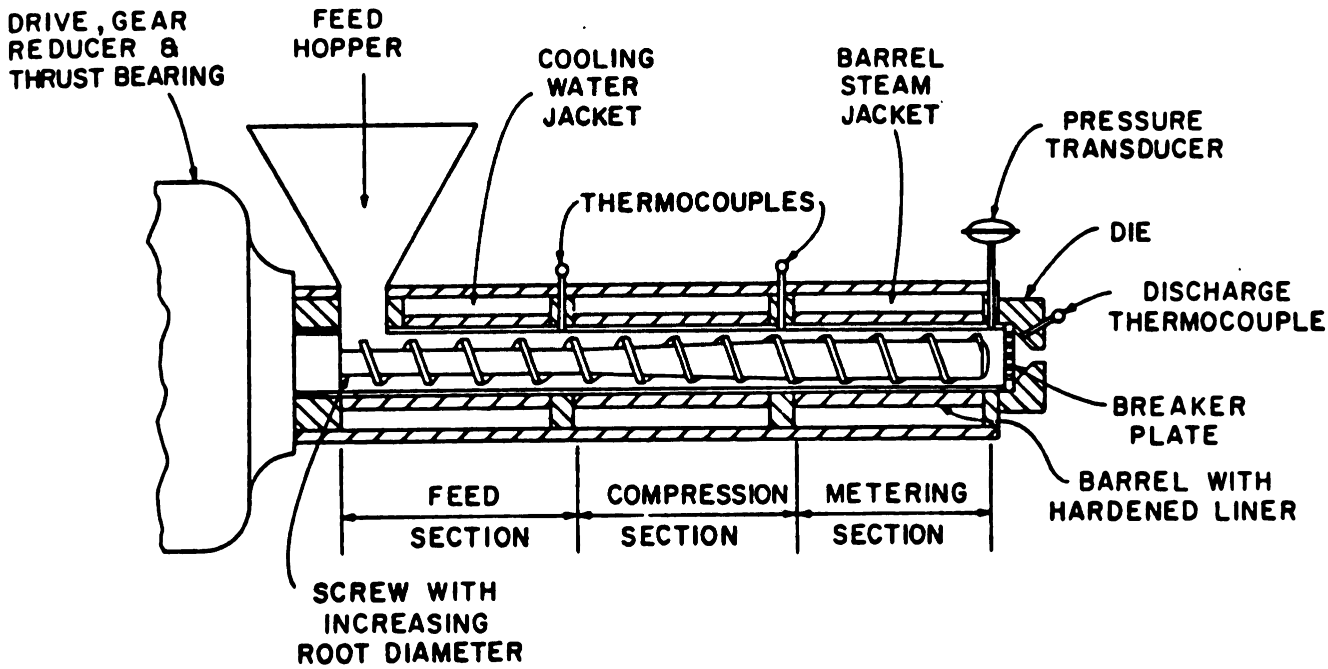

Figure 2.3 Typical Components of Single Screw Cooking Extruders

(Harper, 1978)

single screw extruders based on thermodynamic and functional characteristics showing the overlap between the different extruder types (Figure 2.4). Harper (1985) classified extruders based on shear rate as low shear, moderate shear and high shear extruders (Table 2.1).

2.3 Twin Screw Extruders

Recent focus on extrusion technology is centered on twin screw extruders because of improved process capabilities which include:

(1) a wide range of operating and processing conditions

(2) good mixing and heat transfer characteristics

(3) uniform shear rate profile

(4) narrow residence time distribution

(5) acceptance of a wide range of ingredients

(6) operation over a wide range of moisture contents

(7) control of venting and flashing

(8) facilitation of co-extrusion

2.3.1 Types of Twin Screw Extruders

The two major classifications of twin screw extruders are based on the direction of screw rotation: co-rotating when both screws rotate in the same direction, and counter-rotating when the screws rotate in opposite directions. An additional classification is based on the degree of screw intermesh: non-intermeshing screws, partially intermeshing screws and fully intermeshing screws. Erdmenger (1964) presented a complete classification of twin screw extruders by including the direction of material conveyance (Figure 2.5).

The co-rotating extruders dominate the food industry because they

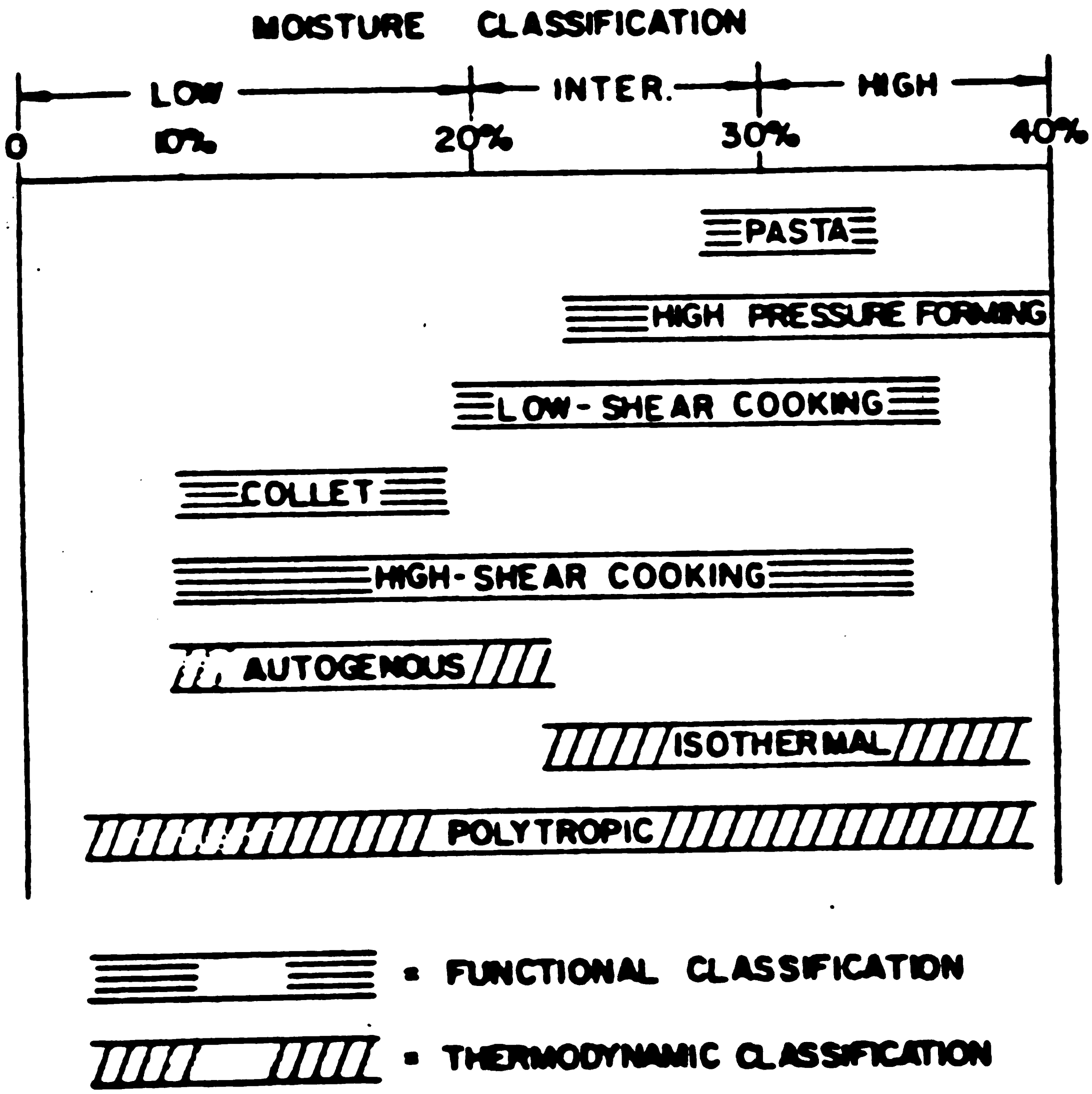

Figure 2.4 Extruder Classifications (Tribelhorn and Harper, 1980)

Table 2.1 Operating Characteristics of Single-Screw Extruders

Operating variable	Low-Shear Forming Extruder	Moderate-Shear Cooking Extruder	High-Shear Cooking Extruder
Feed moisture, % wet basis	23 - 35	20 - 30	12 - 20
Maximum product temperatur (°C)	50 - 80	125 - 175	150 - 200
L/D	5 - 8	10 - 20	4 - 12
D/H	3 - 4.5	5 - 10	7 - 12
Compression ratio	1:1	2 - 3:1	3 - 5:1
Screw speed, s^{-1}	0.08 - 0.11	0.16 - 0.53	0.8 - 1.33
Shear rate, s^{-1}	5 - 10	20 - 100	100 - 180
Net mechanical energy input (KWh/kg)	0.03 - 0.04	0.02 - 0.04	0.1 - 0.14
Heat transfer through barrel jackets (KWh/kg)	-0.01	0.0 - 0.03	-0.03 - 0.0
Steam injection, (KWh/kg)	0.0	0.0 - 0.04	0.0
Net energy input to product (KWh/kg)	0.02 - 0.03	0.02 - 0.11	0.07 - 0.14
Product types	Macaroni RTE cereal pellets, 2nd generation snacks	Soft moist pet foods, Pregelatinized starch, Drink and soup bases, Textured plant protein, RTE breakfast cereals	Pulled starch, Dry pet foods, Modified starch

Source: Harper, 1985.

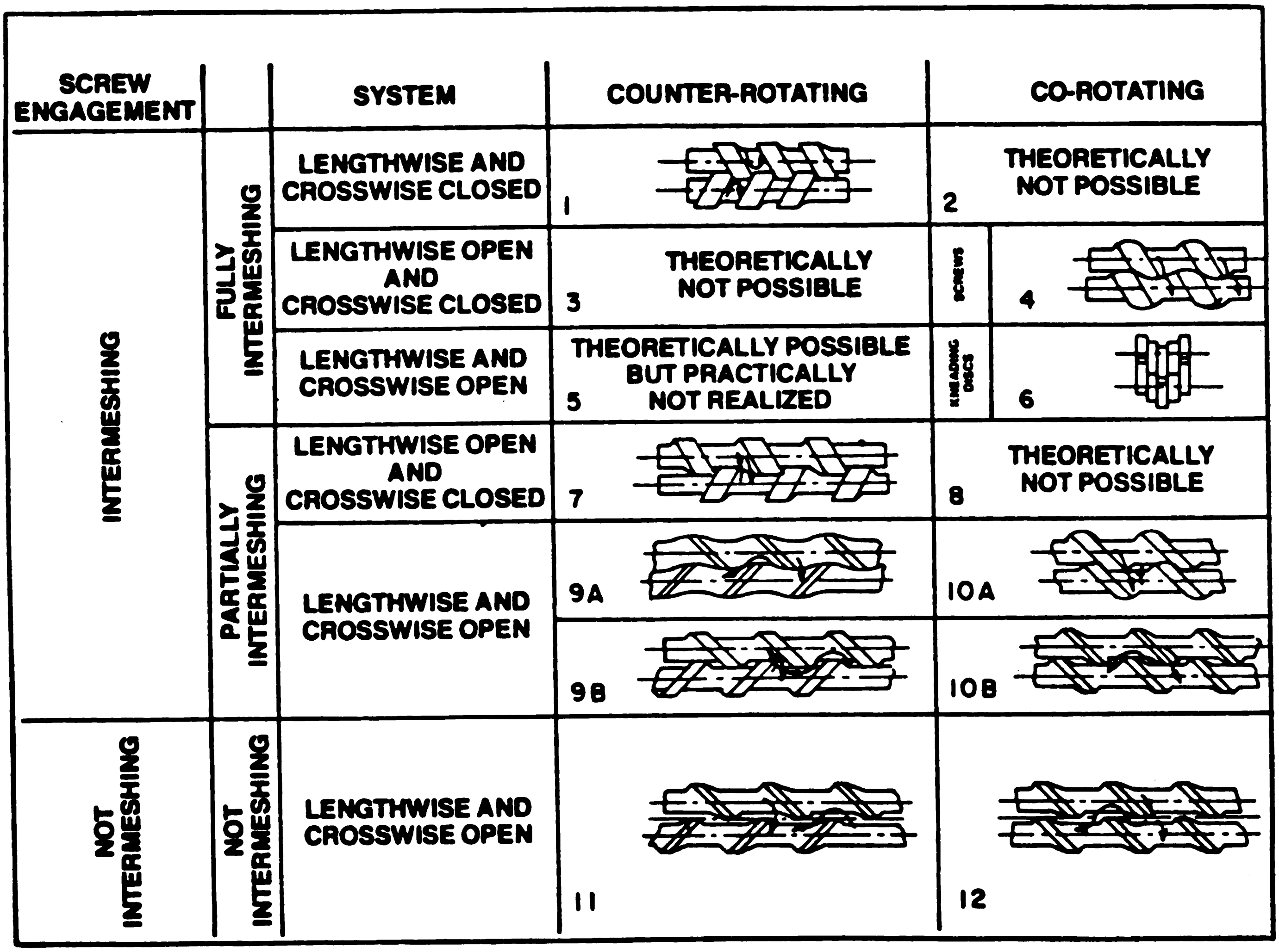

Figure 2.5 Classification of Twin-Screw Mechanisms

(Edmenger, 1964)

can operate at high speed and throughput, generate uniform shear and have good self-cleaning features. The counter-rotating screw extruders provide nearly positive displacement. The operating speeds are generally low because the screw shafts tend to move apart as the speed increases, which causes excessive wear. Operating at low speeds results in low throughput and viscous dissipation.

2.3.2 Counter-rotating Twin screw extruders

This type of extruder is less popular in the food industry, because of their lower throughput, and poor mixing and self-cleaning characteristics. Self cleaning is important for product quality because material that adheres to the screw root and barrel surface might degrade due to broadening residence time. The conveying mechanism of the counter-rotating screw is different from the co-rotating screw because the material is enclosed in C-shaped chambers and is transfered from chamber to chamber as the screws rotate. Schenkel (1966) defined the theoretical throughput as:

$$Q_{th} = 2MNV_c \qquad (2\text{-}2)$$

where:

Q_{th} = theoretical throughput

M = number of thread starts per screw

N = revolutions per minute

V_c = chamber volume

However, the actual throughput is less than the theoretical because of leakage. Janssen (1978) identified four types of leakage (Figure 2.6):

(1) Flight leak (Q_f): the leak through the gap between the flight and the barrel wall

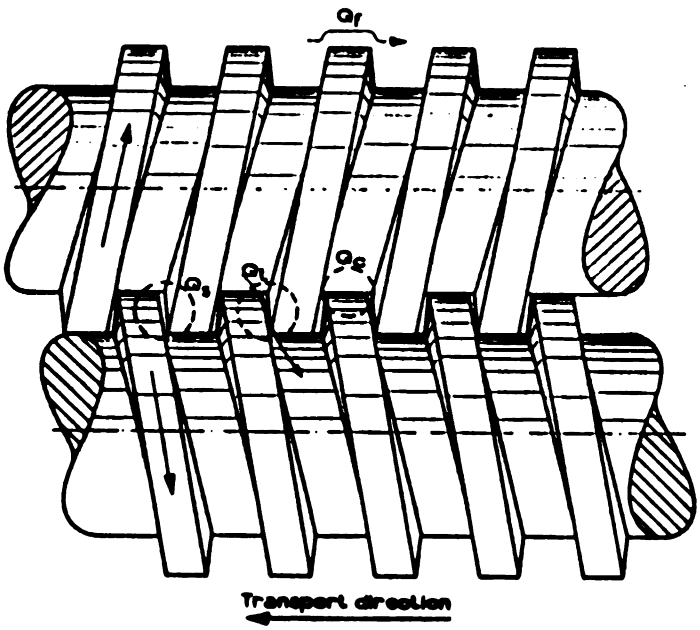

Figure 2.6 Various Leakage Flows in Counter-Rotating Screw Extruders

(Janssen, 1978)

2) **Calender leak (Q_c)** : the leak between the bottom of the channel of one screw and the flight of the other screw

(3) **Tetrahedrom leak (Q_t)**: the leak through the gap that goes from one screw to the other between the flanks of the flights of the two screws

(4) **Side leak (Q_s)**: the leak through the gap between the flanks of the screws perpendicular to the plane through the screw axis

Janssen (1985) defined the acual throughput by incorporating the leakage flow components in the theoretical throughput formula, yielding

$$Q_n = Q_{th} - (Q_f + Q_c + Q_t + Q_s) \qquad (2\text{-}3)$$

2.3.3 Co-rotating Twin Screw Extruders

One of the important features of co-rotating screw extruders is the ability to use different screw configurations that perform different tasks to suit specific process requirements. This is because of the splined shafts that make it possible to assemble various kinds of screw elements such as kneading discs to enhance mixing and increase mechanical energy dissipation (Harper, 1985), reversing screw elements or kneading discs to reduce pressure to facilitate venting, or forward conveying screw elements or kneading discs to increase pressure. The building block principle of assemblying different screw elements provide tremendous potential for process applications and new product development.

Figure 2.7 illustrates how screw configuration design can be used to control pressure to facilitate venting of volatiles and flashing of moisture. It is also possible to add any ingredient down the stream,

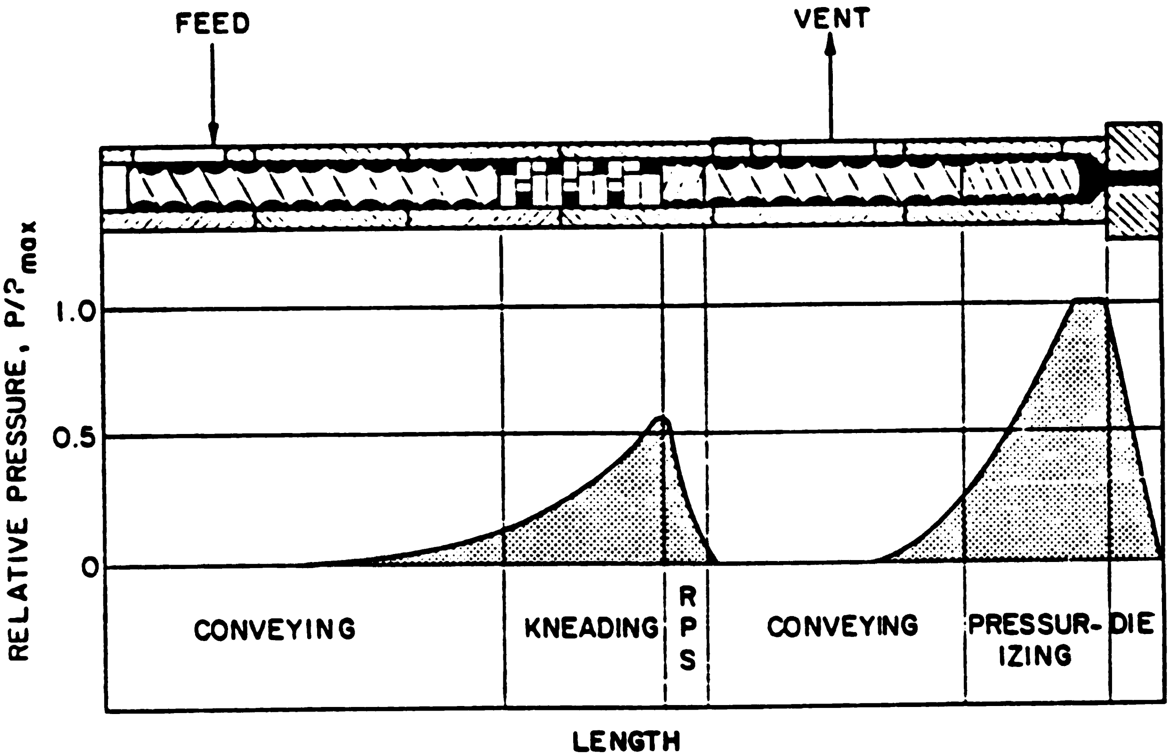

Figure 2.7 Typical Screw and Pressure Profile in a Twin-Screw Extruder

RPS - reverse pitch (Harper, 1985)

especially heat sensitive materials which will not survive the cooking temperature. Screw designs also influence the residence time .

2.3.4 Screw Design

The flexibility of twin screw extruders is due to the different screw designs that are available, which include screw and kneading discs. Screws can be classified into three main categories:

(1) Single lobe: This has relatively good conveying characteristics, can build pressure over a short length at low average shear rates.

(2) Double lobe: This is the standard design for the food industry. It has very good conveying characteristics, good feed intake with low bulk density materials, and relatively low average shear rate (Edmund, 1986).

(3) Triple lobe: This has low volumetric capacity, and can generate very high shear rates. This design is rarely used in the food industry (Edmund, 1986).

Besides the three types of screws discussed above, kneading discs or paddles are also used in twin screw extruders. These have the same cross section as that of double lobe and triple lobe screws (Figure 2.8). Kneading discs are used for performing different processing tasks depending on the number of disks, staggering angle between the discs and the width of the discs.

2.3.5 Residence Time Distribution

The residence time distribution (RTD) is the measure of time the process material spends in the processing equipment. The residence time reveals valuable information about flow patterns, degree of mixing,

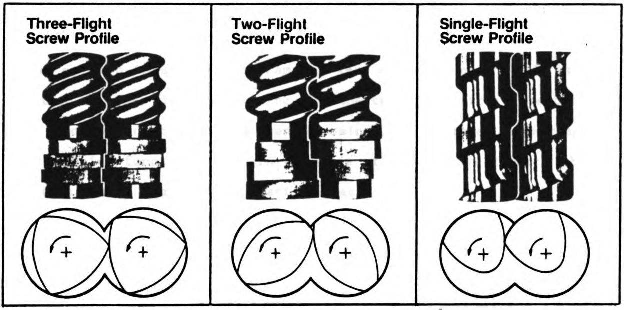

Figure 2.8 Twin-Screw Single-Flighted, Double-Flighted and Triple-Flighted Designs

equipment design, processing conditions and retention time of material in the processing device. For extrusion processes, the study of residence time has received considerable attention (Pinto and Tadmor, 1970; Bigg and Middleman, 1974; Todd, 1975; Janssen et al, 1979; Davidson et al, 1983; Colonna et al, 1983; Wolf et al, 1986; and Altomare and Ghossi, 1986).

Wolf and Resnick (1963) and Levenspiel (1972) developed mathematical models for determining the RTD for chemical reactors. For food extrusion, most of the published works were based on experimental techniques, accomplished by injecting a tracer in a form simulating a pulse or step input. Product samples were collected at the exit as a function of time, starting from the time the tracer was first injected. The tracer concentration was then determined, to generate the exit age distribution function E(t). In the case of an impulse input, the function can be expressed mathematically as:

$$E(t) = \frac{C(t)}{\int_0^\infty C(t)dt} \approx \frac{C(t)}{\int_0^\infty C(t)\Delta t} \qquad (2\text{-}4)$$

where: $C(t)$ = tracer concentration

Δt = samplying time interval

or cumulative distribution function F(t) for a step input. F(t) is related to E(t) by

$$F(t) = \int_0^t E(t)dt \approx \frac{\sum_0^t C(t)\Delta t}{\sum_0^\infty C(t)\Delta t} \qquad (2\text{-}5)$$

The mean residence time $\bar{t}$ is given by

$$\bar{t} = \int_0^\infty tE(t)dt \approx \frac{\sum_0^\infty tC(t)\Delta t}{\sum_0^\infty C(t)\Delta t} \tag{2-6}$$

In some cases, the average residence time is given by

$$\bar{t} = \frac{V}{Q} \tag{2-7}$$

where: V = volume of the processing device

Q = volumetric flow rate

However, equation (2-7) does not give accurate results for twin screw extruders as pointed out by Altomare and Ghossi (1986), because twin screw extruders are starve-fed and the volume occupied by the food dough is not known.

2.3.6 Extruder Die Flow Phenomena

Die assembly is an integral part of the food extrusion system. It plays an important role in shaping and texturizing food products (Harper, 1986). There are a large number of die designs varying in sophistication from single circular die holes to rotating and co-extrusion dies. However, many of the dies were developed by industry, and because of proprietry considerations were never made available to the scientific community. Flow through a food extruder die is very complex due to the complexity of food rheology (Remsen and Clark, 1978; Morgan, 1979 ; Janssen, 1985).

Modelling food extruder dies is complex, due to the combined effects of moisture flashing (puffing) upon exiting from the die and the viscoelastic nature of some food materials that cause jet swell. This leads to a significant problem with regard to scale up of food extruder dies. Quantitative modelling of the effects of moisture flashing (which cause puffing) and normal stress differences (which cause jet swelling) is difficult.

Figure (2.9) shows the pressure drop across the die assembly. The total pressure drop can be written as:

$$\Delta P_t = \Delta P_{ent} + \Delta P_{dhole} + \Delta P_{ex} \qquad (2\text{-}8)$$

where: ΔP_t = total pressure drop

ΔP_{ent} = entrance pressure drop

ΔP_{dhole} = die hole pressure drop

ΔP_{ex} = exit pressure drop

Contribution of ΔP_{ent} to the total pressure drop is significant. Morgan (1979) showed that ΔP_{ent} for soy dough represents 50 to 70 percent of the total pressure drop for capillary extruders with die L/D ratios ranging from two to eight. Remsen and Clark (1978) reported that 20 to 80 percent of the total pressure is lost in the entrance to the die for soy dough extruded in a capillary extruder with L/D ratios ranging from 20 to 80. Modelling of entrance pressure drop for food extruders is still in the early stages of development. Howkins (1987) used dimensional analysis to correlate entrance pressure drop for food materials to flow rate, material rheology and die design. The study of entrance pressure drop for polymers has been extensive, using finite element methods for flow through single circular die holes (Tanner et al, 1975. Boger, 1982; Kenings and Crocket, 1984; Mistoulos et al, 1985) Boger (1982) succeeded in developing a correlation for the entrance

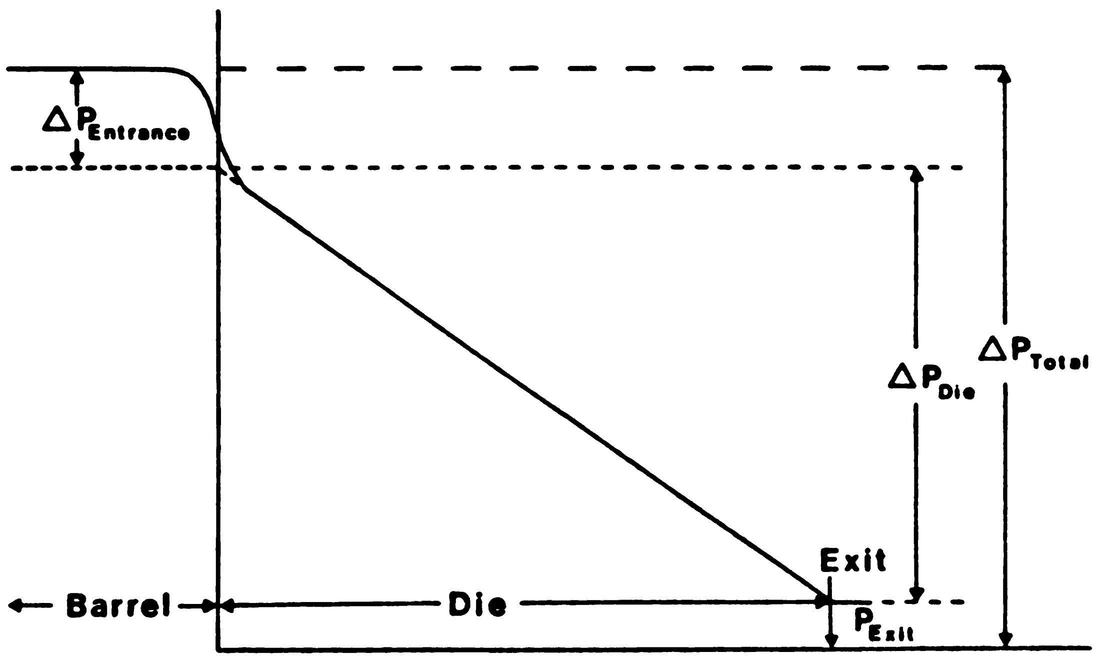

Figure 2.9 Schematic of The Pressure Profile Across an Extruder Die

pressure drop through a circular die for polymers exhibiting non-Newtonian, non-elastic behavior. The correlation is given by

$$\Delta P_{ent} = 2\tau_w \left[\frac{Re'}{32}(C' + 1) + n_c'\right] \qquad (2\text{-}9)$$

where:

$$Re' = \frac{\rho D^n v^{2-n}}{8^{n-1} m \left[\frac{2n+1}{4n}\right]^n} \qquad (2\text{-}10)$$

τ_w = shear stress at the wall

v = average fluid velocity

ρ = fluid density

n = flow behavior index

m = consistency coefficent

C' and n_c' are coefficents that depend on the flow behavior index (Table 2.2). Boger's equation provides a good starting point for modelling entrance pressure loss for foods. However, the key ingredient for successful models is the accurate modelling of dough rheology.

Han (1973) reported values of exit pressure drop between 10 to 30 percent of the entrance pressure loss for low and high molecular weight polymers for shear rates between 100 and 1000 1/s. Howkins (1987) suggested that for foods, $\Delta P_{ex} << \Delta P_{ent}$ and can be neglected, based on the justification of lower viscoelastic properties of food dough compared to polymers.

The flow rate through a die hole is given by the well known Hagen-Poiseuille equation

$$Q = \frac{k\Delta P}{\mu_d} \qquad (2\text{-}11)$$

Table 2.2 Entrance Pressure Drop Coefficients (Eq. 2-9)

Flow Behavior Index n	Loss Coefficient C'	Couette coefficient C_n'
1.0	1.33	0.59
0.9	1.25	0.70
0.8	1.17	0.85
0.7	1.08	1.01
0.6	0.97	1.15
0.5	0.85	1.34
0.4	0.70	1.53
0.3	0.53	1.76

Source: Boger, 1982

where μ_d is the viscosity of the fluid at the die and k is a geometric constant depending on the shape of the die

$$k = \frac{\pi R^4}{8L} \qquad \text{(Circular die)}$$

$$k = \frac{wh^3}{12L} \qquad \text{(Slit die)}$$

$$k = \frac{\pi(R_0 + R_1)(R_0 - R_1)^3}{12L} \qquad \text{(Annular die)}$$

where:

R = radius of the circular die

L = die length

w = width of the slit die

h = height of the slit die

R_0 = outer radius of annular die

R_1 = inner radius of annular die

The shear stress at the wall is given by

$$\tau_w = \frac{\Delta P D}{4L} \tag{2-12}$$

Bagley (1957) proposed that for short capillary dies, the shear stress at the wall can be calculated using

$$\tau_w = \frac{\Delta P}{2[(L/R) + (L^*/R)]} \tag{2-13}$$

where L^* is the equivalent length of the capillary required to account for end effects. The shear rate at the wall for Newtonian fluids flowing through a circular die is given by

$$\dot{\gamma}_w = \frac{4Q}{\pi R^3} \tag{2-14}$$

For a power law fluid, the shear rate at the wall is

$$\dot{\gamma}_w = \frac{3n+1}{4n}\left[\frac{4Q}{\pi R^3}\right] \tag{2-15}$$

2.3.7 Modelling Twin Screw Extruders

Most of the work reported on modelling twin screw extruders is for polymers, where the assumptions of Newtonian fluid and isothermal conditions are used. Modelling for food materials still lags behind due to the complex nature of foods, with most of the development coming as a result of a "cut and try " approach (Harper, 1981).

Janssen's (1978) work on counter-rotating twin screw extruders provided a clear understanding of the conveying mechanism, and paved the way for subsequent development. Riedler (1981) used a quasi three-dimensional finite element scheme to solve for fluid flow, temperature distribution and pressure profiles, within the C-shaped chamber for counter-rotating screws, assuming a Newtonian fluid.

Booy (1978) used kinematics to develop geometric correlations for fully-wiped co-rotating twin screws, including screw surface area and available volume for flow, for different types of screws. Based on Booy's (1978) work, Denson and Hwang (1980) used Galerkin's finite element scheme to solve the equation of motion for two-dimensional flow in co-rotating twin screw extruders. They assumed Newtonian behavior, isothermal conditions and a continuous screw channel, the last assumption being more applicable to single screw extruder analysis. They were able to develop a relation between dimensionless axial pressure gradient and dimensionless volumetric flow rate. Booy (1980) illustrated how the analysis of single screw extruders could be applied to co-rotating twin screw extruders to solve the equation of motion for two-dimensional isothermal flow of a Newtonian fluid.

Eise et al (1981) studied the effects of screw and kneading disc profiles and operating conditions on the degree of fill (ratio of product volume to free channel volume) for a co-rotating screw extruder. They found that, for both the screws and the kneading discs, the degree of fill increases with increases in conveying factor, which was defined as the ratio of the average conveying velocity in the axial direction to the average conveying velocity in the circumferential direction. They also investigated the effect of the conveying factor for kneading discs on the axial mixing coefficient, defined as the ratio of back flow in the kneading discs to the volumetric throughput. They found that the axial mixing coefficient decreases with increases in conveying factor.

Martelli (1983) identified three regions where mechanical energy is dissipated in co-rotating twin screw extruders. These are: (1) between the flight tip of the screw and the inside surface of the barrel; (2) between the flight of one screw and the bottom of the channel of the other screw; and (3) between the flights of opposite screws parallel to each other. Based on Mckelvey's (1962) work for modelling power dissipation within a clearance, Martelli (1983) was able to quantify the viscous dissipation for the three regions using geometric approximations for the clearance depth, surface area and volume. Yacu (1985), based on Martelli's (1983) work of quantifying the mechanical energy dissipation, modelled to a co-rotating twin screw food extruder using a one-dimensional flow model for a non-Newtonian non-isothermal food dough. As a result, the pressure and temperature at the die is predicted with relatively good accuracy. Yacu's work demonstrated the reliability of the one-dimensional flow model for predicting the operating performance of the co-rotating twin screw extruder.

Residence time distribution was used by some authors to study the effects of various parameters on the extrusion process of the twin screw extruder (Todd, 1975; Altomare and Ghossi, 1986). Altomare and Ghossi (1986) presented an excellent paper on the use of RTD to study the effects of screw profile, moisture content, barrel temperature, throughput, screw speed and die design. They found that throughput, screw speed and screw profile have a strong influence on the mean residence time, while die size, moisture content and barrel temperature have no effect on the mean residence time.

2.4 Comparison Between Single and Co-rotating Twin Screw Extruders

The conveying mechanism of a single screw extruder depends mainly on the friction between the material and the screw, and between the material and the barrel. This results in a restricted operating range with regard to product moisture content. On the other hand, the conveying action of intermeshing twin screws is less dependent on friction. Thus, twin screw extruders can operate over a wide range of moisture contents and formula variations. One of the unique and important features of a twin screw extruder is the starve mode of operation. This permits changing product feed rate, screw speeds and barrel temperature independently, providing greater flexibility in attaining the desired shear level, energy inputs and product characeteristics (Altomare and Ghossi, 1986).

Considering the fact that twin screw extruders can operate at low moisture contents, less moisture needs to be removed after extrusion. This results in energy savings which make twin screw extruders 30 percent more efficent than single screw extruders (Anonymous, 1983). Harper (1985) stated that single screw extruders receive 50% of the cooking energy from mechanical energy inputs and the remainder from direct steam injection. On the other hand 70% or more of the cooking energy for twin screw extruders comes from viscous dissipation, the remainder from direct barrel heating. Given this basis, and the fact that steam is the least expensive form of energy, single screw extruders would appear to be more economical. However, when the energy of drying the extrudate is considered, twin screw extruders are more efficent because they can operate at lower moisture level. Dryers have a low energy efficiency (40%), which makes low moisture extrusion more attractive (Harper, 1985). But when low moisture extrusion causes ingredient damage and adversely affects product characteristics, the difference between the two extruders in terms of energy is relatively minor.

Another important factor related to operating cost is the start-up and shut-down time. Twin screw extruders, owing to their self-cleaning characteristic are less subject to jamming and die plugging, both of which interrupt operation. They are also more tolerant to upset in ingredient feed conditions; the extruder can continue to run even if the feeder is shut-off. Also changes in dies and ingredient formulations can be made without stopping the extruder, thus reducing down-time, which translates into greater productivity. But for single screw extruders, a short feed interruption can cause complete shut down requiring machine disassembly, because the extruder requires a continuous flow of ingredients to maintain conveyance (Straka, 1985).

With regard to cost, single screw extruders are superior, simple in design and easy to maintain. On the other hand, twin screw extruders are more expensive, have very sophisticated drive units that include specially designed bearings requiring special attention. Although twin screw extruders have high intial cost, in the long run the numerous advantages mentioned earlier will offset this limitation.

Table 2.3 shows a comparison between single and twin screw extruders on the basis of cost, maintenance, screw design, drive, heat tansfer and operating characteristics.

2.5 Nomenclature

$C(t)$	tracer concentration,
C'	constant (Eq. 2-9)
D	barrel diameter, m
$E(t)$	residence time distribution function, s^{-1}
$F(t)$	cumulative residence time distribution function, dimensionless
h	slit die height, m
K	geometric constant (Eq. 2-11)
Le	screw lead, m
L_d	die length, m
L^*	equivalent die length to account for end effects, m
M	number of thread starts per screw, dimensionless

Table 2.3 Comparison of Single- and Twin-Screw Extruders

Item	Single-Screw	Co-Rotating Twin-Screw
1. Relative cost/unit capacity		
capital		
Extruder	1.0	1.5-2.0
System	1.0	0.9-1.3
2. Relative maintenance	1.0	1.0-2.0
3. Energy		
With preconditioner	Half from steam	Not used
Without preconditioner	Mechanical energy	Mix of mechanical energy and heat exchange
4. Screw		
Conveying angle	$\approx 10^{\circ}$	$\approx 30^{\circ}$
Wear	Highest at discharge and transition section	Highest at restrictions and kneading disks
Positive displacement	No	No
Self-cleaning	No	Self-wiping
Variable flight height	Yes	No
L/D	4-25	10-25
Mixing	Poor	Good
Uniformity of shear rate	poor	Good
Relative RTD spread	1.5	1.0
Venting	Requires two extruders	Yes
5. Drive		
Relative screw speed	1.0-3.0	1.0
Relative thurst bearing capability	Up to 5.0	1.0
Relative torque/pressure	Up to 5.0	1.0
Gear reducer	Simple	Complex
6. Heat transfer	Poor-jackets control barrel wall temperature and slip at wall	Good in filled section
7. Operation		
Moisture (%)	12-35	6 to very high
Ingredients	Flowing granular materials	wide range
Flexibility	Narrow operating	Greater operating

Source: Harper, J.M. 1985

m power law consistency coefficient, Pa-s^n

n power law flow behavior index, dimensionless

N screw speed, RPM

n_c' constant (Eq. 2-9)

Q volumetric flow rate, m^3/hr

Q_c calender leak flow, m^3/hr

Q_f leakage through screw flight, m^3/ hr

Q_n actual throughput, m^3/hr

Q_s side leak flow, m^3/hr

Q_t tetrahedrom leak, m^3/hr

Q_{th} theoretical throughput, m^3/hr

R circular die radius, m

Re' Reynolds number, (Eq. 2.9)

R_i inner radius of annular die, m

R_o outer radius of annular die, m

$\bar{t}$ average residence time, s

v average fluid velocity, m/s

V process device volume, m^3

V_c screw chamber volume, m^3

w slit die width, m

Greek Sympols

ΔP	pressure drop, Pa
ΔP_{dhole}	die hole pressure drop, Pa
ΔP_{ent}	entrance pressure drop, Pa
ΔP_{ex}	exit pressure drop, Pa
ΔP_{t}	total pressure drop, Pa
ρ	fluid density, kg/(m^3)
τ_w	shear stress at the wall, Pa
$\dot{\gamma}$	shear rate, s^{-1}
μ_d	viscosity at the die, Pa-S
Φ	screw helix angle, degree

2.6 Literature Cited

Altomare, E. and Ghossi, P. 1986. An Analysis of Residence Time Distribution Patterns in a Twin Screw Cooking Extruder. Biotech. Prog. 2(3):157-163

Anonymous 1983. Single Vs. Twin Screw. Food Eng. June:103

Bagley, E. B. 1957. End Correction in The Capillary Flow of Polyethylene. J. Appl. Phys. 28(5):624

Bigg, D. and Middleman, S. 1974. Mixing in Screw Extruders. A model for Residence time Distribution in Melt Screw Extruders. Poly. Eng. and Sci. 10:279

Boger, D. V. 1982. Circular Entry Flow of Inelastic and Viscoelastic Fluids. In: Advancess in Transport Process. John Wiley and Sons, New York

Booy, M. L. 1978. Geometry of Fully Wiped Twin-Screw Equipment. Polym. Eng. and Sci. 18(12):973-984

Booy, M. L. 1980. Isothermal Flow of Viscous Liquids in Co-Rotating Twin Screw Devices. Polym. Eng. and Sci. 20(18):1220-1228

Colonna, P., Melcion, J. P., Vergnes, B. and Mercier, C. 1983. Flow, Mixing and Residence Time Distribution of Maize Starch Within a Twin Screw Extruder With Longitudinally Split Barrel. J. Cereal Sci. 1:115

Davidson, V. J., Daton, D., Diosady, L. L. and Spralt, W. A. 1983. Residence time distribution for wheat starch in single screw extruders. J. of Food Sci. 48:1157

Denson, C. D. and Hwang Jr, B. K. 1980. The Influence of The Axial Pressure Gradient on Flow Rate For Newtonian Liquids in Self Wiping, Co-Rotating Twin Screw Extruders. Polym. Eng. and Sci. 20(14):965-971

Edmund, W. S. 1986. Twin- Screw Extrusion Cooking Systems For Food Processing. Cereal Foods World. 31(6):414-416

Eise, K., Herrmann, H., Jakopin, S. and Burkhardt, U. 1981. An Analysis of Twin- Screw Extruder Mechanisms. Advances in Plastic Technology. 1(2):18

Erdmenger, R. 1964. Mehrwellen-Schnecken in der Verahrens Technik. Chemie-Ing. Techn. 36. Jahrgang. Nv. 3:175-185

Han, C. D. 1973. Influence of The Die Entrance Pressure Drop, Recoverable Elastic Energy, and Onset of Flow Instability in Polymer Melt Flow. J. Appl. Poly. Sci. 17(5):1403-1413

Harper, J. M. 1978. Extrusion Processing of Foods. Food Technol. 32(7):67-72

Harper, J. M. 1979. Food Extrusion. Crit. Rev. Food Sci. Nutr. 11(2):155-215

Harper, J. M. 1981. Extrusion of Food. Vols. 1 and 2. CRC Press Boca Raton, Fl.

Harper, J. M. 1985. Processing Characteristics of Food Extruders. Food Engineering and Process Application Vol. 2. Unit Operation Ed. Lemanguer, M and Jelen, P.

Harper, J. M. 1986. Extrusion Texturization of Foods. Food Technol. 40(3):70

Howkins, M. D. 1987. A Predictive Model For Pressure Drop in Food Extruder Dies. M.S. Thesis, Michigan State University, East Lansing, MI. USA.

Janssen, L. P. B. M. 1978. Twin Screw Extrusion. Elsevier Scientific Publ. Co. Amsterdam.

Janssen, L. P. B. M., Hollunder, R. W., Spoor, M. W. and Smith, J. M. 1979. Residence Time Distribution in Plasticating Twin Screw Extruders. AIChE. Journal. 25(2):345-351

Janssen, L. P. B. M. 1985. Models For Cooking Extrusion. Food Engineering and Process Applications Vol. 2. Unit Operation Ed. Lemaguar, M. and Jelen, P.

Keunings, R. and Crocket, M. J. 1984. Numerical Simulation of The Flow Of Viscoelastic Fluid Through an Abrupt Contraction. J. Non-Newtonian Fluid Mech. 14(1):279-299

Levenspiel, O. 1972. Chemical Reaction Engineering, 2nd Ed. John Wiley and Sons, New York.

Mans, J. 1982. Exruders. Prepared Foods. 11:60-63

Martelli, F. G. 1983. Twin Screw Extruders: A basic Understanding. Van Nostrand Reinhold Comparce, New York.

Mckelvey, J. M. 1962. Polymer Processing. John Wiley and Sons, New York.

Mistoulis, E., Vlachopoulos, J. and Mirza, F. A. 1985. A Numerical Study of The Effect of Normal Stresses and Elongational Visscosity on Entry Vortex Growth of Extrudate Swell. Polym. Eng. and Sci. 25(11):677-689

Morgan, R. G. 1979. Modelling Effect of Temperature- Time History, Temperature, Shear Rate and Moisture Content on Viscosity of Defatted Soy Flour Dough. PhD. Dissertation, Texas A&M University, USA.

Pinto, G. and Tadmor, Z. 1970. Mixing and Residence Time Distribution In Melt Screw Extruders. Polym. Eng. and Sci. 10(5):279-288

Remsen, C. and Clark, P. 1978. A Viscosity Model For a Cooking Dough. J. Food Process Eng. 2:39-64

Riedler, J. 1981. Quasi Three-Dimensional Finite Element Solution For Twin Screw Extruder. In Numerical Methods In Laminar and Turbulent Flow, Conference Proc., Taylor, C., Schrefter, B. A. Eds. Pineridge Press, Swansea, UK. PP. 191-206.

Rossen, J. L. and Miller, R. C. 1973. Food Extrusion. Food Technol. 27:40-55

Schenkel, G. 1966. Plastic Extrusion Technology and Theory. Iliffe Books LTD. American Elsevier Publishing Company INC. New York.

Straka, R. 1985. Twin and Single-Screw Extruders for The Cereal and Snack Industry. Cereal Food World. 30(5):329

Tanner, R. I., Nickell, R. E. and Bilger, R. W. 1975. Finite Element Methods For The Solution of Some Incompressible Non-Newtonian Fluid Mechanics, Problem With Free Surfaces. Computer Method in Appl. Mech. and Eng. 6(1):155-174

Todd, D. 1975. Residence Time Distribution in Twin Screw Extruders. Polym. Eng. and Sci. 15:437

Tribelhorn, R. C. and Harper, J. M. 1980. Extrusion-Cooker Equipment. Cereal Foods World. 25:134-136

Wolf, D. and Resnick, W. 1963. Residence Time Distribution in Real Systems. Ind. Eng. Chem. Fundam. 2:287

Wolf, D. and White, D. H. 1976. Experimental Study of The Residence Time Distribution in Plasticating Extruders. AIChE. J. 22:122

Wolf, D., Holin, N. and White, D. H. 1986. Residence Time Distribution in Commercial Twin-Screw Extruders. Polym. Eng. and Sci. 26(9):640-646

Yacu, W. 1985. Modelling a Twin Screw Co-Rotating Extruder. J. Food Proc. Eng. 8:1-21

CHAPTER 3

MODELLING THE AVERAGE SHEAR RATE IN A TWIN SCREW CO-ROTATING EXTRUDER

3.1 Abstract

The modelling of the shear rate for co-rotating twin screw extruders has been approached in a manner similar to that used with mixers. Both Newtonian and non-Newtonian standards have been used to estimate an average shear rate for three screw configurations of a Baker Perkins (MPF-50D) twin screw extruder. The estimated shear rate was found to correlate with screw speed.

3.2 INTRODUCTION

Modelling of twin screw extruders is hindered significantly by the lack of adequate models for evaluating the shear rate inside the extruder. The shear rate is an important parameter for evaluating viscous dissipation, which constitutes the major source of heat energy for cooking extruders. The approach generally used for modelling the shear rate in twin screw extruders is similar to the one used commonly with single screw extruders, for which the shear rate is defined as the ratio of the screw tip velocity and the channel or clearance depth (Martelli, 1971; Yacu, 1985; Meijer and Eleman, 1988). The main drawback of this approach is the difficulty in accurately quantifying the shear rate at the different shearing zones of the twin screw extruder, primarily because of the geometric complexity of the extruder. Furthermore, twin screw extruders provide a good degree of mixing

(Harper, 1985) which disrupts the velocity profile and raises questions about the applicability of the single screw model to twin screw extruders. The good mixing characteristic of twin screw extruders suggest that a mixer approach might be more appropriate for modelling the shear rate.

The primary objectives of this analysis are:

(1) To present a procedure for estimating the average shear rate for co-rotating twin screw extruders.

(2) To develop correlations for the average shear rate of three Baker-Perkins screw configurations: single flighted screw (single lead) with pitch= 0.25D, double flighted screw (feed screw) with pitch=1D, and kneading discs staggered at 30 degrees forwarding (30F)

3.3 Power Input To Extruders

Changes in kinetic energy during extrusion are generally negligible due to the relatively low velocities in the extruder (Harper, 1981). Therefore, for the extruder the steady state macroscopic mechanical energy balance (Bernoulli Equation) for a given control volume i reduces to

$$\hat{P}_{wi} = \hat{E}_{vi} + \Delta p_i/\rho \qquad (3\text{-}1)$$

where, $\hat{P}_{wi}$ is the rate of power input, E_{vi} is the rate of viscous dissipation of mechanical energy, Δp_i is the pressure drop, and ρ is the fluid density. Multiplying Eq. 3-1 by the mass flow rate yields

$$P_{wi} = E_{vi} + \Delta p_i Q \qquad (3\text{-}2)$$

where, Q is the volumetric flow rate.

For extruders the flow work term in the mechanical energy balance is due to the flow through the die (net flow) and the back flow (pressure flow). Therefore the extruder is divided into two control volumes (Figure 3.1). Applying the mechanical energy balance to control volume #1 yields

$$P_{w1} = E_{v1} + \Delta p_1 Q_p \qquad (3\text{-}3)$$

Similarly for control volume #2 we get

$$P_{w2} = E_{v2} + \Delta p_2 Q_n \qquad (3\text{-}4)$$

Adding Eqs. 3-3 and 3-4 yield

$$P_w = E_v + \Delta p Q_p + \Delta p Q_n \qquad (3\text{-}5)$$

where

$$P_w = P_{w1} + P_{w2} \qquad (3\text{-}6)$$

$$E_v = E_{v1} + E_{v2} \qquad (3\text{-}7)$$

$$\Delta P = \Delta P_1 = \Delta P_2 \qquad (3\text{-}8)$$

Q_p (pressure flow) and Q_n (net flow) which are related by

$$Q_n = Q_d - Q_p \qquad (3\text{-}9)$$

where Q_d is the drag flow. In most food extrusion applications, the drag flow is much larger than the pressure flow (Harper, 1981). Therefore, the net flow is closer to the drag flow. Neglecting the power consumed in back flow reduces Equation 3-5 to

$$P_w = E_v + \Delta p Q_n \qquad (3\text{-}10)$$

In food extrusion, the flow work is generally very small compared to viscous dissipation, due to the relatively high viscosities of food

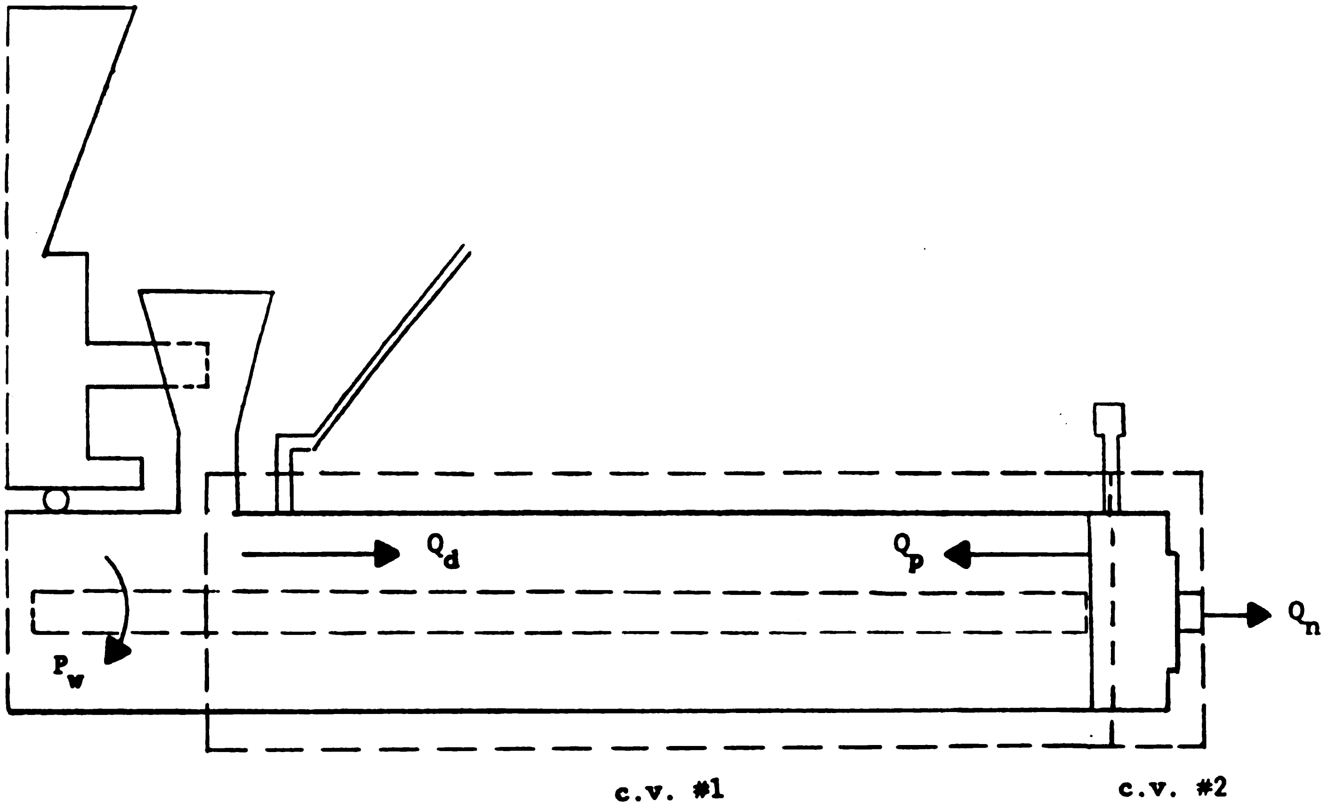

Figure 3.1 Schematic of The Extruder Showing Two Control Volumes Used in The Development of The Macroscopic Mechanical Energy Balance

doughs and the low pressure drops (Harper, 1981). From Eq. 3-10, the power consumed in viscous dissipation can be expressed as

$$E_v = P_w - \Delta p Q_n \tag{3-11}$$

The power consumption in mixing vessels is usually expressed in terms of a dimensionless power number which can be defined for twin screw etruders as

$$P_o = \frac{E_v}{\rho N^3 D_h^5} \tag{3-12}$$

where P_o = power number

N = screw speed

D_h = extruder hydraulic diameter

Power consumption in mixing a Newtonian fluid in the laminar region is inversly proportional to the Reynolds number (Metzner and Otto, 1957; Rieger and Novak, 1973). For twin screw extruders, the Reynolds number is defined as

$$Re = \frac{D_h^2 N \rho}{\mu} \tag{3-13}$$

where Re = Reynolds number

μ = Newtonian viscosity

3.4 Hydraulic Diameter

The concept of a hydraulic diameter has been used extensively in fluid dynamics to characterize the geometry of complex shapes. For twin screw extruders, use of the barrel diameter as a characteristic dimension does not provide useful information, because different screw configurations provide different processing characteristics. Therefore, use of the hydraulic diameter as a characteristic dimension provides more information about the screw characteristics. Conventionally, the hydraulic diameter is defined as

$$D_h = \frac{4V_w}{A_w} \qquad (3\text{-}14)$$

where V_w and A_w are the wetted volume and area per unit length, respectively.

The hydraulic diameters for the three screw configurations used in this study were determined as follows:

(1) Single Lead

In order to calculate the hydraulic diameter, a 5.08 cm (2-inch) screw length was taken as a basis. The wetted volume was estimated by

$$V_w = V_b - 2V_s \qquad (3\text{-}15)$$

where V_b = barrel volume

V_s = screw volume for a 5.08 cm long screw

Figure (3-2) shows the cross-sectional area of the barrel. The barrel volume and surface area can be calculated by

$$V_b = A_{bc}L \qquad (3\text{-}16)$$

$$A_{bs} = P_{bs}L \qquad (3\text{-}17)$$

$$A_{bc} = 2(\pi - \psi)R^2 + C_L R \sin(\psi) \qquad (3\text{-}18)$$

and

$$P_{bp} = 2D(\pi - \psi) \qquad (3\text{-}19)$$

where A_{bc} = barrel cross-sectional area

A_{bs} = barrel surface area

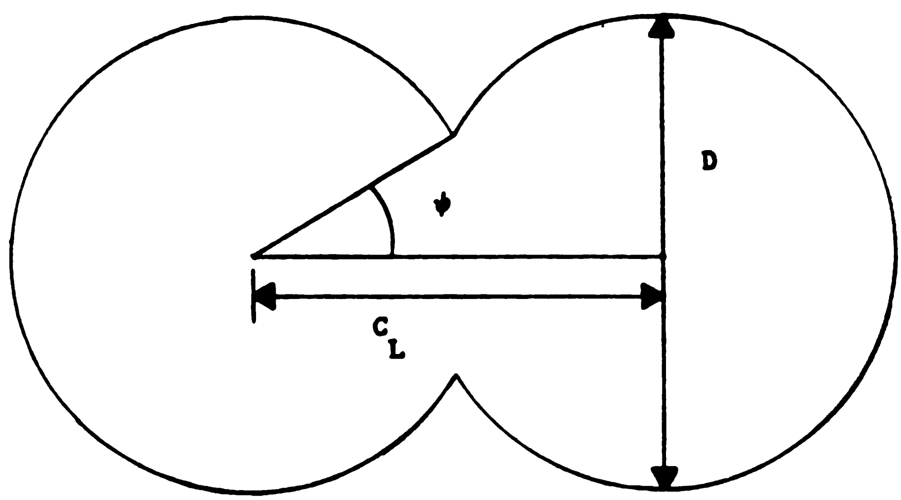

Figure 3.2 Twin Screw Extruder Barrel Cross-section

P_{bp} = barrel perimeter

D = barrel diameter

L = barrel length

The screw volume was estimated by sealing both ends of the screw, and immersing it into a beaker of water with a marked level. The volume of water displaced is equivalent to the screw volume.

The wetted surface area was estimated by

$$A_w = A_{bs} + 2A_s \tag{3-20}$$

$$A_s = A_t + A_r + A_f \tag{3-21}$$

$$A_t = Z_t e \tag{3-22}$$

$$A_r = Z_r W \tag{3-23}$$

$$A_f = 2HZ_t \tag{3-24}$$

where A_s is the screw surface area and A_t, A_r and A_f are the screw tip, root and flange area, respectively. Z_t and Z_r are the length along the helix of the screw tip and root, respectively, and H is the channel depth. Tables 3.1a and 3.1b show the different values for the screw and the barrel, as well as the calculated values of the volumes and surface areas.

<u>(2) Feed Screws</u>

The wetted volume was estimated in a manner similar to the single lead. The screw surface area was estimated by combining the flange and root area. Since the screw has a parabolic shape, the flange and root area are related by

$$A_r + A_f = 2BZ_t \tag{3-25}$$

Table 3.1a Single lead screw and barrel geometry

Barrel diameter (D)	50.76 (mm)
Screw major diameter (D_s)	50.23 (mm)
Screw root diameter (D_r)	28.56 (mm)
Screw channel depth (H)	11.10 (mm)
Screw tip width (e)	2.64 (mm)
Screw channel bottom width (E)	5.26 (mm)
Screw shafts center distance (C_L)	40.0 (mm)
Screw helix angle (ϕ)	4.6 (degree)
ψ	38 (degree)
Z_t	633.40 (mm)*
Z_r	342.39 (mm)*

* Based on a 5.08 cm (2-inch) axial length

Table 3.1b Volume and surface area for single lead and barrel

Screw volume (V_s)	51.5 (cm^3)
Barrel volume (V_b)	193.16 "
Wetted volume (V_w)	90.16 "
Barrel surface area (A_{bs})	127.81 (cm^2)
Screw tip area (A_t)	16.72 "
Screw root area (A_r)	18.04 "
Screw flange area (A_f)	140.62 "
Wetted area (A_w)	478.57 "

Volume and surface area are based on a 5.08 cm (2-inch) axial length where B is the channel perimeter. The tip area is given by

$$A_t = 2Z_t e \qquad (3\text{-}26)$$

The value of the screw constants and results of the calculations are presented in Tables 3.2a and 3.2b

<u>(3) 30 Degree Forwarding (30 F)</u>

A similar procedure to the one used with single lead and feed screws was used to estimate the wetted volume. The wetted area for kneading discs staggered at 30 degree forwarding (30 F) consist of tip area, side area and flange area. The tip and side area can be estimated from routine measurements, but the flange area is measured by a scale drawing of the discs with the staggered angle on graph paper (Figure 3.3) and estimating the wetted area (unhatched area).

For 5.08 cm of barrel length and 1.27 cm disc width, four discs are required per shaft. This adds up to three flange areas and four tips and side areas. Therefore the total disc surface area is given by

$$A_s = 2(3A_f + 4A_t + 4A_{ds}) \qquad (3\text{-}27)$$

where A_{ds} is the disc side area. Table 3.3 gives a summary of the calculations for the kneading discs.

Table 3.4 shows the estimated values of the hydraulic diameter of the three types of screw.

3.5 Modelling The Shear Rate

Martelli (1983) identified four regions where the material is subjected to shear inside a co-rotating twin screw extruder. These are

1) between screw tip and barrel

2) between screw tip of one screw and channel bottom of the other

Table 3.2a Feed screw geometry

Screw major diameter (D_s)	50.02	(mm)
Screw root diameter (D_r)	29.26	"
Screw channel depth (H)	10.38	"
Screw tip width (e)	1.5	"
Z_t	165.8	" *
Screw helix angle (ϕ)	17.85	"

* Based on a 5.08 cm (2-inch) axial length

Table 3.2b Volume and surface area for feed screw and barrel

Screw root and flange area (A_r+ A_f)	105.6	(cm^2)
Screw tip area (A_t)	4.95	"
Wetted area (A_w)	348.91	"
Screw volume (V_s)	52.4	(cm^3)
Wetted volume (V_w)	88.36	"

All measurments are based on a 5.08 cm (2-inch) axial length

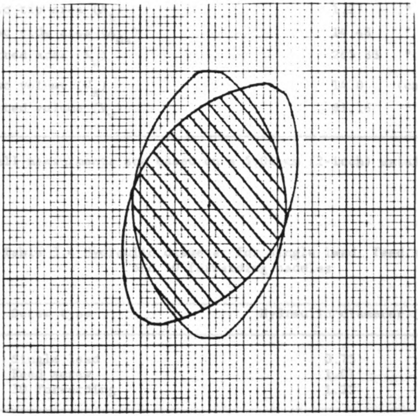

Figure 3.3 Cross-Sectional View of Kneading Discs Staggered at 30 Degree Forwarding

Table 3.3 Volume and surface area for 30F paddles and barrel

Discs flange area (A_f)	1.92	(cm^2)
Disc tip area (A_t)	1.27	"
Disc side area (A_{ds})	14.48	"
Wetted area (A_w)	265.33	"
Disc volume (V_s)	14.0	(cm^3)
Wetted volume (V_w)	81.16	"

All measurments are based on a 5.08 cm (2-inch) axial length

Table 3.4 Hydraulic diameter for single lead, feed screw and 30 forwarding paddles

Screw type	Hydraulic diameter (cm)
Single lead	0.75
Feed screw	1.01
30 Forwarding	1.22

screw

3) within the screw channel

4) between parallel screw flanges

Based on the ideal definition of shear rate as the ratio of screw tip velocity to channel or clerance depth, Martelli (1983) estimated the shear rate at various regions using some approximation to the extruder geometry. This definition of shear rate is based on the assumption of pure drag flow, which is not the prevailing mode for twin screw extruders. In addition, the transfer of material between the screws disrupts the velocity profile, severely reducing the accuracy of this method.

The strategy used for estimating the average shear rate for twin screw extruders in this study is analogous to the traditional method suggested by Metzner and Otto (1957) for mixers. It is also based on the argument presented by Rao and Cooley (1984): if two identical mixing systems, one containing a Newtonian and the other a non-Newtonian fluid, are operating in the laminar region with identical impeller speeds, and the viscosity of the Newtonian is varied by diluting or thickening until the power measured on each are the same, then the apparent viscosity of the non-Newtonian fluid must be the same as the Newtonian fluid viscosity. This concept is used for estimating the average shear rate for twin screw extuders.

The term average shear rate is used because for non-Newtonian fluids the apparent viscosity varies with the shear rate inside the extruder. Since an average shear rate is assumed, the apparent viscosity at this shear rate is termed "average apparent viscosity", which is assumed to be equivalent to the Newtonian viscosity at the same power number and screw speed.

The procedure used for calculating the average shear rate is as follows:

(1) From the extruder data of a Newtonian fluid, calculate the power number (P_o) and Reynolds number (Re), using Eqs. (3-12) and (3-13).

(2) Use regression analysis to correlate P_o and Re.

(3) From the extruder data of the non-Newtonian fluid, calculate the power number (P_o^*) using equation (3-12).

(4) Use the value of (P_o^*) from (3) in (2) to calculate the corresponding (Re^*)

(5) Calculate the average apparent viscosity (η_a) on the basis of the Re^* obtained in step 4, using Eq. (3-13), with μ repaced by η_a.

(6) Use a viscometer to obtain a correlation between apparent viscosity and shear rate for the non-Newtonian fluid.

(7) Use the average apparent viscosity (η_a) to calculate an average shear rate ($\dot{\gamma}_a$) using the correlation in (6).

(8) Correlate ($\dot{\gamma}_a$) to screw speed and throughput.

3.6 Experimental Procedure

Newtonian and non-Newtonian standards were used to obtain the data needed to estimate the effective shear rate. A polymer (polybutene) was chosen as the Newtonian standard, because it has high viscosity and is available in melt form at room temperature. The fluid was obtained from the Amoco Company. The non-Newtonian standard was prepared by mixing seven percent soy polysaccharide (SPS) with pure honey. The sample was left overnight to allow the air bubbles to settle out of the fluid before extrusion.

3.6.1 Rheological Data

A conccentric cylinder viscometer (Haake) was used with measuring head M-150, and SVI and SVII sensors. The viscometer was connected to a Haake speed programmer, a Hewlett-Packard 3495 data acquisition system, and a Hewlett-Packard 85 computer to facilitate data collection and analysis. Also a Hakke F3-C temperature controller was used to control the product temperature.

The samples used to determine the rheological properties, for both the Newtonian and the non-Newtonian fluids, were taken from the same batch used for the extrusion runs. Data for both fluids were taken at different temperatures over as wide a shear rate range as possible.

3.6.2 Twin Screw Extrusion Data

A Baker Perkins (MPF-50) twin screw co-rotating extruder was used for this work. All the extrusion runs were performed over 15 L/D, using a configuration made up of one type of screw at a time. A special die with a gate valve was constructed and used in all the extrusion runs to control die pressure and, hence, percent fill. A K-tron feeder (K-tron corporation) with controllable auger speed was used to feed the material into the extruder.

During the extrusion run, the barrel temperature was controlled by circulating chilled water to maintain low product temperature and high torque readings. One of the main objectives during these runs was to maintain near 100 pecent fill levels. This was achieved by manipulating both the feeder and the die pressure until the channel was filled, which was monitored by observing the material back up to the feed port. When 100 percent fill was achieved, the extruder was left to run for a while before taking measurements to make sure steady state conditions were attained. Screw speed, torque, barrel temperature, product temperature and die pressure were recorded at the controller panel. The flow rate was measured by measuring extrudate weight over a given time span. The product temperature at the die was measured by inserting a thermocouple probe through the die openning. Measurements were made for all three screw configurations on both Newtonian and non-Newtonian standards.

3.7 Results And Discusion

3.7.1 Determination of Rheological Properties

3.7.1.1 Newtonian Standard

The shear stress versus shear rate data for polybutene are presented in Figure 3.4 for temperatures of 40, 60 and 80 ^{o}C. The plots indicate clearly that polybutene is Newtonian, because of the linear relation between the shear stress and the shear rate. Also when the data was fitted to the power law model given by

$$\tau = K\dot{\gamma}^{n} \qquad (3\text{-}28)$$

where τ = shear stress

K = consistency coefficent

and n = flow behavior index

The results of the regression show that n=1, which is the case for a Newtonian fluid. Table 3.5 summarizes the results of the regression

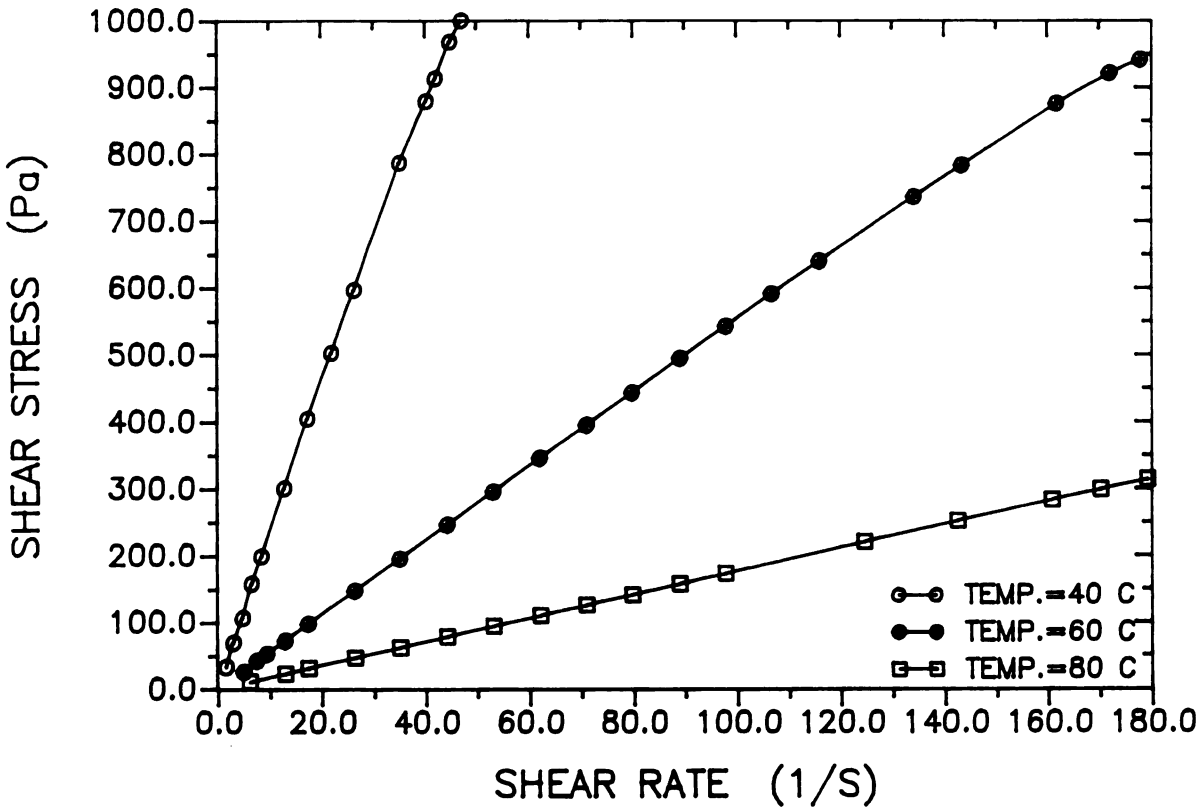

Figure 3.4 Shear Stress Versus Shear Rate For Polybutene

Table 3.5 Rheological properties of Polybutene

Temperature (C)	K (Pa s^n)	n	R^2
40	19.31	1.03	0.99
60	5.44	1.00	1.00
80	1.80	0.99	1.00

analysis.

Temperature effects on the Newtonian viscosity can be expressed using an Arrhenius relation of the form

$$\mu = \mu_o \exp(\Delta E/RT) \qquad (3\text{-}29)$$

where μ = Newtonian viscosity

μ_o = reference viscosity

ΔE = activation energy

R = gas constant

T = absolute temperature, ^oK

Figure 3.5 shows the plot of log μ versus 1/T, the slope of which gives an activation energy of 12995 cal/g mole.

3.7.1.2 Non-Newtonian Standard

A plot of shear stress versus shear rate for honey-SPS is shown in Figure 3.6. Regression analysis on the data revealed a power law fit (Table 3.6). For non-Newtonian fluids, the viscosity is usually refered to as an apparent viscosity beacuse it is a function of the shear rate. For power law fluids the apparent viscosity is given by

$$\eta = K\dot{\gamma}^{n-1} \qquad (3\text{-}30)$$

The temperature effect on the consistency coefficent may be expressed as an Arrhenius relationship:

$$K = K_o \exp(\Delta E/RT) \qquad (3\text{-}31)$$

where K_o is a reference consistency coefficent. When the effect of temperature is incorporated, the viscosity is given by

$$\eta = K_o \dot{\gamma}^{n-1} \exp(\Delta E/RT) \qquad (3\text{-}32)$$

Figure 3.7 Shows a plot of log K against 1/T, with the slope giving

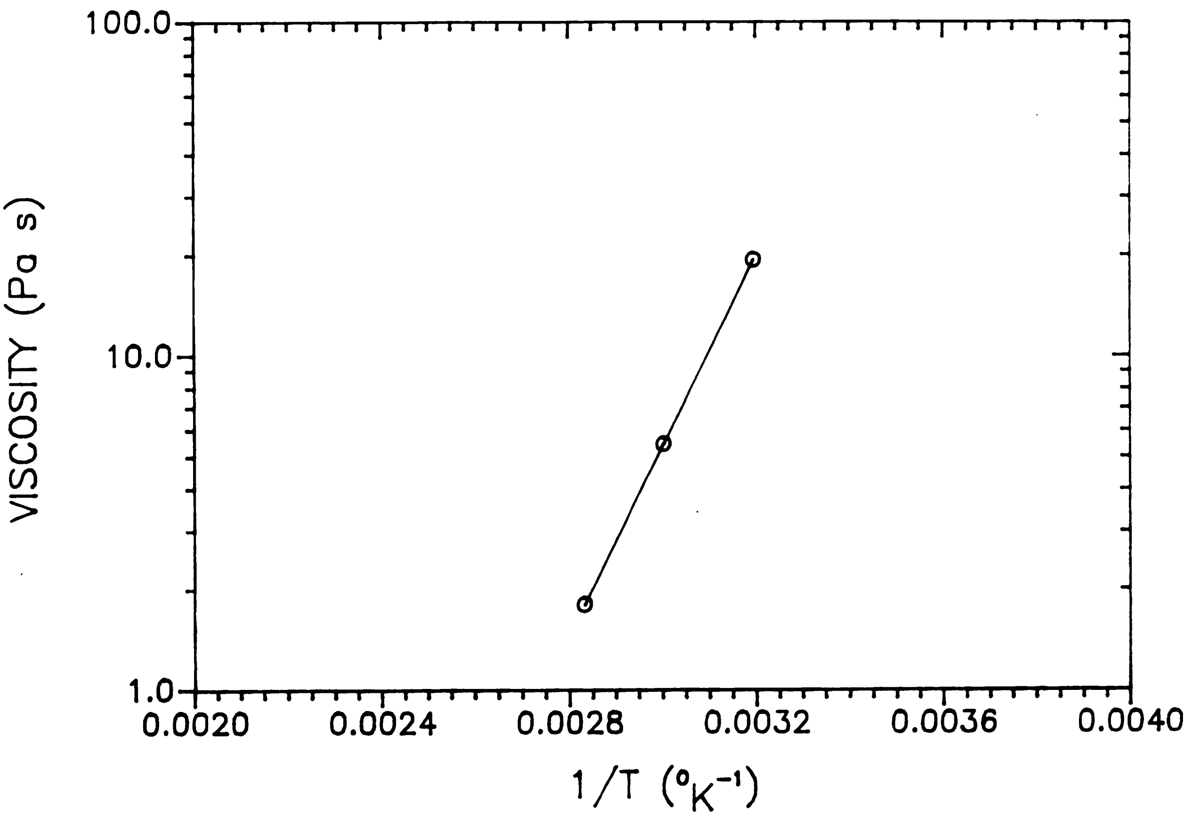

Figure 3.5 Viscosity Versus Inverse Temperature For Polybutene

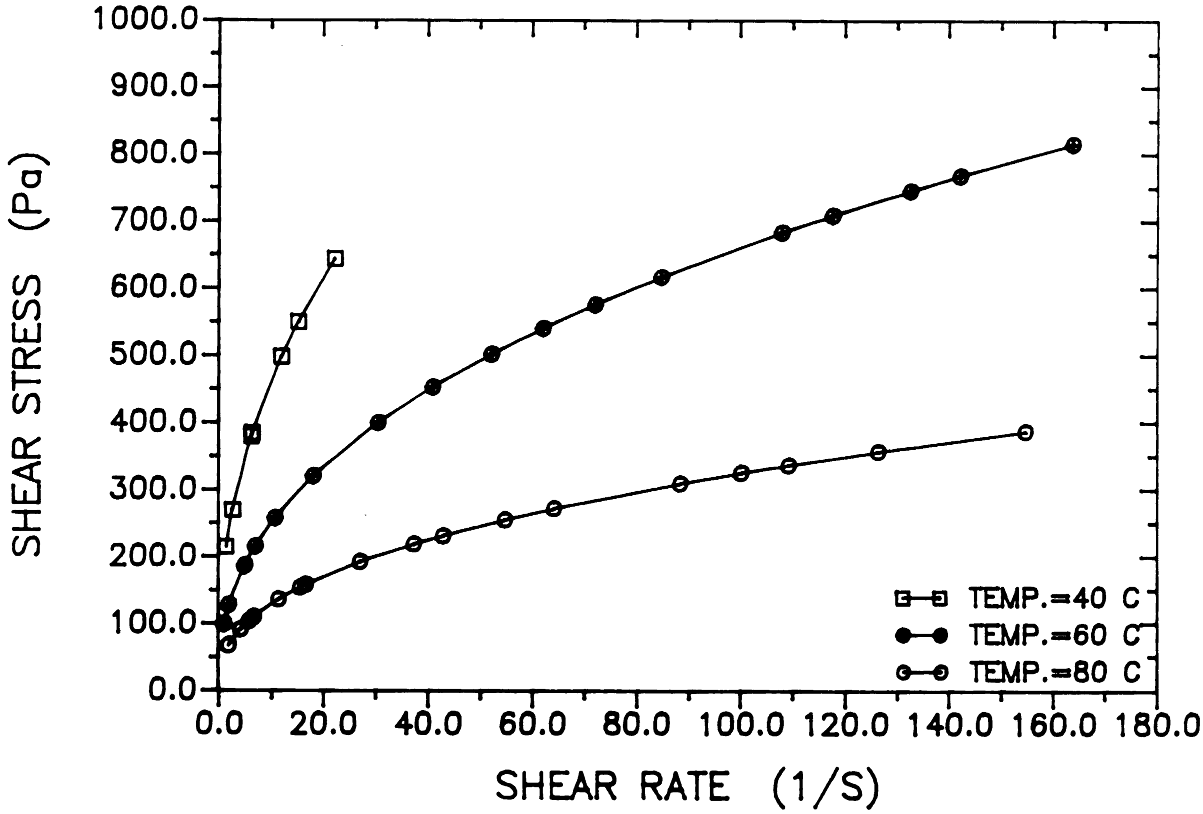

Figure 3.6 Shear Stress Versus Shear Rate For a Mixture of 7% SPS and 93% Honey

Table 3.6 Rheological Properties of a Mixure of 7% SPS and 93% Honey

Temperature	K (Pa s^n)	n	R^2
40	172.609	0.422	0.98
60	93.071	0.425	0.97
80	50.884	0.402	0.97

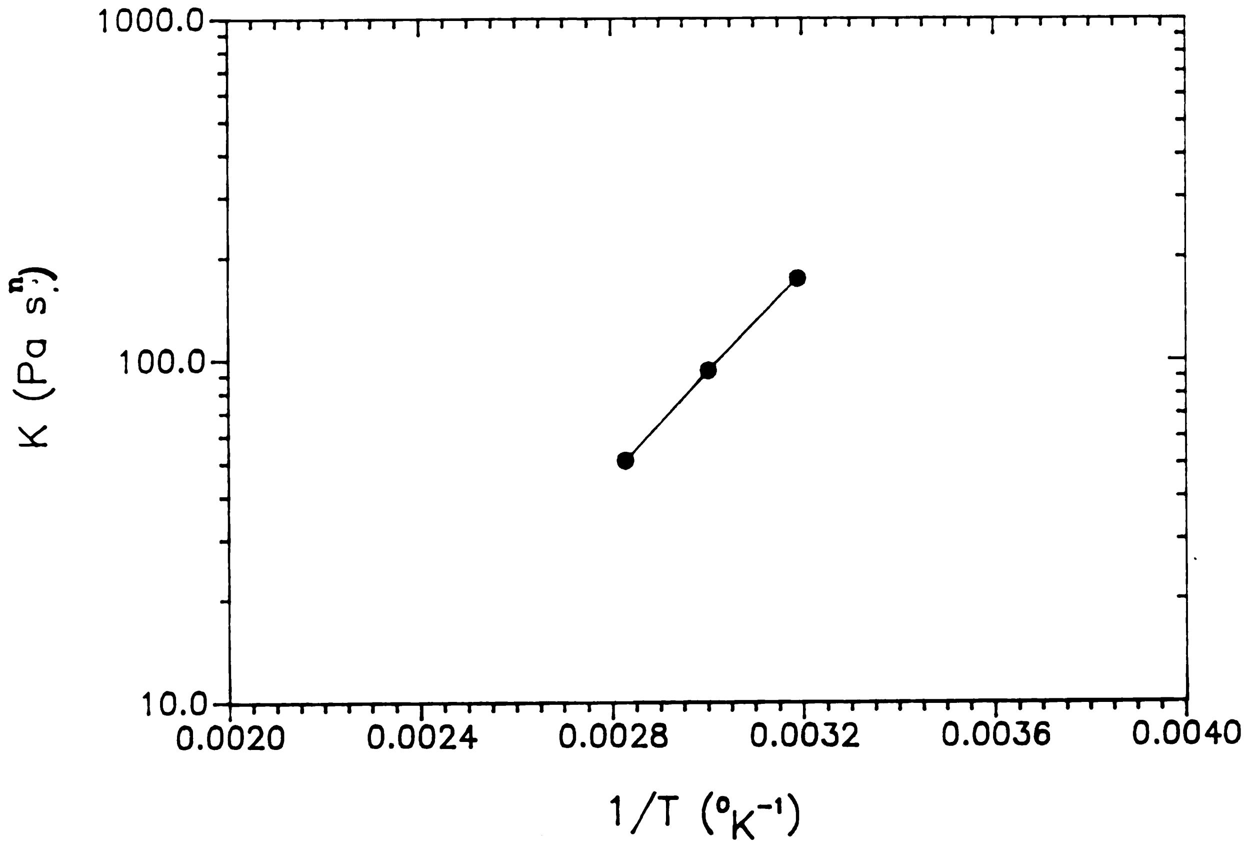

Figure 3.7 Consistency Coefficient Versus Inverse Temperature For a Mixture of 7% SPS and 93% Honey

an activation energy of 7904 cal/g mole.

3.7.2 Estimation Of The Average Shear Rate

As outlined in section 3.2, the power used for calculating the dimensionless power number is that used in shearing the material. The total power input to the extruder was calculated from the torque reading, using the manufacturer's correlation given by

$$P_w = 0.354(\%\ \text{torque})N \qquad (3\text{-}33)$$

where the screw speed (N) is in revolutions per second. Equations 3-11, 3-12 and 3-33 were used to calculate the power number. The Reynolds number was calculated by Eq. 3-13, with the viscosity evaluated at the average of the temperature of the product at the inlet and outlet of the extruder. Plots of power number versus Reynolds number for the three screw configurations are shown in Figure 3.8, using the Newtonian data.

In mixing systems, the plot of $\log(P_o)$ against $\log(Re)$ usually yields a slope close to one. For twin screw extruders, because there is conveying as well as mixing, the following general model is proposed for correlating the power number to the Reynolds number

$$P_o = \frac{\beta}{Re^{\lambda}} \qquad (3\text{-}34)$$

where β and λ are constants depending on the screw configuration.

To simplify the regression analysis, Eq. 3-34 was transformed to

$$\log(P_o) = \log(\beta) + \lambda \log(Re) \qquad (3\text{-}35)$$

The parameter β and λ were evaluated using linear regression. The results of the regression are shown in Table 3.7, and indicate an excellent fit. It is worth noting that the proportionality between P_o and Re shown here is the same as observed for mixers. However,the

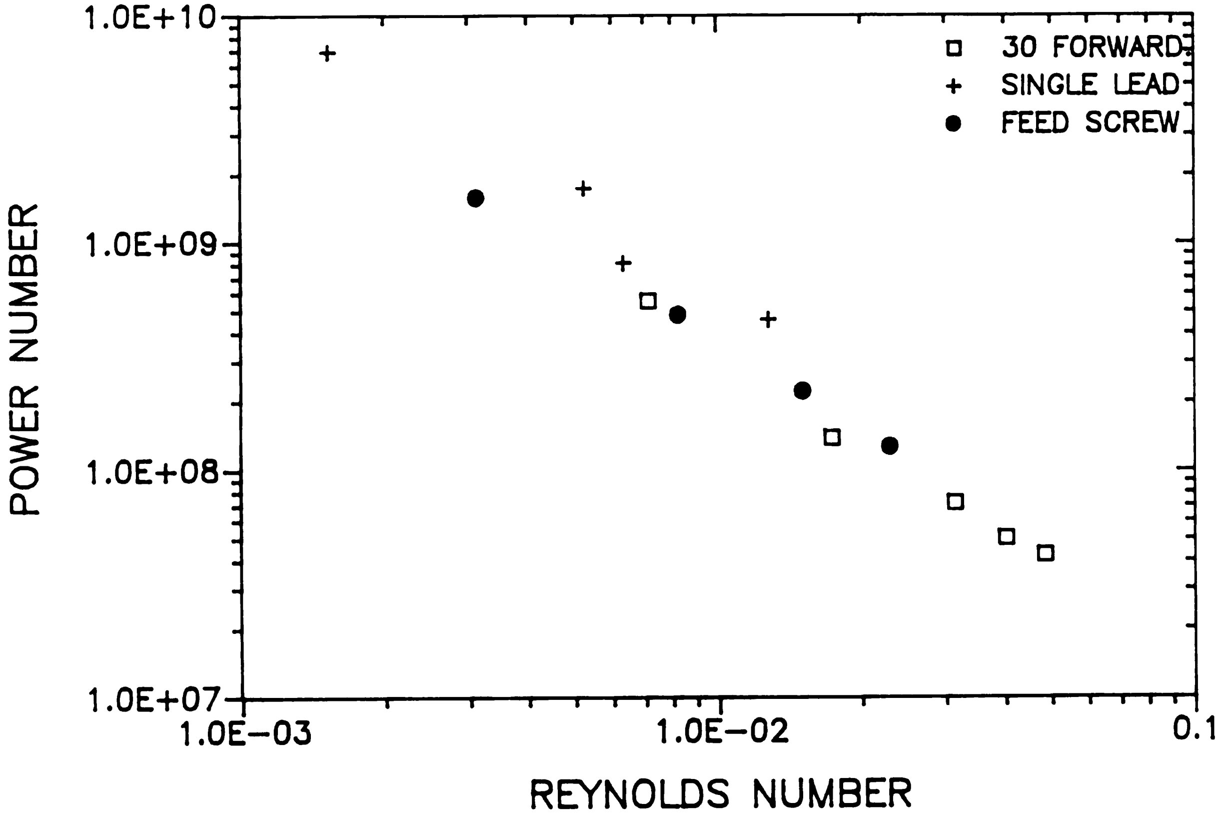

Figure 3.8 Power Number Versus Reynolds Number For The Newtonian Standard (Polybutene)

Table 3.7 Results of regression analysis of Eq. 3-35 for the three screw configurations

Screw	Log(β)	λ	R^2
Single lead	6.15054	-1.31	0.97
Feed screw	6.04225	-1.26	0.98
30 forward.	5.8389	-1.34	0.98

parameter λ is usually unity for mixers. The different value obtained here is most probably because the twin screw extruder provides pumping as well as mixing, as mentioned previously.

The power number was also calculated for the non-Newtonian case for each of the three screw configurations. As previously explained, the power number for the non-Newtonian material was based on the correlation developed for the Newtonian fluid. The calculated Reynolds number is used to calculate the equivalent effective viscosity for the non-Newtonian fluid by

$$\eta_a = \frac{\rho_n D_h^2 N}{Re^*} \tag{3-36}$$

where η_a = average apparent viscosity

ρ_n = density of the non-Newtonian fluid

and Re^* = the equivalent non-Newtonian Reynolds number

Then, using the viscosity correlation developed from the viscometer measurement with η replaced by η_a, an average shear rate can be found using

$$\dot{\gamma}_a = \left[\frac{\eta_a}{K_o \exp(\Delta E/RT_a)}\right]^{1/(n-1)} \tag{3-37}$$

where T_a is the average product temperature.

Table 3.8 shows the calculated values of the average shear rate for the three screw configurations. The average shear rate for the kneading discs is the highest, followed by the feed screw and single lead, as would be expected. There is no published data on the shear rate of twin screw extruders for comparison. Rossen and Miller (1973) published

Table 3.8 Average shear rates for three screw configurations

a) Single Lead Screws

Screw speed (RPM)	M (kg/s)	$\dot{\gamma}_a$ (s^{-1})
100	0.01497	23.4
150	0.02434	28.8
200	0.02268	33.0
300	0.02011	36.6
400	0.02676	42.5

b) Feed Screws

Screw speed (RPM)	M (kg/s)	$\dot{\gamma}_a$ (s^{-1})
100	0.02162	35.3
200	0.02374	56.1
250	0.04732	64.2
300	0.03084	67.8
400	0.03841	72.5

c) 30F Paddles

Screw speed (rps)	M (kg/s)	$\dot{\gamma}_a$ (s^{-1})
100	0.01889	53.3
150	0.00695	62.1
200	0.02419	79.8
300	0.03025	85.8
400	0.04641	99.1

shear rate data for various single screw extruders which appear to be of the same order of magnitude as those obtained in this work.

Eise et al. (1982) and Altomare and Ghossi (1986) indicated that for twin screw extruders, screw speed and throughput are the major variables that affect shear rate. Therefore, the following models are proposed for correlating the average shear rate of twin screw extruders

$$\dot{\gamma}_a = \alpha_1(N)^{\alpha 2} \tag{3-38}$$

$$\dot{\gamma}_a = \beta 1(N)^{\beta 2}(\dot{M})^{\beta 3} \tag{3-39}$$

where N is the screw speed (rev/sec), $\dot{M}$ is the throughput (kq/sec), and $\alpha 1$, $\alpha 2$, $\beta 1$, $\beta 2$ and $\beta 3$ are constants depending on the screw configuration.

Equations 3-38 and 3-39 are nonlinear. To simplify the parameter estimation procedure, the following transformation was made to convert it to a linear parameter estimation problem.

$$\log(\dot{\gamma}_a) = \log(\alpha 1) + \alpha 2 \log(N) \tag{3-40}$$

$$\log(\dot{\gamma}_a) = \log(\beta 1) + \beta 2 \log(N) + \beta 3 \log(\dot{M}) \tag{3-41}$$

A modified form of a computer program developed by Beck (1978) was used to estimate the parameters in Eqs. 3-40 and 3-41, using least squares based on the sequential parameter estimation method. The results of the regression analysis are presented in Tables 3-9 and 3-10 for single lead screws, Tables 3-11 and 3-12 for feed screws, and Tables 3-13 and 3-14 for 30F paddles. The results showed that both model 3-40 and 3-41 fit the data well for the three screw configurations, with slight differences in the error sum of squares. A student t-test was performed

Table 3.9 Regression results for fit of Eq. 3-40 for single lead screws

a) Regression Coefficients

Regression Coefficient	Estimated Regression coefficient	Estimated Standard Error	t^*
Log(β1)	1.287663	0.016165	79.657
β2	0.412928	0.028149	14.669

b) Analysis of Variance

Source of Error	Sum of Squares	Degree of Freedom	Mean Squares	F^*
SSR	0.038762	1	0.038762	
SSE	0.000543	3	0.000181	213.987
SST	0.039306			

Standard Error = 0.0134589 R^2 = 0.9862

Table 3.10 Regression results for fit of Eq. 3-41 for single lead screws

a) Regression Coefficients

Regression Coefficient	Estimated Regression coefficient	Estimated Standard Error	t^*
$\mathrm{Log}(\beta 1)$	1.539756	0.106028	14.522
$\beta 2$	0.373809	0.024806	15.069
$\beta 3$	0.138435	0.058023	2.385

b) Analysis of Variance

Source of Error	Sum of Squares	Degree of Freedom	Mean Squares	F^*
SSR	0.039143	2	0.019571	
SSE	0.000163	2	0.000082	239.905
SST	0.039306			

Standard Error = 0.0090306 $R^2 = 0.9958$

c) Test Of Hypothesis For $\beta 3$

H_o: $\beta 3 = 0.0$

H_a: $\beta 3 \neq 0.0$

For a level of significane of 0.05, t(.975,2) = 4.303

$t^* = 2.385 < t(.975,2) = 4.303$

Accept H_o and conclude that $\beta 3 = 0$

Table 3.11 Regression results for fit of Eq. 3-40 for feed screws

a) Regression Coefficients

Regression Coefficient	Estimated Regression coefficient	Estimated Standard Error	t^*
Log(β1)	1.447797	0.038416	37.687
β2	0.539190	0.062737	8.594

b) Analysis of Variance

Source of Error	Sum of Squares	Degree of Freedom	Mean Squares	F^*
SSR	0.060102	1	0.060102	
SSE	0.002457	3	0.000819	73.392
SST	0.062559			

Standard Error = 0.0286167 R^2 = 0.9607

Table 3.12 Regression results for fit of Eq. 3-41 for feed screws

a) Regression Coefficients

Regression Coefficient	Estimated Regression coefficient	Estimated Standard Error	t^*
Log($\beta 1$)	1.564318	0.289840	5.397
$\beta 2$	0.509700	0.102988	4.949
$\beta 3$	0.065966	0.162469	0.406

b) Analysis of Variance

Source of Error	Sum of Squares	Degree of Freedom	Mean Squares	F^*
SSR	0.060272	2	0.030136	
SSE	0.002287	2	0.001143	26.354
SST	0.062559			

Standard Error = 0.0338156 $R^2 = 0.9634$

c) Test Of Hypothesis For $\beta 3$

H_o: $\beta 3 = 0.0$

H_a: $\beta 3 \neq 0.0$

For a level of significane of 0.05, t(.975,2) = 4.303

$t^* = 0.406 < t(.975,2) = 4.303$

Accept H_o and conclude that $\beta 3 = 0$

Table 3.13 Regression results for fit of Eq. 3-40 for 30F paddles

a) Regression Coefficients

Regression Coefficient	Estimated Regression coefficient	Estimated Standard Error	t^*
Log(β1)	1.631419	0.029050	56.159
β2	0.448046	0.050584	8.521

b) Analysis of Variance

Source of Error	Sum of Squares	Degree of Freedom	Mean Squares	F^*
SSR	0.045636	1	0.045636	
SSE	0.001755	3	0.000585	78.0139
SST	0.047391			

Standard Error = 0.0241862 R^2 = 0.9630

Table 3.14 Regression results for fit of Eq. 3-41 for 30F paddles

a) Regression Coefficients

Regression Coefficient	Estimated Regression coefficient	Estimated Standard Error	t^*
$Log(\beta 1)$	1.709653	0.134859	12.677
$\beta 2$	0.413874	0.078972	5.255
$\beta 3$	0.035004	0.060955	0.596

b) Analysis of Variance

Source of Error	Sum of Squares	Degree of Freedom	Mean Squares	F^*
SSR	0.045894	2	0.022947	
SSE	0.001497	2	0.000748	30.658
SST	0.047391			

Standard Error = 0.0273581 $R^2 = 0.9684$

c) Test Of Hypothesis For $\beta 3$

H_o: $\beta 3 = 0.0$

H_a: $\beta 3 \neq 0.0$

For a level of significane of 0.05, t(.975,2) = 4.303

$t^* = 0.596 < t(.975,2) = 4.303$

Accept H_o and conclude that $\beta 3 = 0$

to to test for whether the addition of the flow rate term to model 3-38 has any significance, using the following test of hypothesis:

$$H_o: \beta 3 = 0$$

and $$H_a: \beta 3 \neq 0$$

H_o implies that flow rate has no effect on the average shear rate. For a level of significance of 0.05, we require t(0.975,2)=4.303, with the decision rule:

$$\text{if} \quad t^* \leq 4.303, \text{ conclude } H_o$$

$$\text{if} \quad t^* > 4.303, \text{ conclude } H_a$$

The results for all the screw configurations suggested that $\beta 3 = 0$ (Tables 3.10, 3.12 and 3.14). Thus we conclude that the flow rate term has no significance on the average shear rate. It is also clear from the regression results that the three-parameter model has a relatively higher standard error for the parameters in comparison with the two-parameters model. Thus, based on the test of hypothesis results and the principle of parsimoney which emphasize the use of the model with the smallest number of parameters for adequate representation (Box and Hunter, 1962), the two-parameter model will be more appropriate for this situation.

The prediction equations for single lead screws, feed screws and the 30F paddles are:

(single lead) $$\hat{\dot{\gamma}}_a = 19.3938\ N^{0.413} \qquad (3\text{-}42)$$

(Feed Screws) $$\hat{\dot{\gamma}}_a = 28.041\ N^{0.539} \qquad (3\text{-}43)$$

(30F Paddles) $$\hat{\dot{\gamma}}_a = 42.7976\ N^{0.448} \qquad (3\text{-}44)$$

Table (3.15) shows the residuals and percent error using Equations 3-41, 3-42 and 3-43. The maximum error obtained is 8% which indicates that the model is accurate . Also examination of the residuals indicates that none of the assumptions of additive, zero mean, constant variance, independent, and normal error appear to be violated. Therefore, the least squares method provides accurate estimation of the parameter in this case (Beck and Arnold, 1977).

This modelling technique provides a sound basis for twin screw extruders because it gives a weighted average value of the shear rate, and takes the shearing effect of the different zones of the extruder into consideration. It is worth noting that although the data are limited due to cost constraints, they were collected over a wide range of screw speeds (100 - 400 RPM), typical of what might be encounterd in industry. Also some of the data were checked and confirmed for reproducibility.

3.8 Conclusions

A procedure has been established for estimating the average shear rate for twin screw extruders. The average shear rate obtained in this analysis is a weighted average value, and takes into account the shearing effects from the different regions within the extruder. At a given screw speed, the 30 forwarding paddles generate the highest shear rate followed by feed screws and single lead screws.

The average shear rate correlates well with screw speed. There is no data available in the literature to provide comparison with this

Table 3.15 Comparison Between Observed and Predicted average Shear Shear Rates For Three Screw Configurations

a) Single Lead Screws

N (RPM)	Observed $\dot{\gamma}_a$ (1/s)	Predicted $\hat{\dot{\gamma}}_a$ (1/s)	Residuals $\dot{\gamma}_a - \hat{\dot{\gamma}}_a$ (1/s)	% Error
100	23.4	23.9	-0.5	-2.14
150	28.8	28.3	+0.5	+1.74
200	33.0	31.9	+1.1	+3.33
300	36.6	37.7	-1.1	-3.01
400	42.5	42.4	+0.1	+0.23

b) Feed Screws

N	Observed	Predicted	Residuals	% Error
100	35.3	36.9	-1.6	-4.53
200	56.1	53.7	+2.4	+4.27
250	64.2	60.5	+3.7	+5.76
300	67.8	66.8	+1.0	+1.47
400	72.5	78.0	-5.5	-7.58

c) 30F Paddles

N	Observed	Predicted	Residuals	% Error
100	53.3	53.8	-0.5	-0.94
150	62.1	64.5	+2.4	+3.86
200	79.8	73.4	+6.4	+8.02
300	85.8	88.0	-2.2	-2.56
400	99.1	100.1	-1.0	-1.01

work. However, the model may be incorporated in a predictive model for the temperature profile to test its validity.

3.9 Nomenclature

A_{bc} barrel cross-sectional area, cm^2

A_{bs} barrel surface area, cm^2

A_f screw flange area, cm^2

A_r screw root area, cm^2

A_s screw surface area, cm^2

A_{ns} kneading disc side area, cm^2

A_t screw tip area, cm^2

A_w wetted area, cm^2

B feed screw channel perimeter, cm

D barrel diameter, mm

D_h hydraulic diameter, cm

e screw tip width, mm

E screw channel bottom width, mm

E_v viscous dissipation of mechanical energy, W

$\hat{E}_v$ viscous dissipation of mechanical energy per mass flow rate, W/(kg/s)

E_{v1} viscous dissipation of mechanical energy to c.v. #1 (Fig. 3.1), W

E_{v2} viscous dissipation of mechanical energy to c.v. #2 (Fig. 3.1), W

F^* calculated F-statistic (MSR/MSE), dimensionless

H channel depth, mm

k consistency coefficient, Pa-s^n

k_o reference consistency coefficient, Pa s^n

L barrel length, m

MSE mean squares due to error

MSR mean squares due to regression

n flow behavior index, dimensionless

P_o power number, dimensionless

P_o^* power number of non-Newtonian fluid, dimensionless

P_{bp} barrel perimeter, cm

P_w total power input to extruder (shaft work), W

$\hat{P}_w$ total power input to extruder per mass flow rate, W/(kg/s)

P_{w1} power input to control volume #1 (Fig. 3.1), W

P_{w2} power input to control volume #2 (Fig. 3.1), W

Q_d drag flow rate, m^3/hr

Q_n net flow rate, m^3/hr

Q_p pressure flow rate, m^3/hr

R gas constant, cal/(gm-mole^{o}K)

Re Reynolds number

Re^{*} equivalent Reynolds number for a non-Newtonian fluid

SSE sum of squares due to error

SSR sum of squares due to regression

SST total sum of squares

t^{*} calculated t-value (est. param./ std. error of the para.)

T temperature, ^{o}C

T_o reference temperature, ^{o}C

V_b barrel volume, cm^3

V_s screw volume, cm^3

V_w wetted volume, cm^3

Z_t length along the screw helix at the tip, cm

Z_r length along the screw helix at the root, cm

Greek Sympols

$\alpha 1$ constant (Eq. 3-38)

$\alpha 2$ constant (Eq. 3-38)

β constant (Eq. 3-34)

β_1 constant (Eq. 3-39)

β_2 constant (Eq. 3-39)

β_3 constant (Eq. 3-39)

ΔE activation energy, cal/(g mole)

ΔP pressure drop, Pa

ρ Newtonian fluid density, 900 kg/(m^3)

ρ_n non-Newtonian fluid density, 1230 kg/(m^3)

μ Newtonian viscosity, Pa s

μ_o Newtonian reference viscosity, Pa s

η non-Newtonian apparent viscosity, Pa s

η_a average non-Newtonian apparent viscosity, Pa s

$\dot{\gamma}$ shear rate, s^{-1}

$\dot{\gamma}_a$ average shear rate, s^{-1}

τ shear stress, Pa

λ constant (Eq. 3-34)

ψ angle shown in Figure 3.1

ϕ helix angle

3.10 Literature Cited

Altomare, E. and Ghossi, P. 1986. Analysis Of Residence Time Distribution Pattern in a Twin Screw Cooking Extruder. Biotech. Progr. 2(3):157-163

Beck, J. V. 1987. Nonlinbg, unpublished computer Program, Michigan State Unviversity

Beck, J. V. and Arnold, K. J. 1977. Parameter Estimation in Engineering and Science. John Wiley and Sons, New York.

Box, G.E.P. and Hunter, W.G. 1962. A Useful Method For Model-Building. Technometrics. 4:301-318

Eise, K., Herrmann, H., Jakopin, S., and Burkhardt, U. 1981. An Analysis of Twin-Screw Extruder Mechanisms. Advances In Plastic Technology. 2(1):18-39

Harper, J. M. 1981. Extrusion of Food. Vol. 1. CRC Press Boca Raton, Fl

Harper, J. M. 1985. Processing Characteristics of Food Extruders. Food Engineering and Process Application. Vol. 2. Unit Operation Eds. Lemanguer, M. and Jelen, P.

Martelli, F. G. 1971. Twin-Screw Extruders - A Separate Breed. SPE. J. 27(1)P:25-30

Martelli, F. G. 1983. Twin screw Extruders: A Basic Understanding. Van Nostrand Reinhold Compance. New York

Meijer, H. E. H. and Eleman, P. H. M. 1988. The Modelling of a Continuous Mixer. Part 1: The Co-Rotating Twin-Screw Extruder. Polym. Eng. and Sci. 28(5):275-290

Metzner, A. B., and Otto, R. E. 1957. Agitation of Non-Newtonian Fluids. AIChE. J. 3(1):3-10

Rao, M. A. and Cooley, H. J. 1984. Determination Of Effective Shear Rates in Rotating Viscometers With Complex Geometry. J. Texture Studies. 15:327-335

Rieger, F. and Novak, V. 1973. Power Consumption Of Agitators in Highly Viscous Non-Newtonian Liquids. Trans. Inst. Chem. Engrs. 51:105-111

Rossen, J. L. and Miller, R. C. 1973. Food Extrusion. Food Technol. 27:46-53

Yacu, W. 1985. Modelling a Twin Screw Co-Rotating Extruder. J. Food Proc. Eng. 8:1-21

CHAPTER 4

MODELLING THE AVERAGE HEAT TRANSFER COEFFICIENT IN A TWIN SCREW CO-ROTATING EXTRUDER

4.1 Abstract

A numerical and experimental procedure has been developed to estimate the average heat transfer coefficient for twin screw extruders. The procedure is based on the one-dimensional heat transfer equation for a non-Newtonian food dough. The estimated heat transfer coefficient correlates well with the Brinkman and Graetz numbers. The model will be useful in modelling heat transfer in twin screw extruders.

4.2 Introduction

The majority of published studies on modelling of twin screw extruders are based on the simplified assumptions of Newtonian fluids and isothermal flow (Wyman, 1975; Denson and Hwang, 1980; Booy, 1980). However, most extruded materials, whether foods or polymers, are non-Newtonian. In addition, they usually either require heating through the barrel in order to achieve certain processing requirements, or rely entirely on viscous dissipation of mechanical energy to provide heat energy. This generates a significant temperature profile, making the isothermal approximation unrealistic for extrusion modelling. With the exception of Yacu (1985), who reported a single value of 500 W/(m^2-^oC) for the heat transfer coefficient, no published literature has addressed the problem of heat transfer in the non-Newtonian non-isothermal flow of foods in a co-rotating twin screw extruder.

An understanding of the heat transfer during the cooking extrusion process is of paramount industrial importance, because it enables proper control over the performance of the extruder, and the optimization of the process. One of the missing links in modelling heat transfer is the lack of published data on heat transfer coefficients in twin screw extruders. Knowledge of the heat transfer coefficient in food extrusion is important for scale-up and for design of extruder temperature control systems (Levine and Rockwood, 1986).

The main objectives of this study are:

(1) To develop a procedure for estimating the average heat transfer coefficient for twin screw extruders.

(2) To correlate the average heat transfer coefficient to the rheological properties of the fluid, extruder geometry, and operating conditions.

4.2 Rheological Model

Rheological properties are important for extrusion process design, control and scale up. However, most foods undergo physiochemical changes during extrusion cooking due to starch gelatinization and protein denaturation which complicate the development of models for cooking extruders. Therefore, the availability of rheological models that take these changes into consideration is a fundamental requirement for successful extrusion process modelling.

Most shear stress shear rate data for extruded materials appear to fit the power law model (Harper et al., 1971; Chen et al., 1978; Remsen and Clark, 1978; Jao et al. 1978; Cervone and Harper, 1978; Levine, 1982), expressed as

$$\tau = K\dot{\gamma}^{n} \tag{4-1}$$

where, τ is the shear stress, n is the flow behavior index, K is the consistency coefficient and $\dot{\gamma}$ is the shear rate. For this analysis, the power law model was chosen because of simplicity and adequacy in fitting most shear stress versus shear rate data. When temperature effects are incorporated, the power law viscosity can be written as:

$$\eta = K_{o}\dot{\gamma}^{(n-1)}\exp[(\Delta E/R)(1/T - 1/\ T_{o})] \tag{4-2}$$

4.4 Model Development

4.4.1 Provisions of the model

The primary emphasis in this analysis is the estimation of an average heat transfer coefficient for twin screw extruders. The approach adopted is a combination of numerical and experimental techniques. The estimation of the average heat transfer coefficients follows the solution of the one-dimensional energy equation for the average heat flux. The temperature profile along the barrel was determined experimentally, and incorporated into the energy equation to solve for the average heat flux.

The energy equation was developed for the filled zone only, using a non-Newtonian non-isothermal viscosity model. The effect of viscous dissipation is included in the model.

4.4.2 Assumptions

The following assumptions were made in the development of the model:

(1) Steady state

(2) Incompressible dough

(3) Constant thermal properties (specific heat and thermal conductivity)

(4) Viscous forces are dominant compared to inertial and gravity forces

(5) Viscosity is independent of strain and time temperature history

(6) The temperature is uniform in the direction perpendicular to the screw shafts

(7) Negligible heat losses from screw shafts.

4.5 The Energy Equation

One of the main assumptions of this model is negligible temperature variation in the direction perpendicular to the screw shafts, which implies the temperature variation is only in the axial direction. This assumption is based on the fact that co-rotating twin screw extruders maintain a good degree of mixing (Eise et al. 1982; Martelli, 1983; Harper, 1985 and Yacu, 1985). Furthermore, the energy equation is developed for a configuration made up of kneading discs only, to assure a significant level of mixing (Harper, 1986).

The macroscopic mechanical energy balance for the control volume gives

$$\hat{P}_w = \hat{E}_v + \Delta p/\rho \qquad (4\text{-}3)$$

where $\hat{E}_v$ is the rate of viscous dissipation of mechanical energy, Δp is the pressure drop and ρ is the fluid density.

By the first law of Thermodynamics,

$$\hat{\Delta H} = \hat{Q}_h + \hat{P}_w \tag{4-4}$$

where $\hat{\Delta H}$, $\hat{Q}_h$ and $\hat{P}_w$ are enthalpy, heat transfer at the boundary of the control volume and power input to the control volume, respectively. The enthalpy of an incompressible fluid can be expressed as

$$\hat{\Delta H} = C_p \Delta T + \Delta p/\rho \tag{4-5}$$

where C_p is the specific heat, and ΔT is the change in product temperature between the inlet and outlet of the control volume.

Substituting Eqs. 4-3 and 4-5 into Eq. 4-4 gives

$$C_p \Delta T = \hat{E}_v + \hat{Q}_h \tag{4-6}$$

Multiplying Eq. 4-6 by the mass flow rate yields

$$MC_p \Delta T = E_v + Q_h \tag{4-7}$$

in a twin screw extruder the viscous dissipation per unit volume ($\overset{*}{E}_v$) can be approximated by

$$\overset{*}{E}_v = \eta_a \dot{\gamma}_a{}^2 \tag{4-8}$$

The heat transfer from the control volume bounded by x and ($x+\Delta x$) (Figure 4.1) is

$$Q_h = q[2D(\pi - \psi)]\Delta x \tag{4-9}$$

In Eqs. 4-8 and 4-9 η_a and $\dot{\gamma}_a$ are, respectively, the average apparent viscosity and the average shear rate, q is the heat flux, D is the extruder diameter and ψ has the same definition as in chapter 3.

Substituting Eqs. 4-8 and 4-9 into Eq. 4-7 yields

$$MC_p \Delta T = q[2D(\pi - \psi)\Delta x + A_1 \eta_a \dot{\gamma}_a{}^2 \Delta x \tag{4-10}$$

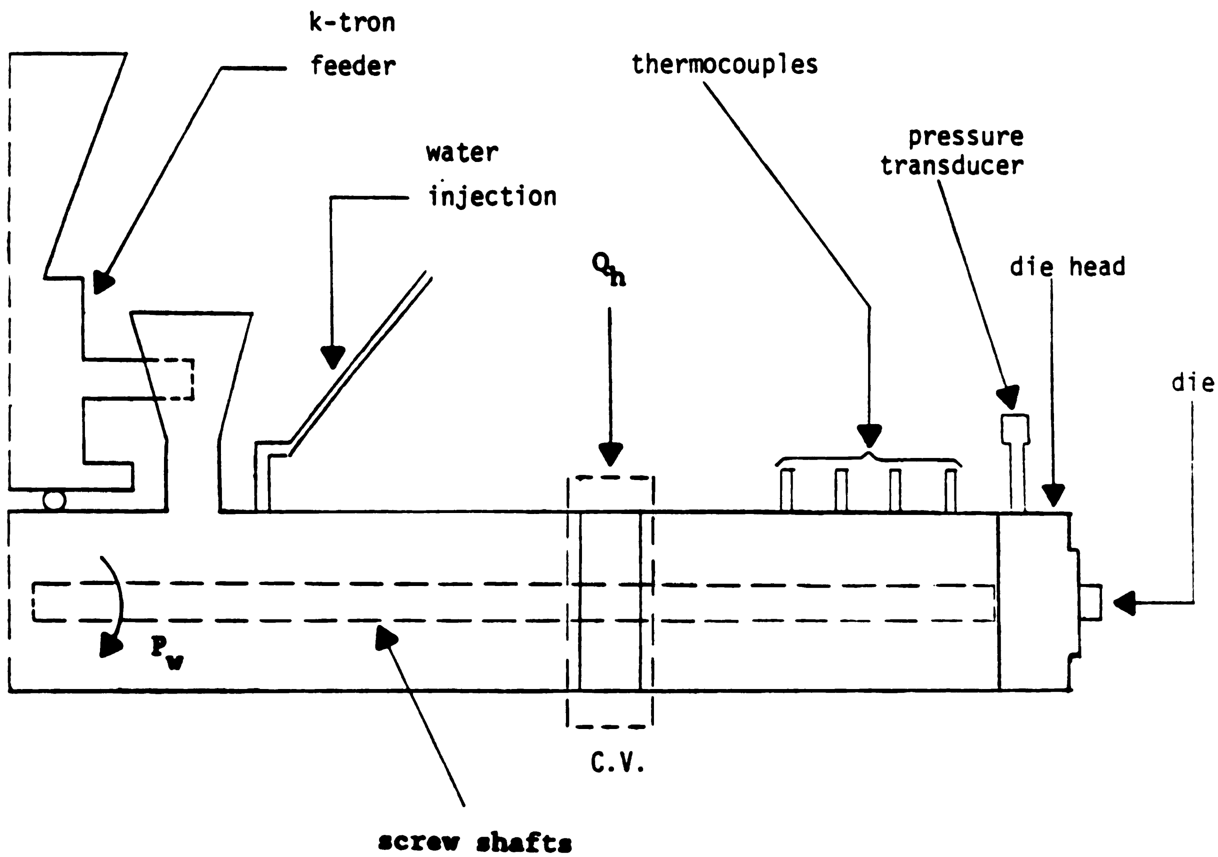

Figure 4.1 Schematic of The Extruder Showing Control Volume Used in Developing The Energy Equation

Dividing Eq. 4-10 by Δx, and taking the limit as Δx approches zero,

$$MC_p \frac{dT}{dx} = q[2D(\pi - \psi)] + A_i \eta_a \dot{\gamma}_a^2 \qquad (4\text{-}11)$$

where A_i is the available flow area. Substituting Eq. 4-2 into Eq. 4-11 with η replaced by η_a and $\dot{\gamma}$ by $\dot{\gamma}_a$ yields

$$MC_p \frac{dT}{dx} = q[2D(\pi - \psi)] + A_i K_o \dot{\gamma}_a^{(n+1)} \exp[(\Delta E/R)(1/T - 1/T_o)] \qquad (4\text{-}12)$$

To make Eq. 4-12 dimensionless, define

$$\theta = \frac{T - T_o}{T_w - T_o} \qquad \chi = x/L \qquad (4\text{-}13)$$

where T_o and T_w are the reference temperature and barrel temperature, respectively, and L is a characteristic length (filled length in this study). Incorporating the dimensionless terms into equation 4-12 yields

$$MC_p \frac{(T_w - T_o)}{L} \frac{d\theta}{d\chi} = 2qD(\pi - \psi) + A_i K_o \dot{\gamma}_a^{(n+1)} \exp[\frac{-\Delta E}{RT_o}] \exp[\frac{\Delta E}{R(\theta(T_w - T_o)+T_o)}]$$

------------------ (4-14)

Dividing Eq. 4-14 by $k(T_w - T_o)$ gives

$$\frac{MC_p}{kL} \frac{d\theta}{d\chi} = \frac{q2D(\pi - \psi)}{k(T_w - T_o)} + \frac{A_i K_o \dot{\gamma}_a^{(n+1)}}{k(T_w - T_o)} \exp[\frac{-\Delta E}{RT_o}] \exp[\frac{\Delta E}{R(\theta(T_w - T_o)+T_o)}] \qquad (4\text{-}15)$$

where k is the thermal conductivity. Multiplying and dividing the last term of equation 4-15 by L^2 yields

$$Gz \frac{d\theta}{d\chi} = \overset{*}{q} - Br \frac{A_i}{L^2} \exp[\frac{\Delta E}{R(\theta(T_w - T_o) + T_o)}] \qquad (4\text{-}16)$$

where $$Gz = \frac{MC_p}{kL} \qquad \text{(Graetz number)} \qquad (4\text{-}17)$$

$$Br = \frac{K_o L^2 \dot{\gamma}_e^{(n+1)}}{k(T_o - T_w)} \exp[\frac{-\Delta E}{RT_o}] \quad \text{(Brinkman number)} \tag{4-18}$$

and $$\overset{*}{q} = \frac{2D(\pi - \psi)q}{k(T_w - T_o)} \quad \text{(dimensionless heat flux)} \tag{4-19}$$

Eq. 4-16 can be rearranged to solve for the heat flux:

$$\overset{*}{q} = Gz\frac{d\theta}{d\chi} + Br\frac{A_1}{L^2} \exp[\frac{\Delta E}{R(\theta(T_w - T_o) + T_o)}] \tag{4-20}$$

The average dimensionless heat flux can be defined as

$$\bar{\overset{*}{q}} = \int_0^1 \overset{*}{q} \, d\chi \tag{4-21}$$

To solve for the average dimensionless heat flux, integrate Eq. 4-20 to obtain

$$\bar{\overset{*}{q}} = Gz \int_0^1 (\frac{d\theta}{d\chi}) \, d\chi + \frac{A_1}{L^2} Br \int_0^1 \exp[\frac{\Delta E}{R(\theta(T_w - T_o) + T_o)}] \, d\chi \tag{4-22}$$

which may be simplified to give

$$\bar{\overset{*}{q}} = Gz\theta \begin{matrix} 1 \\ 0 \end{matrix} + \frac{A_1}{L^2} Br \int_0^1 \exp[\frac{\Delta E}{R(\theta(T_w - T_o) + T_o)}] \, d\chi \tag{4-23}$$

To complete the solution of equation 4-23, the temperature profile must be known. This can be found from an experimental measurement of the temperature at different points along the barrel. A regression of the data can then be used to establish a correlation between temperature and position.

Having obtained the average dimensionless heat flux, the average heat flux ($\bar{q}$) can be obtained from

$$\bar{q} = \frac{\bar{\overset{*}{q}} \, k(T_w - T_o)}{2D(\pi - \psi)} \tag{4-24}$$

The average heat flux can also be calculated from

$$\bar{q} = \bar{h}\ (\bar{T} - T_w) \tag{4-25}$$

where, $\bar{h}$ is the average heat transfer coefficient, and $\bar{T}$ is the average temperature, defined as:

$$\bar{T} = \frac{1}{L} \int_0^L T(x)dx \tag{4-26}$$

The average heat transfer coefficient can therefore be estimated from

$$\bar{h} = \frac{\bar{q}}{(\bar{T} - T_w)} \tag{4-27}$$

4.6 Materials and Methods

Soy polysaccharide (SPS) obtained from Raltson Purina (St. Louis, Mo) was chosen as the test material because it consists mainly of soy fiber which is a relatively inert material. A moisture content of 70 % (wet basis) was used for all extrusion runs. The dough was prepared inside the extruder by mixing SPS flour with injected water.

A Baker Perkins (MPF-50D) twin screw co-rotating extruder was used for this work, with 15 L/D of kneading discs (staggered at 30 degree forwarding). A pair of three-hole dies (length = 2.58 cm and diameter = 0.3175 cm) were mounted on a twin-hole die head. Thermocouples with probes that penetrate the product were installed on all available ports on the barrel and were connected to a data acquisition system (model PCA-96 Sc-Pd-Rs) and an IBM PC computer to facilitate product temperature measurements. Product temperatures from all thermocouples were displayed continuously on the computer screen.

The flour was metered by a K-tron feeder (K-tron Corporation) with adjustable auger speed. Water was injected at the first port next to the feeding port by a Bran and Lubbe injection pump (type N-P33). The control of all extruder operations except water injection rates were done from a control panel which also displayed readings of torque, barrel temperature, product temperature, feed rate, die pressure and screw speed.

Before each extrusion run, the feeder and the water injection pump were calibrated to determine the appropriate feeder and pump settings that give the desired moisture content for the different flow rates. The heat exchanger unit was turned on to circulate water and help maintain a uniform barrel temperature. Three levels of throughput were used (31, 45 and 60 kg/hr). For each throughput, three screw speeds were used, ranging from 150 to 450 RPM.

During the extrusion run, product temperature, die pressure and torque readings were monitored. When the readings were stable, steady state conditions were assumed, and the product temperature, barrel temperature, torque reading and die pressure were recorded. Also, product temperatures at the screw tip (just before the die) were measured by inserting a thermocouple with a long probe through the die hole. The flow rate was determined by measuring extrudate weight for a known period of time. For each extrusion run, the extruder was "dead-stopped" and the barrel dismantled within 2 to 5 minutes to determine the length of the filled section.

4.7 Results and Discussion

4.7.1 Thermal and Rheological Properties of Soy Polysaccharide

As discussed previously, thermal properties (specific heat and thermal conductivity) as well as rheological properties are required to obtain the average heat transfer coefficient. Thermal conductivity was estimated from Andersen's (1950) empirical correlation

$$k = k_w MC + (1\text{-}MC)ks \qquad (4\text{-}28)$$

where k_w is the thermal conductivity of water at 20 °C (0.597 W/(M-K)) and k_s is the thermal conductivity of the solid, which was assumed to be 0.259 W/(M-K). As illustrated by Mohsenin (1980), Eq. 4-28 is more accurate at high moisture contents, which is the case for the SPS used in this analysis (70 % MC). Ordinanz (1946) reported specific heats of 1.883 to 2.176 KJ/(Kg-K) for doughs in the temperature range of 0 - 100 °C. For this analysis, a value in the middle of the range was chosen (2.05 KJ/(Kg-K)) .

Howkins (1987) and Vega (1988) measured the rheological properties of SPS at different temperature and moisture contents using a capillary rheometer. They found that the power law model fit the experimental data adequately. Howkins (1987) estimated an activation energy of 4520 (cal/g-mole) which appears to be within the range reported by Harper (1981) for food materials. The power law model of SPS at 70% moisture content and 20 °C was estimated by Vega (1988) as

$$\tau = 6700\ \dot{\gamma}^{\,0.25} \qquad (4\text{-}29)$$

in this study equation 4-29 along with Howkin's (1987) activation energy was used, since moisture content does not significantly affect the activation energy (Remsen and Clark, 1978).

4.7.2 Temperature Profile

Experimental measurements of temperture were used to establish a correlation between temperature and position for the filled zone. Figure 4.2 shows the locations of the thermocouples over the filled length, since the interest in this analysis is on the filled zone. Measurements of the filled zone showed that the filled length varies from 24 to 30 cm. Therefore, a filled length of 23.495 (cm) was chosen as the reference for all calculations, to guarantee that all thermocouples within this length are actually in the filled zone.

Two models were considered for correlating the data:

$$T(\chi) = \alpha_1 + \alpha_2 \chi \qquad (4\text{-}30)$$

$$T(\chi) = \alpha_{11} + \alpha_{22}\chi + \alpha_{33}\chi^2 \qquad (4\text{-}31)$$

It was found from the regression analysis that Eq. 4-31 fit the data slightly better than Eq. 4-30 with regard to R^2. Nevertheless, model (4-30) was chosen because it provides an acceptable fit of the data, and has fewer parameters (Table 4.1)

4.7.3 Estimation of The Average Heat Transfer Coefficient

The average heat transfer coefficients were obtained from solution of the energy equation for the average heat flux. However, the solution of the energy equation requires knowledge of the temperature distribution in the axial direction. The temperature distribution was obtained from experimental measurements of the temperature along the extruder and correlation of the temperatures with position.

The mathematical development of the energy equation was given in section (4.4). The solution for the average heat flux starts by

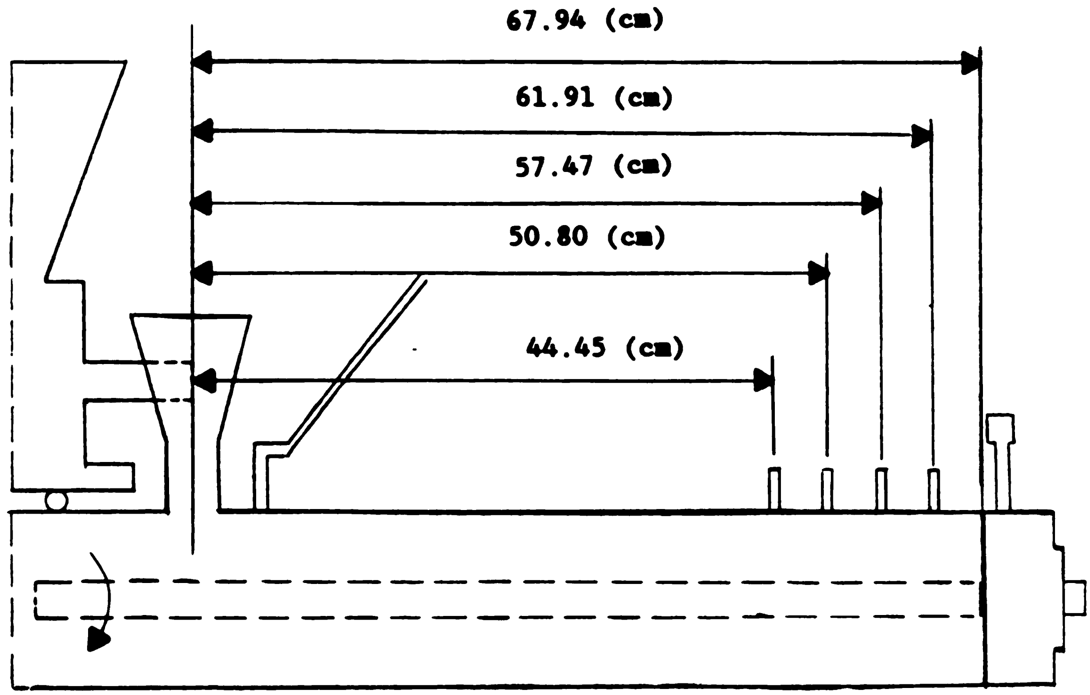

Figure 4.2 Locations of Thermocouples in The Filled Zone of The Extruder

Table 4.1 Regression results for fit of Eq. 4-30

Screw speed (RPM)	M (Kg/hr)	α_1	α_2	R^2
150	33	22.43216	34.76811	0.97
350	33	22.46774	43.66993	0.98
350	46	26.11963	36.24580	0.97
250	46	26.91004	27.43104	0.95
450	46	23.50323	47.98553	0.99
250	60	25.10903	28.94809	0.90
350	60	26.49018	35.36839	0.93
450	60	25.79449	41.02305	0.97

evaluating the Graetz and Brinkman numbers, the ratio of the heat transfer by convection to that by conduction in the axial direction, and the ratio of viscous heat dissipation to heat transferd through the barrel, respectively. The shear rate in the Brinkman number was evaluated using equation 3-44. The flow area (A_i) was estimated as explained in the previous chapter (A_i= 15.976 cm^2). The filled length (L) was 23.495 (cm).

A computer program was written to solve for the average heat transfer coefficient, using Eqs. 4-22 to 4-27. Simpson's rule was used to evaluate the integral in equation 4-22, using the parameters given in Table 4.1 and solving for the average heat transfer coefficients. A summary of the results is given in Table 4.2. It is important to point out that the values of the average heat transfer coefficients obtained are for a wide range of operating conditions, including screw speeds from 250 to 450 RPM, which is typical of the operating range in the industry and throughputs of 33 to 60 kg/hr. These ranges are both typical of the operating ranges of many industrial applications.

The average heat transfer coefficient varies from 191 to 768 W/(m^2-^oC). Lack of published data on the heat transfer coefficient for twin screw extruders makes it difficult to make a comparison. The only data found in the literature for twin screw co-rotating extruders was given by Yacu (1985), where a single value of 500 W/(m^2-^oC) was reported for the filled zone. No explanation was provided on how this value was obtained. Yacu's (1985) data is, however, within the range of values obtained in this work. Recently, Levine and Rockwood (1986) reported

Table 4.2 Calculated values of the average heat transfer coefficients

N (RPM)	$\dot{M}$ (Kg/hr)	Gz	Br	$\bar{h}$ (W/m^2- ^{o}C)
250	33	161.18	4.4975	191
350	33	161.18	6.3324	274
350	46	228.19	6.6684	416
250	46	228.19	5.4272	313
450	46	228.19	9.9438	656
250	60	294.10	4.9961	560
350	60	294.10	7.1713	669
450	60	294.10	9.1158	768

data for single screw extruders in the range 170 - 420 $W/(m^2\text{-}^oC)$, and Mohamed et al. (1988) reported data for single screw extruders in the range 136 - 420 $W/(m^2\text{-}^oC)$. Both data appear to be within the range of the twin screw extruder. The higher values obtained for the twin screw extruder are most likely due to its excellent mixing attributes which enhance heat transfer.

The data in Table 4.2 shows that the average heat transfer coefficient increases with increasing Brinkman and Graetz numbers, which suggests that these may be used as the primary variables in modelling the average heat transfer coefficient. An examination of Equ. 4-16 leads to a similar conclusion. Therefore, the following model is proposed for correlating the average heat transfer coefficient:

$$\bar{h} = \beta_1 Gz^{\beta_2} Br^{\beta_3} \tag{4-32}$$

where β_1, β_2 and β_3 are constants. Equation 4-32 was linearized by a logarithmic transformation.

$$\log(\bar{h}) = \log(\beta_1) + \beta_2 \log(Gz) + \beta_3 \log(Br) \tag{4-33}$$

The parameters in Eq. 4-33 were estimated using least square analysis, based on the sequential parameter estimation method (Beck and Arnold, 1977). The results of the regression analysis are summarized in Table 4.3. To test for whether the proposed model is adequate for fitting the data, the following hypothesis was tested:

$$H_o: \beta_1 = 0.0,\ \beta_2 = 0.0 \text{ and } \beta_3 = 0.0$$

$$H_a: \beta_1 \neq 0.0,\ \beta_2 \neq 0.0 \text{ and } \beta_3 \neq 0.0$$

The F test was used. From Table 4.3 the statistic F^* is 71.881, using a

Table 4.3 Regression results for fit of Eq. 4-33

a) Regression Coefficients

Regression Coefficient	Estimated Regression coefficient	Estimated Standard Error	t^*
$Log(\beta_1)$	-1.375760	0.374183	3.676
β_2	1.405937	0.170438	8.414
β_3	0.850644	0.157130	5.248

b) Analysis of Variance

Source of Error	Sum of Squares	Degree of Freedom	Mean Squares	F^*
SSR	0.317591	2	0.158795	
SSE	0.011046	5	0.002209	71.881
SST	0.328637			

Standard Error = 0.0470013 R^2 = 0.9664

level of significance of 0.05, we require $F(.95;2,5) = 5.79$. The decision rule is:

$$\text{If } F^* \le 5.79, \text{ conclude } H_o$$

$$\text{If } F^* > 5.79, \text{ conclude } H_a$$

Since $F^* > 5.79$, we conclude H_a, which implies that all the parameters of the model are important. For further confirmation of the F test conclusion, a student t test was also used with the following alternatives:

$$H_o: \beta_i = 0.0 \qquad i = 1,2,3$$

$$H_a: \beta_i \neq 0.0 \qquad i = 1,2,3$$

At a level of significance of 0.05, $t(.975;5) = 2.57$. From Table (4.3) $t_i^* > t(.975;5) = 2.57$ for all the parameters, therefore we accept H_a and conclude that none of the parameters is zero, which is the same conclusion reached by the F-test. Neter et al. (1985) indicated that for multiple regression when there is multicollinearity between the independent variables the F-test and the student t-test might lead to contradictory conclusion, which is not the case with this model. Therefore, the model is adequate for correlating the data. Furthermore, the coefficent of determination (R^2) is 0.966 which is considered to be good. The prediction equation can be written as

$$\hat{h} = 0.0421\ Gz^{1.406} Br^{0.851} \qquad (4\text{-}34)$$

Table 4.4 shows that the maximum percent error in predicting the

Table 4.4 Comparison between observed and predicted heat transfer coefficients

observed ($\bar{h}$) (W/(m^2 ^{o}C)	predicted ($\hat{h}$) W/(m^2 ^{o}C)	Residual W/(m^2 ^{o}C)	% Error
191	192	- 1	- 0.52
274	257	+17	+ 6.29
416	438	-22	- 5.29
313	367	-54	-17.25
656	615	+41	+ 6.25
560	489	+71	+12.68
669	665	+ 4	+ 0.59
768	816	-48	- 6.25

average heat transfer coefficent using Eq. 4-34 is 17%, which is reasonable. Examination of the residuals in Table 4.4 indicates that none of the assumptions of additive, zero mean, constant variance, uncorrelated and normal errors appear to have been violated. Therefore, the least square method provides an accurate parameter estimation in this case (Beck and Arnold, 1977). Eq. 4-34 can be written in a more convenient form by using the Nusselt number:

$$\bar{Nu} = 0.0042\ Gz^{1.406} Br^{0.851} \qquad (4\text{-}35)$$

where

$$\bar{Nu} = hD/k \qquad (4\text{-}36)$$

$\bar{Nu}$ is the average Nusselt number, D is the extruder diameter and k is the thermal conductivity

4.8 Conclusions

A model for estimating the average heat transfer coefficient has been developed, based on the one-dimensional energy equation, with the aid of experimentally determined temperature profiles. The model uses experimental data collected for 30 degree forwarding kneading discs to ensure complete mixing and hence assure the assumption of uniform temperature in the direction perpendicular to the screw shafts

The estimated average heat transfer coefficient correlates satisfactorily with the Brinkman and Graetz numbers ($R^2 = 0.966$). Due to lack of published data on twin screw extruders no comparisons could be made with the results of this study. The only data found in the literature was a single value from Yacu (1985). However, this data appears to be within the range of the results obtained in this study.

4.9 Nomenclature

A_i available area for flow, m^2

Br Brinkman number, dimensionless

C_p specific heat, kJ/(kg- ^oK)

E_v viscous dissipation of mechanical energy, W

E_v^* viscous dissipation of mechanical energy per unit volume, $W/(m^3)$

$\hat{E}_v$ rate of viscous dissipation of mechanical energy W/(Kg/hr)

D barrel diameter, m

Gz Graetz number, dimensionless

$\bar{h}$ observed average heat transfer coefficient, $W/(m^2- {}^oC)$

$\hat{h}$ predicted average heat transfer coefficient, $W/(m^2- {}^oC)$

H enthalpy, W

$\hat{H}$ H/M , W/(Kg/hr)

k thermal conductivity, $W/(m-{}^oK)$

K consistency coefficient, Pa s^n

K_o reference concistency coefficient, Pa s^n

k_s thermal conductivity of the solid phase, $W/(m-{}^oK)$

k_w thermal conductivity of water $W/(m -{}^oK)$

L length of the filled zone, m

MC moisture content (wet basis), dimensionless

$\dot{M}$ throughput, Kg/hr

n flow behavior index, dimensionless

$\bar{Nu}$ average Nusselt number, dimensionless

$\hat{P}_w$ rate of work input, W/(Kg/hr)

q heat flux at the barrel, W/m^2

$\bar{q}$ average heat flux at the barrel, W/m^2

q^* dimensionless heat flux at the barrel

$\bar{q}^*$ average dimensionless heat flux at the barrel

Q_h heat transfer through the boundary, W

$\hat{Q}_h$ rate of heat transfer through the boundary, W/(kg/hr)

R gas constant, cal/(g mole ^oK)

T product temperature, ^oC

$\bar{T}$ average product temperature, ^oC

T_o reference temperature, 40 ^oC

T_w barrel temperature, ^oC

x dimension in the axial direction, m

<u>Greek Sympols</u>

α_1 constant, (Eq. 4-30)

α_2 constant, (Eq. 4-30)

α_{11} constant, (Eq. 4-31)

α_{22} constant, (Eq. 4-31)

α_{33} constant, (Eq. 4-31)

β_1 constant, (Eq. 4-32)

β_2 constant, (Eq. 4-32)

β_3 constant, (Eq. 4-32)

η non-Newtonian apparent viscosity, Pa s

η_a non-Newtonian average apparent viscosity, Pa s

$\dot{\gamma}$ shear rate, s^{-1}

$\dot{\gamma}_a$ average shear rate, s^{-1}

χ dimensionless axial length

τ shear stress, Pa

Θ dimensionless temperature

4.10 Literature Cited

Andersen, S. A. 1950. Automatic Refrigeration. Maclaren and Son Ltd. for Donfoss. Nordborg, Denmark.

Beck, J.V. and Arnold, K.J. 1977. Parameter Estimation in Engineering and Science, John Wiley and Sons, New York.

Booy, M. L. 1980. Isothermal Flow Of Viscous Liquids in Co-Rotating Twin Screw Devices. Polym. Eng. and Sci. 20(18):1220-1228

Cervone, N. W. and Harper, J. M. 1978. Viscosity of Intermediate Moisture Dough. J. Food Proc. Eng. 2:83-96

Chen, A. H., Jao, Y. C. Larkin, J. W. and Goldstein, W. E. 1978. Rheological Model of Soy Dough in Extrusion. J. Food Proc. Eng. 2:337-342

Denson, C. D. and Hwang Jr, B. K. 1980. The Influence of The Axial Pressure Gradient on Flow Rate for Newtonian Liquids in Self Wiping Co-Rotating Twin Screw Extruder. Polym. Eng. and Sci. 20(14):965-971

Eise, K., Herrmann, H., Jakopin, S. and Burkhardt, U. 1981. An Analysis of Twin-Screw Extruder Mechanisms. Advances in Plastic Technology. 1(2):18-39

Harper, J. M., Rhodes, T. P. and Wanniger, L. A. 1971. Viscosity Model For Cooked Cereal Doughs. AIChE. J. Symp. Ser. 67(108):40-43

Harper, J. M. 1981. Extrusion of Food, Vols. 1 and 2. CRC Press Boca RAton, Fl.

Harper, J. M. 1985. Processing Characteristics of Food Extruders. Food Engineering and Process Application Vol. 2. Unit Operation Eds. Lemanguer, M. and Jelen, P.

Harper, J. M. 1986. Extrusion Texturization of Foods. Food Technol. 40(3):70

Howkins, M. D. 1987. A Predictive Model For pressure Drop in Food Extruder Dies. M.S. Thesis, Michigan State University, East Lansing, MI, USA.

Jao, Y. C., Chen, A. H., Lewandowski, D. and Irwin, W. E. 1978. Engineering Analysis of Soy Dough Rheology in Extrusion. J. Food Proc. Eng. 2:97-112

Levine, L. 1982. Estimating Output and Power of Food Extruders. J. Food Proc. Eng. 6:1-13

Levine, L. and Rockwood, J. 1986. A correlation For Heat Transfer Coefficients in Food Extruders. Biotech. Prog. 2(2):105-108

Martelli, F. G. 1983. Twin-Screw Extruders: A Basic Understanding. Van Nostrand Reinhold Comparce New York.

Mohamed, I. O., Morgan, R. G. and Ofoli, R. Y. Average Convective Heat Transfer Coefficients in Single Screw Extrusion of Non-Newtonian Food Materials. Biotech. Prog. 4(2):68-75

Mohsenin, N. N. 1980. Thermal Properties of Foods and Agricultural Materials. Gordon and Breach Science Publ.

Neter, J., Wasserman, W. and Kutner, M.H. 1985. Applied Linear Statistical Models. 2nd. Ed., Richard D. Irwin, Inc. Homewood, Illinois 60430.

Ordinanz, W. O. 1946. Specific Heat of Foods in Cooling. Food Industries. 18(12):101

Remsen, C. H. and Clark, J. P. 1978. A Viscosity Model For A Cooking Dough. J. Food Proc. Eng. 2:39-64

Vega, V. 1988. Personal Comunications.

Yacu, W. 1985. Modelling a Twin Screw Co-Rotating Extruder. J. Food Proc. Eng. 8:1-21

Wyman, C. E. 1975. Theoretical Model For Intermeshing Twin Screw Extruders: Axial Velocity Profile For Shallow Channels. Polym. Eng. and Sci. 15(8):606

CHAPTER 5

PREDICTION OF THE TEMPERATURE PROFILE IN CO-ROTATING TWIN SCREW EXTRUDERS, INCORPORATING THE EFFECTS OF VISCOUS DISSIPATION

5.1 Abstract

A heat transfer model which accounts for viscous dissipation effects has been developed to predict product temperature profiles inside a co-rotating twin screw extruder. Three types of screw configurations were used to investigate the temperature predictions of the model. Temperature profiles were also determined experimentally to be compared with the simulation. Excellent agreement was obtained for 30F paddles. Predictions for feed screws were generally good, with the exception of some deviation at low throughput. Predictions for single lead screws were poor, most probably due to the poor mixing characteristics of this type of screw, in contrast to the assumption of uniform temperature in the direction perpendicular to screw shafts.

5.2 Introduction

Most of the limitations of the single screw extruder have been overcome with the design of the co-rotating twin screw extruder, which allows for greater operating flexibility. Twin screw extuders, unlike single screw extruders, can operate in starve mode, where most of the screw channels are only partially filled with material. This results in decoupling the screw speed and throughput, because conveyance of the product does not depend entirely on friction between the product and screw and barrel surfaces as in single screw extruders.

Twin screw extruders have two distinct zones: a) the partially filled zone, which has poor heat transfer characteristics and very low heat generation from viscous dissipation, and b) the filled zone, which has good heat transfer characteristics and a significant amount of heat generation from viscous dissipation, which enhances the cooking process.

The problem of heat transfer in twin screw extruders is of great importance. However, heat transfer models are still in the early stages of development, due to the complexity of the extruder geometry and the flow dynamics inside the extruder. For cooking extruders, knowledge of the heat transfer mechanisms is important for proper control and optimization of the cooking process. Also, knowledge of the product temperature before the die is useful for die design and hence better control of product shape and texture (Harper, 1986).

The predominant heat transfer modes in extrusion are convective heat transfer through the barrel and viscous dissipation. However, the contribution of viscous dissipation to the heat energy required for cooking can reach 100% depending on extruder design, operating conditions and moisture content (Rossen and Miller, 1973). The difficulty in modelling heat transfer in twin screw extruders and accounting for viscous dissipation stems from the difficulty in assessing the shear rate inside the extruder and lack of data on the heat transfer coefficient.

The primary objectives of this analysis are:

(1) To develop a predictive heat transfer model for the temperature profile in the axial direction, incorporating viscous dissipation

effects for knneading discs staggered at 30 degree forwarding (30F), single flighted screw (single lead), and a two-flighted screw (feed screws).

(2) To conduct experimental tests to verify the model.

5.3 Mathematical Development

Based on the assumption of uniform temperature in the direction perpendicular to screw shafts, a one-dimensional energy equation will be developed to describe product temperature variation in the axial direction. For single lead and feed screws the energy equation was used to describe temperature variation along the screw helix, and then transformed to describe the variation in the axial energy. For kneading discs, from a macroscopic energy balance around a control volume, a differential equation was developed to describe temperature variation in the axial direction.

5.3.1 Assumptions

The following assumptions were made in the development of the governing differential equation:

(1) Steady state

(2) Constant thermal properties (specific heat and thermal conductivity)

(3) Incompressible fluid

(4) Viscous forces are dominant compared to inertial and gravity forces

(5) Viscosity is independent of strain and time temperature history

(6) The temperature is uniform in the direction perpendicular to the screw shafts

(7) Negligible heat losses from screw shafts

5.3.3 The Energy Equation for Feed and Single Lead Screws

As in Chapter 4, the energy balance gives

$$MC_p\Delta T = Q_h + E_v \tag{5-1}$$

where M is the mass flow rate, C_p is the specific heat, ΔT is the temperagerge change between the inlet and outlet of the control volume, Q_h is the heat added or removed from the control volume at the boundary, and E_v is the viscous dissipation of mechanical energy. It is assumed that the viscous dissipation per unit volume ($\overset{*}{E}_v$) can be represented by

$$\overset{*}{E}_v = \eta_a\dot{\gamma}_a^2 \tag{5-2}$$

where η_a and $\dot{\gamma}_a$ are, respectively, the average apparent viscosity and the average shear rate. The heat transfer from the control volume bounded by z and $(z+\Delta z)$ can be written as

$$Q_h = qW\Delta z \tag{5-3}$$

where z is the direction along the screw helix, q is the heat flux, and W is the channel width. Substituting Eqs. 5-2 and 5-3 into Eq. 5-1 yields

$$MC_p\Delta T = qW\Delta z + \eta_a\dot{\gamma}_a^2A_x\Delta z \tag{5-4}$$

Dividing Eq. 5-4 by Δz, and taking the limit as Δz approaches zero,

$$MC_p\frac{dT}{dz} = qW + \eta_e\dot{\gamma}_e^2\,A_x \tag{5-5}$$

The rheology of a great majority of extruded materials can be described by the power law model (Harper et al. 1971; Chen et al. 1978; Remsen and Clark, 1978; Jao et al. 1978; Cervone and Harper, 1978;

Levine, 1982). Assuming the power law describes the rheology of the material in this study, the apparent viscosity can be expressed as:

$$\eta = K_o\dot{\gamma}^{(n-1)}\exp(\frac{\Delta E}{R})[\frac{1}{T} - \frac{1}{T_o}] \qquad (5\text{-}6)$$

where K_o is the consistency coefficient, n is the flow behavior index, ΔE is the activation energy, R is the gas constant and T_o is a reference temperature. The heat flux at the wall can be defined as

$$q = \bar{h}(T - T_w) \qquad (5\text{-}7)$$

where $\bar{h}$ is the average heat transfer coefficient, and T and T_w are the product and the barrel temperatures, respectively. Assuming that the shear rate inside the extruder can be represented by an average value ($\dot{\gamma}_a$), and substituting Eq. 5-6 with $\dot{\gamma}$ replaced by $\dot{\gamma}_a$, and Eq. 5-7 into Eq. 5-5 yields

$$MC_p\frac{dT}{dz} = W\bar{h}(T - T_w) + A_xK_o\dot{\gamma}_a^{(n+1)}\exp[(\frac{\Delta E}{R})(\frac{1}{T} - \frac{1}{T_o})] \qquad (5\text{-}8)$$

From Eq. 5-8 the energy equation in the axial direction can be written as

$$MC_p\sin\Phi\,\frac{dT}{dx} = W\bar{h}(T - T_w) + A_xK_o\dot{\gamma}_e^{(n+1)}\exp[(\frac{\Delta E}{R})(\frac{1}{T} - \frac{1}{T_o})] \qquad (5\text{-}9)$$

where Φ is the screw helix angle. To make Eq. 5-9 dimensionless, define

$$\theta = \frac{T - T_o}{T_w - T_o} \quad , \qquad \chi = x/L \qquad (5\text{-}10)$$

where L is the filled length. Incorporating the dimensionless terms into Eq. 5-9 yields

$$MC_p \frac{(T_w - T_o)}{L} \sin\Phi \frac{d\theta}{d\chi} = W\bar{h}(T - T_w) + A_x K_o \dot{\gamma}_a^{(n+1)} \exp(\frac{-\Delta E}{RT_o})$$

$$\exp[\frac{\Delta E}{R(\theta(T_w - T_o) + T_o)}] \;\ldots\ldots\; (5\text{-}11)$$

Dividing Eq. 5-11 by $k(T_w - T_o)$ gives

$$\frac{MC_p}{kL} \sin\Phi \frac{d\theta}{d\chi} = \frac{W\bar{h}(T - T_w)}{k(T_w - T_o)} + \frac{A_x K_o \dot{\gamma}_e^{(n+1)}}{k(T_w - T_o)} \exp(\frac{-\Delta E}{RT_o}) \exp[\frac{\Delta E}{R(\theta(T_w - T_o) + T_o)}]$$

$$\ldots\ldots\ldots\ldots\ldots\ldots\ldots\; (5\text{-}12)$$

where k is the thermal conductivity. Multiplying and dividing the last term of Eq. 5-12 by L^2 yields

$$Gz \sin\Phi \frac{d\theta}{d\chi} = \frac{W\bar{h}(\theta - 1)}{k} - Br \frac{A_x}{L^2} \exp[\frac{\Delta E}{R(\theta(T_w - T_o) + T_o)}] \qquad (5\text{-}13)$$

where $\quad Gz = \frac{MC_p}{kL} \quad$ (Graetz number) $\quad (5\text{-}14)$

and $\quad Br = \frac{K_o L^2 \dot{\gamma}_a^{(n+1)}}{k(T_o - T_w)} \exp[\frac{-\Delta E}{RT_o}] \quad$ (Brinkman number) $\quad (5\text{-}15)$

Equation 5-13 is a first order non-linear differential equation which can be solved numerically, subject to the boundary condition

$$\text{at} \quad \chi = 0 \qquad \theta = \frac{T_i - T_o}{T_w - T_o} \qquad (5\text{-}16)$$

where T_i is the inlet temperature to the filled zone.

5.2.3 The Energy Equation For Kneading Discs

The energy equation for the kneading discs was developed in Section 4.5, and can be written in the following form

$$Gz \frac{d\theta}{d\chi} = \frac{2D(\pi - \psi)q}{k(T_w - T_o)} - Br \frac{A_i}{L^2} \exp[\frac{\Delta E}{R(\theta(T_w - T_o) + T_o)}] \qquad (5\text{-}17)$$

where D is the barrel diameter, and A_1 is the net flow area in the axial direction. Substituting Eq. 5-7 into Eq. 5-17,

$$Gz \frac{d\theta}{d\chi} = \frac{2D(\pi - \psi)}{k} \bar{h}(\theta - 1) - Br\frac{A_1}{L^2} \exp\left[\frac{\Delta E}{R(\theta(T_w - T_o) + T_o)}\right] \qquad (5\text{-}18)$$

Equation 5-18 can be solved numerically, subject to the boundary condition given by Eq. 5-16.

5.4 Materials and Methods

A Baker Perkins (MPF-50D) twin screw co-rotating extruder was used for this work. Three types of screw configurations were used: feed screw, single lead, and kneading discs staggered at 30 degree forwarding. For each of the screw configurations, a barrel length of 15 L/D was used, with a pair of three-hole dies (length = 2.58 cm, diameter = 0.3175 cm). Soy polysaccharide (SPS) obtained from Raltson Purina (St. Louis, Mo) was chosen as the test material. A moisture content of 70 % (wet basis) was used for all the extrusion runs. Three throughputs were used (33, 46, and 60 kg/hr). For each throughput, three screw speeds were used. The same procedure as described in Section 4.6 for running the extruder and collecting the data was used. For some of the extrusion runs the extruder was "dead-stopped", the barrel was dismantled quickly and the length of the filled zone was measured.

5.5 Results And Discussion

5.5.1 Numerical Solution Of The Differential Equations

The differential equations developed earlier for both the kneading discs and the feed screws are nonlinear first order differential equations. A numerical scheme was used to solve the quations, using a fourth order Runge-Kutta method. A computer program was written in

Fortran to perform all necessary calculations. The rheological and thermal properties used were the same as given in Chapter 4, since the same product at the same moisture content was also used in this analysis. The geometric constants of the screws and the kneading discs in the differential equations were estimated as follows:

a) feed screw

$W = 0.025$ m

$A_x = 0.0003$ m^2

$\Phi = 17.85^\circ$

b) single lead

$W = 0.0127$ m

$A_x = 0.0001$ m^2

$\Phi = 4.75^\circ$

c) 30F paddles

$A_i = 0.001596$ m^2

Booy (1980) showed that the number of parallel channels formed by intermeshing screws with small tips is given by

$$n_c = 2n_t - 1 \qquad (5\text{-}19)$$

where n_c is the number of parallel channels, and n_t is the number of screw tips. Thus the number of parralel channels for a feed screw is three.

The solution of the differential equations requires knowledge of the inlet temperature to the filled zone. Since there are no models available which predict the temperature at the end of the partially filled zone (which corresponds to the inlet of the filled zone), experimental measurements were made to obtain the inlet temperature. The temperature obtained from the first thermocouple in the filled zone was chosen as the inlet temperaure. The location of this thermocouple was determined by a measurement of the filled length after "dead-stopping" the extruder. It was found to be L = 23.495 cm for the kneading discs, and L = 10.125 cm for the feed screws and single lead. For the estimation of the average heat transfer coefficient, a characteristic length of 23.495 cm was used to calculate Gz and Br for all the screw configurations. The computational scheme is illustrated by the flow-chart in Figure 5.1

5.5.2 Simulated Versus Experimental Temperature Profiles

The computer program discussed in Section 5.5.1 was used to obtain the temperature profile for three throughputs (33, 46, and 60 kg/hr). For each of the three throughputs, three screw speeds were used (200, 300, and 400 RPM) to cover a wide range of operating conditions.

Computer predictions and experimental results are plotted for each of the extrusion runs. The results for the 30 forwarding paddles are shown in Figures 5.2 to 5.4. Good agreement is obtained between the simulation and the experimental results, especially in the prediction of the pre-die temperature. Some of the experimental data showed some deviation from the simulation results in the mid-sections of the filled length. However, this does not invalidate the model, because the pre-die temperature measurement is the most reliable data. This value was obtained by inserting a thermocouple with a long probe through the die hole; the other values were obtained with extruder sensors which may be slightly influenced by the barrel temperature.

The results of the simulated and experimental temperature profiles for feed screws are shown in Figures 5.5 to 5.7. The model under-estimates the pre-die temperature at low and medium throughputs (Figures 5.5 to 5.6) by a maximum of seven and two degrees respectively. Results at medium and high flow rates, however, showed good agreement between simulated and the experimental results (Figure 5.8). The reason for this might be due to the fact that at medium to high throughputs a good degree of mixing was achieved, in agreement with the main assumption of uniform temperature in the direction perpendicular to the screw shafts. Excellent mixing also explains why the kneading discs show very good agreement between the simulated and experimental results; kneading discs provide a good degree of mixing. For single lead screws, the prediction of the temperature profile is very poor (Figure 5.8). This can be attributed to the poor mixing characteristics, which suggests the presence of a temperature gradient in the direction perpendicular to the screw shafts.

This was confirmed by inserting a thermocouple at different positions in the direction perpendicular to the screw shafts, after "dead-stopping" the extruder. Also, if the dough has a yield stress, this may induce a plug flow region at the screw root, causing material in the region closer to the barrel to be subjected to a high shear rate (and hence result in higher viscous dissipation) which would produce a higher temperature in the region closer to the barrel surface. In addition, the relatively wider screw tip for the single lead could generate higher levels of viscous dissipation at the screw tip clearance.

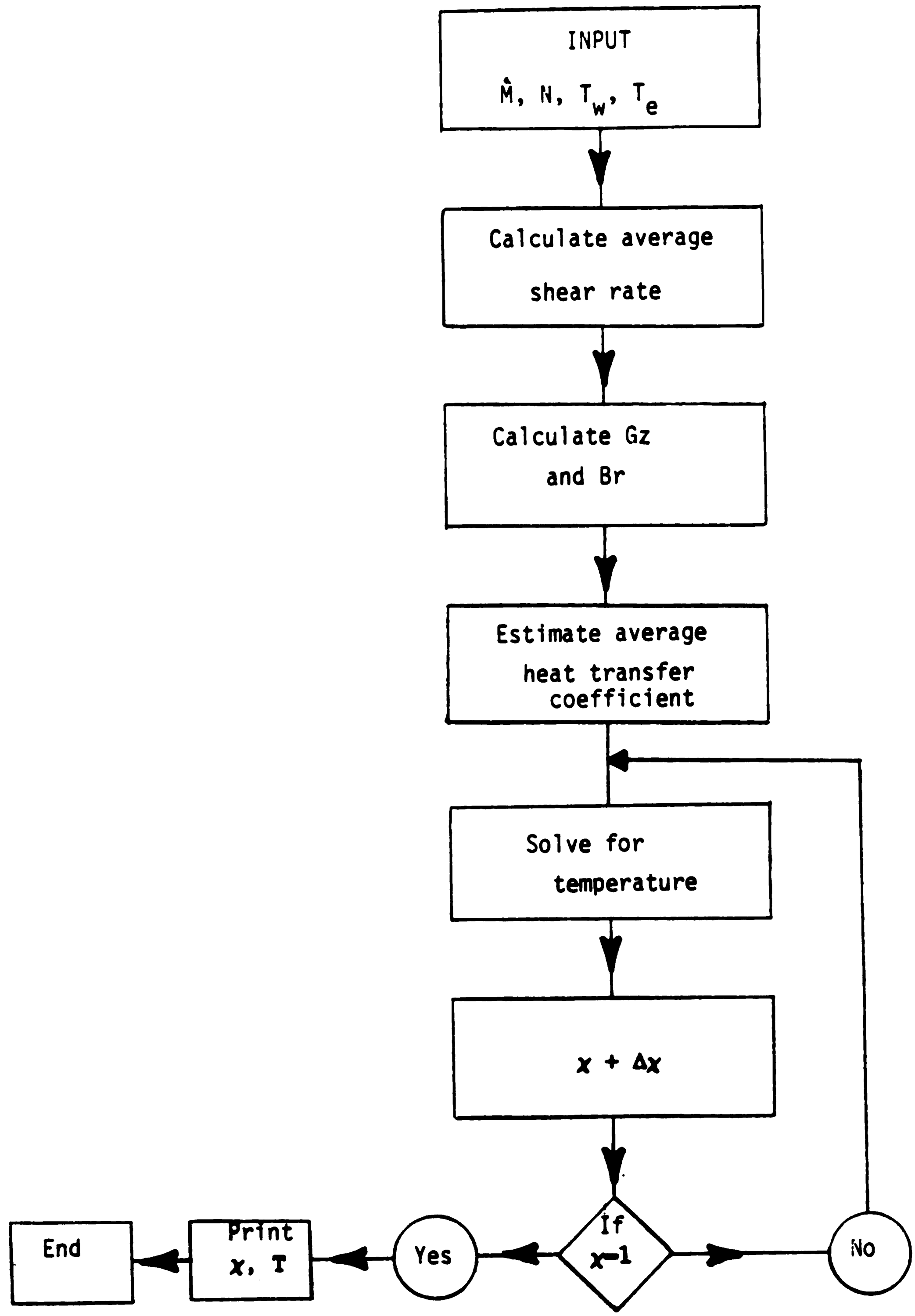

Figure 5.1 Flow Chart Showing The Calculation Scheme For The Solution of The Temperature Profile

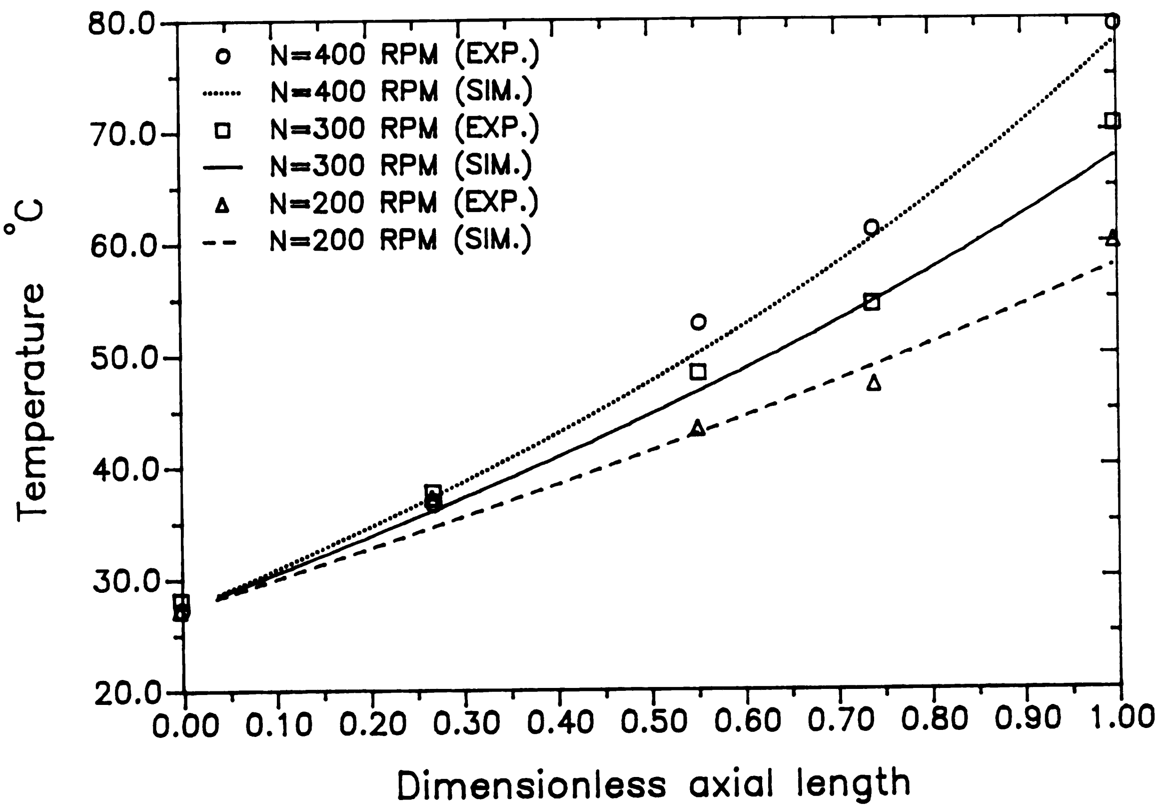

Figure 5.2 Simulated Versus Experimental Temperature Profiles

(30F Paddles, M = 33 kg/hr)

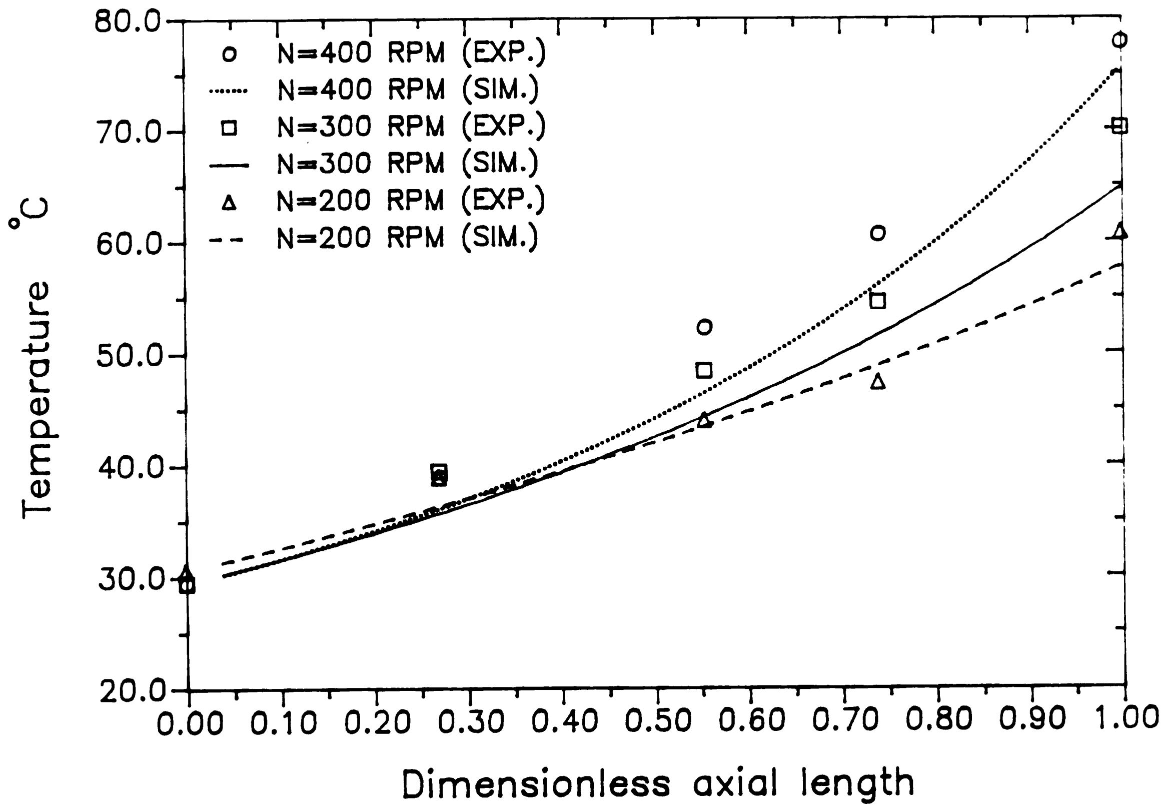

Figure 5.3 Simulated Versus Experimental Temperature Profiles

(30F Paddles, M = 46 kg/hr)

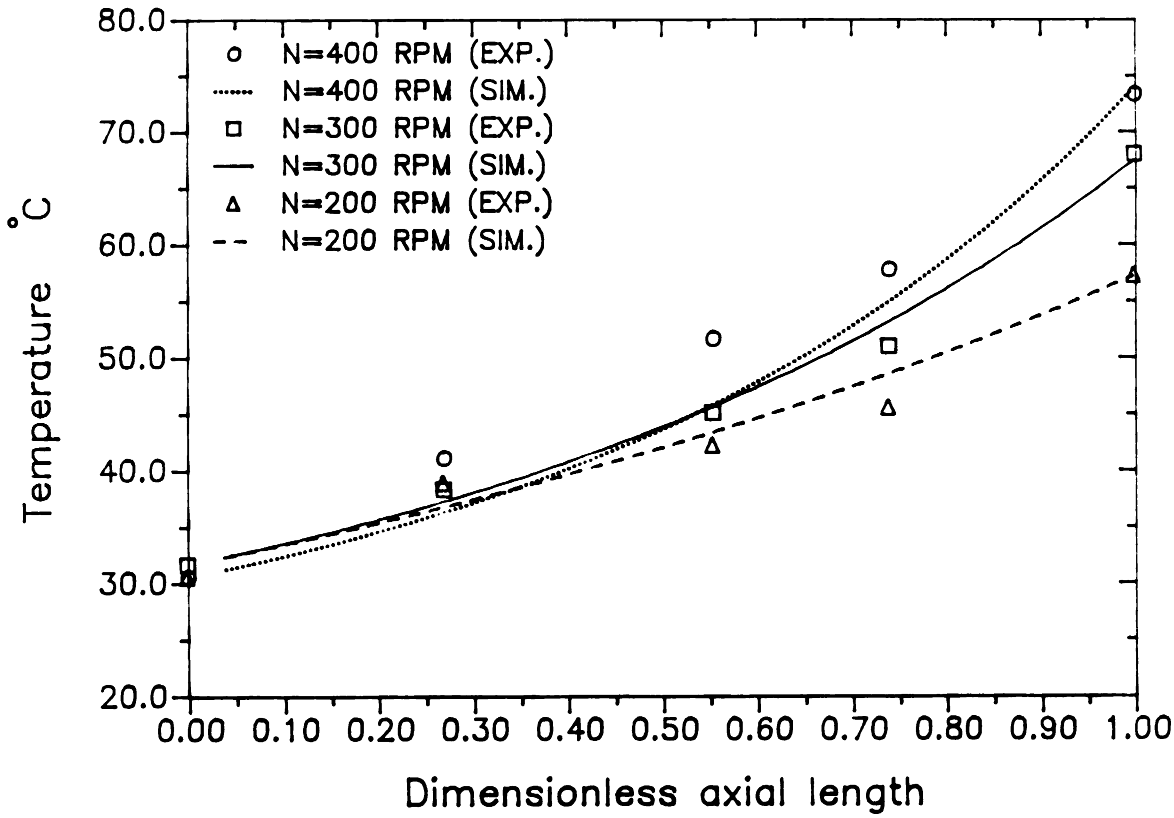

Figure 5.4 Simulated Versus Experimental Temperature Profiles

(30F Paddles, M = 60 kg/hr)

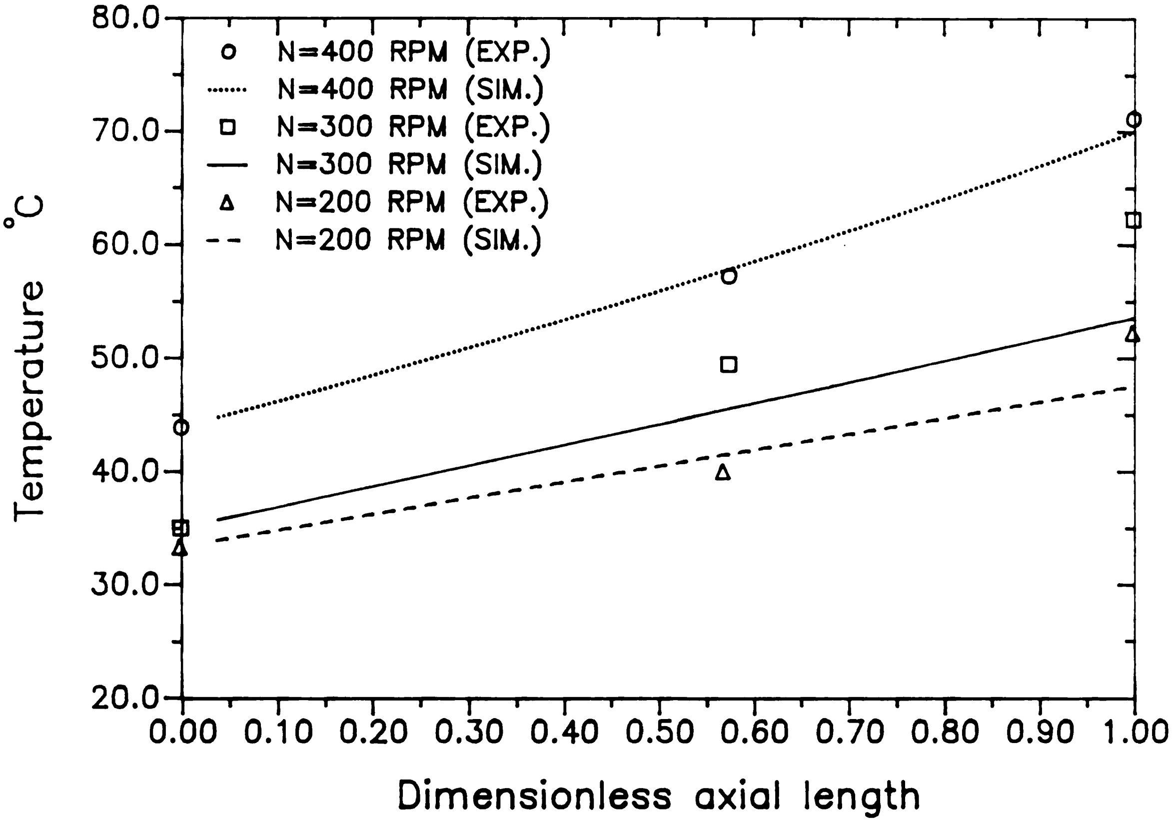

Figure 5.5 Simulated Versus Experimental Temperature Profiles

(Feed Screws, M = 33 kg/hr)

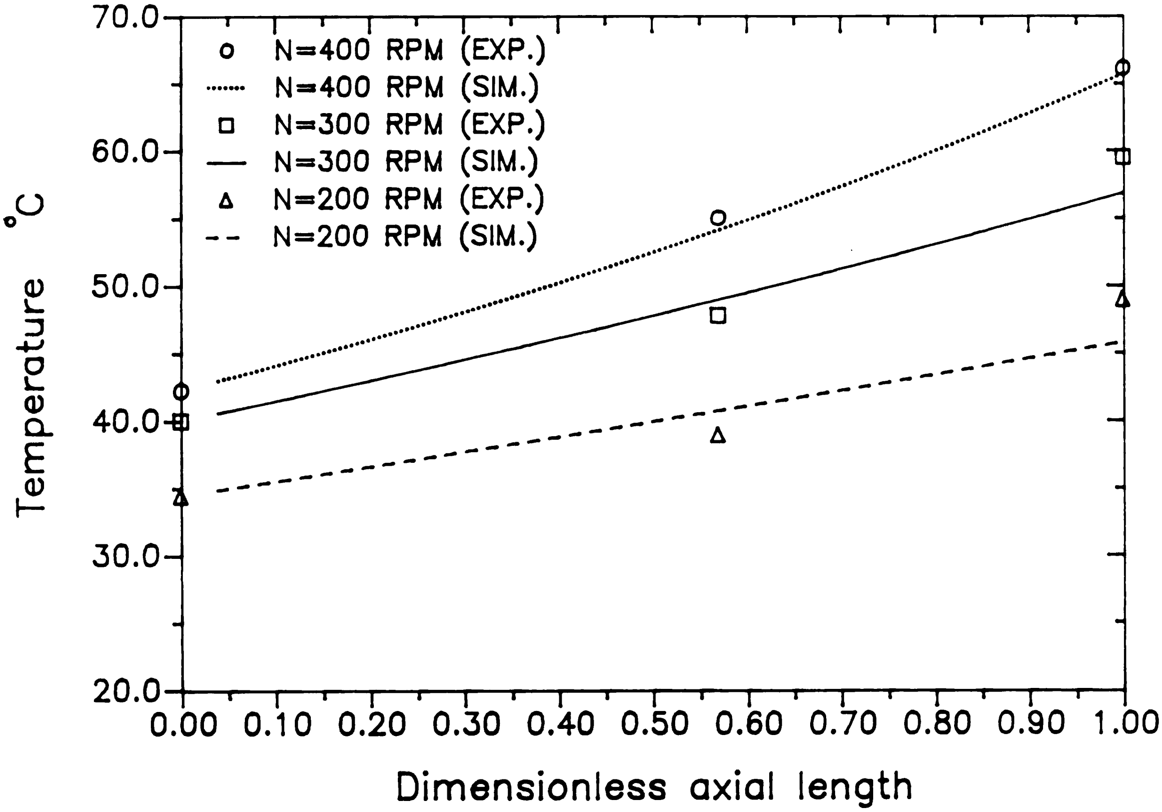

Figure 5.6 Simulated Versus Experimental Temperature Profiles

(Feed Screws, M = 46 kg/hr)

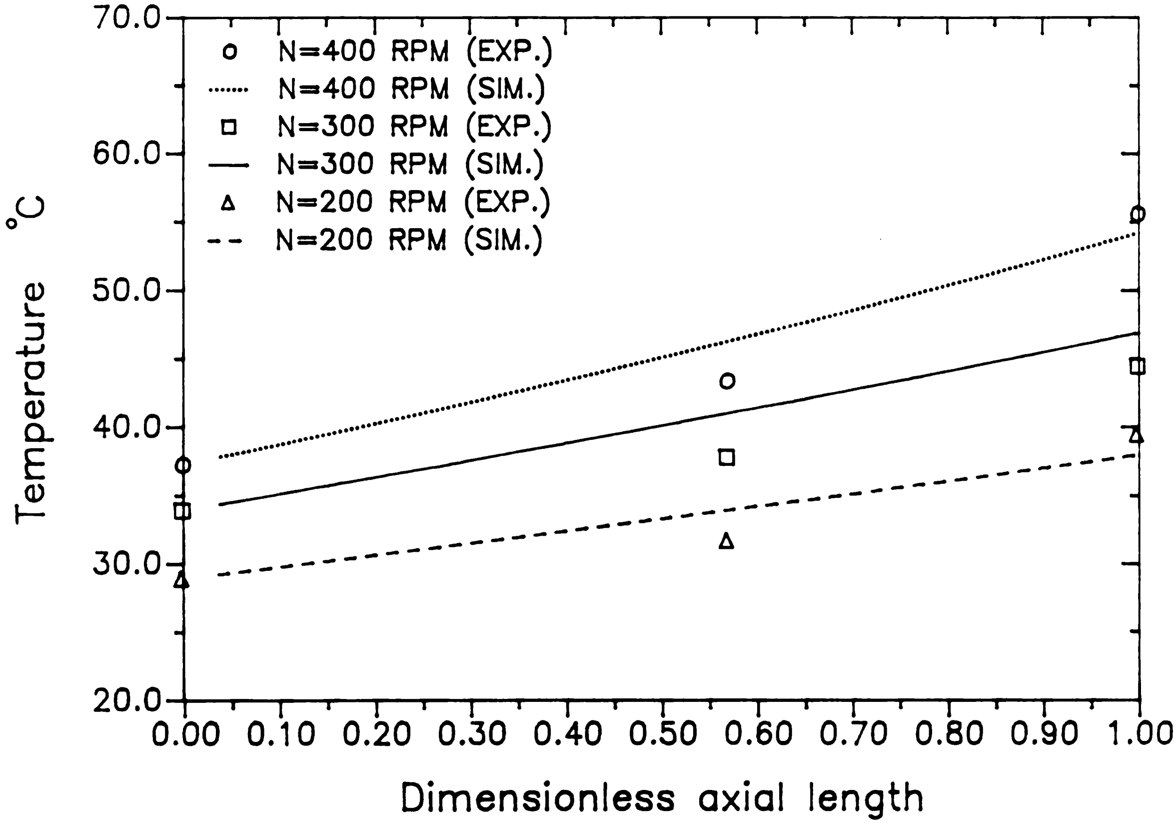

Figure 5.7 Simulated Versus Experimental Temperature Profiles

(Feed Screws, M = 60 kg/hr)

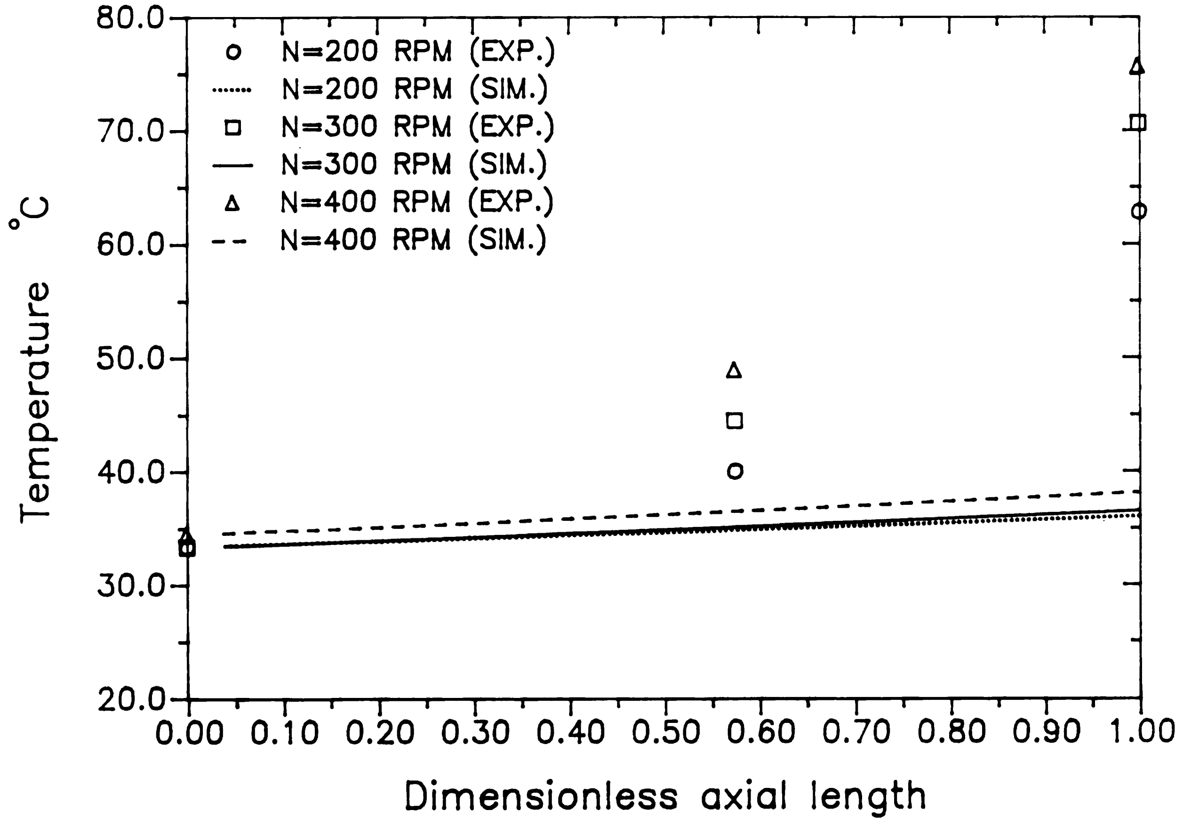

Figure 5.8 Simulated Versus Experimental Temperature Profiles

(Single Lead Screws, M = 46 Kg/hr)

Examining the results for the 30 forwarding paddles, much practical and valuable information can be obtained from the simulation. For example, for a given throughput, increasing the screw speed increases the Brinkman number, and hence the level of viscous dissipation, which is reflected in the higher product temperature (Figures 5.2, 5.3 and 5.4). Also for a given screw speed, increasing throughput increases the Graetz number and hence the average heat transfer coefficient, which results in a smaller temperature gradient between the product and the barrel as can be seen from the slopes of the profiles (Figure 5.9). This shows the dominant effect of convective cooling over viscous dissipation at high throughput and low screw speeds. At high screw speeds and low throughputs viscous heating dominates convective cooling.

5.6 Conclusions

A model incorporating viscous dissipation effects has been developed for predicting the temperature profile for non-Newtonian non-isothermal food doughs inside a twin screw extruder. The predicted temperature profiles were compared to experimental values, using three screw configurations. Excellent agreement with the experimental data was obtained for 30F paddles. Feed screws provide good predictions at medium and high flow rates, and slightly under predict at low flow rates. Single lead screws gave poor predictions of the temperature profile. This is most likely due to the fact that single lead screws provide a poor level of mixing; thus the assumption of uniform product temperature in the direction perpendicular to screw shafts is not satisfied.

The results also show that viscous dissipation effects overcome convective cooling effects at lower feed rates and high screw speed,

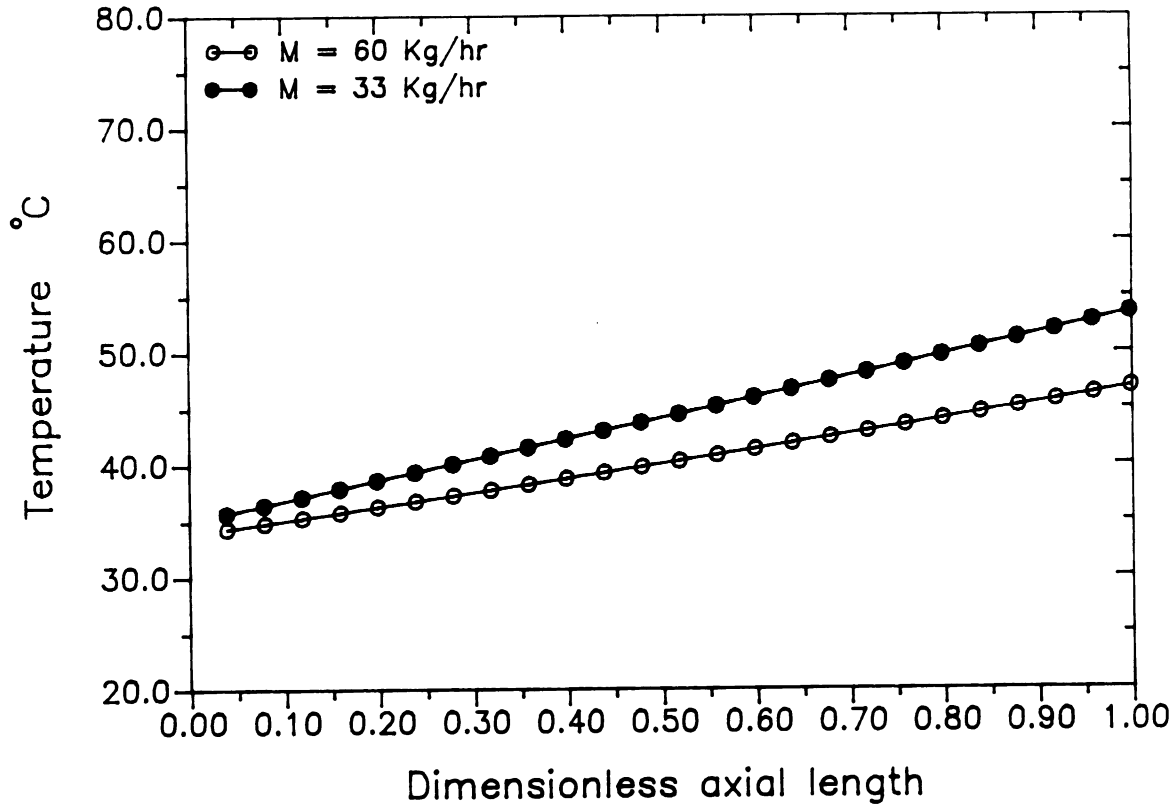

Figure 5.9 Simulated Versus Experimental Temperature Profiles

(Feed Screws, N = 300 RPM)

while convective cooling dominates viscous heating at high flow rates and low screw speeds. This kind of information is useful in design, control and optimization of the cooking extrusion process.

5.7 Nomenclature

A_i flow area for the 30 forwarding paddle, m^2

A_x cross-sectional area of screw channel, m^2

Br Brinkman number, dimensionless

C_p specific heat, kJ/(kg-^oK)

D barrel diameter, m

E_v viscous dissipation, W

$\overset{*}{E}_v$ viscous dissipation per unit volume, w/(m^3)

Gz Graetz number, dimensionless

$\bar{h}$ average heat transfer coefficient, W/(m^2 K)

k thermal conductivity, W/(m - ^oK)

K_o reference consistency coefficient, Pa s^n

L filled length, m

$\dot{M}$ throughput, kg/hr

n flow behavior index

n_c number of parralel channels

n_t number of screw tips

q heat flux, W/m^2

Q_h heat transfer at the control volume boundary, W

R gas constant, cal/(g-mole-^oK)

T product temperature, ^oC

T_i inlet product temperature, ^oC

T_o reference temperature (40), ^oC

T_w wall temperature, ^oC

x axial direction co-ordinate, m

z direction along screw helix, m

Greek Sympols

ΔE activation energy, cal/(g-mole)

η apparent viscosity, Pa s

η_a average apparent viscosity, Pa s

$\dot{\gamma}$ shear rate, s^{-1}

$\dot{\gamma}_e$ average shear rate, s^{-1}

Θ dimensiomless temperature

Φ helix angle, degree

5.8 Literature Cited

Booy, M. L. 1980. Isothermal Flow of Viscous Liquid in Co-Rotating twin screw devices. Polym. Eng. and Sci. 20(18):1220-1228

Cervone, N. W. and Harper, J. M. 1978. Viscocity of Intermediate Moisture Dough. J. Food Proc. Eng. 2:83-96

Chen, A. H., Jao, Y. C., Larkin, J. W. and Goldstein, W. E. 1978. Rheological Model of Soy Dough in Extrusion. J. Proc. Eng. 2:337

Harper, J. M., Rhodes, T. P. and Wanniger, L. A. 1971. Viscosity Model For Cooked Cereal Dough. AIChE. Symp. Ser. 67(108):40-43

Harper, J. M. 1986. Extrusion Texturization of Foods. Food Technol. 40(3):70

Jao, Y. C., Chen, A. H., Lewandowski, D. and Irwin, W. E. 1978. Engineering Analysis of Soy Dough Rheology In Extrusion. J. Food Proc. Eng. 2:97-112

Levine, L. 1982. Estimating Output and Power of Extruders. J. Food Proc. Eng. 6:1-13

Remsen, C. H. and Clark, J. P. 1978. A Viscosity Model For a Cooking Dough. J. Food Proc. Eng. 2:39-64

Rossen, J. L. and Miller, R. C. 1973. Food Extrusion. Food Technol. 27:46-53

CHAPTER 6

SUMMARY AND CONCLUSIONS

Mixer analysis techniques were applied to a twin screw extruder to estimate the average shear rate. Three screw configurations were investigated: single lead, feed screw and 30 degree forwarding paddles. The estimated shear rate was correlated to screw speed.

A one-dimensional energy equation was developed for 30 forwarding paddles and solved numerically to obtain the average heat flux, using the shear rate model developed in this study. The experiment was conducted on a Baker Perkins (MPF-50D), twin screw co-rotating extruder, using only 30 forwarding paddles with soy polysaccharide at 70% moisture content as the test material. From the estimated heat flux, average heat transfer coefficients were calculated and correlated to Brinkman and Graetz numbers.

The shear rate and the average heat transfer coefficients were incorporated into the one-dimensional energy equations developed for the feed and single lead screws and the 30 forwarding paddles. Each equation was solved numerically for the temperature profiles, using a fourth order Runge-Kutta method, with the inlet temperature determined by an experimental measurement of the product temperature at the beginning of the filled zone.

The following conclusions were drawn from this investigation:

1) The average shear rate correlates well with screw speed

2) For a given screw speed, 30 forwarding paddles have the highest shear rate, followed by feed screws and single lead screws.

3) The average heat transfer coefficients correlate well with Brinkman and Graetz numbers.

4) The average heat transfer coefficients are higher for twin screw extruders than for single screw extruders.

5) The one-dimensional energy equation is adequate for modelling heat transfer in mixing paddles and feed screws, but inappropriate for single lead screws.

6) At low throughput and high screw speeds, viscous dissipation exceeds convective cooling capacity.

7) At high throughput and low screw speeds convective cooling capacity is higher than the rate of viscous dissipation.

CHAPTER 7

SUGGESTIONS FOR FUTURE RESEARCH

1) Extension of this work to kneading discs staggered at 45, and 60 degrees forwarding and 30, 45 and 60 degrees reversing.

2) Determination of the variables which affect the filled length and the level of fullness, and correlation of the fill level to appropriate parameters.

3) Modelling of heat transfer in the partially filled zone.

4) Modelling of the effects of reaction kinetics on dough viscosity, and the incorporation of these models into heat transfer analysis.

5) Modelling shear rate and heat transfer in food doughs with a yield stress.

6) Modelling heat transfer in single flighted screws.

7) Defining, and modelling the degree of mixing for different screw configurations.

APPENDIX A: Data From Twin Screw Extrusion of Polybutene, Using Several Screw Configurations

Single Lead Screws

N (RPM)	% Torque	M (Lb/min)	Δp (Lb/in^2)	T_a (^oF)
100	20	1.52	60	77
200	20	1.14	110	80
300	21	1.65	150	85
400	21	1.77	90.5	95.5

Feed Screws

N (RPM)	% Torque	M (Lb/min)	Δp (Lb/in^2)	T_a (^oF)
100	21	2.57	280	80
200	25	2.78	410	87
300	26	4.50	400	92
400	26	5.23	320	95.5

30F Paddles

N (RPM)	% Torque	M (Lb/min)	Δp (Lb/in^2)	T_a (^oF)
100	18	0.91	100	91
200	18	2.14	90	96
300	21	3.21	100	101
350	20	3.60	90	103
400	22	4.65	90	105

T_a is the average feed and die product temperature

APPENDIX B: Data From Extrusion of a Mixture of 7% SPS and 93% Honey, Using Several Screw Configurations

Single Lead Screws

N (RPM)	% Torque	$\dot{M}$ (Lb/min)	Δp (Lb/in^2)	T_a (^oF)
100	12	1.98	88	88.0
150	18	3.22	210	76.5
200	15	1.50	90	95.0
300	15	2.66	20	102.0
400	15	3.54	20	108.0

Feed Screws

N (RPM)	% Torque	$\dot{M}$ (Lb/min)	Δp (Lb/in^2)	T_a(^oF)
100	14	1.25	210	81.5
200	15.5	1.57	190	83.0
250	18	6.25	300	73.0
300	17	2.04	180	85.0
400	18.5	2.54	180	87.5

30F paddles

N (RPM)	% Torque	$\dot{M}$ (Lb/min)	Δp (Lb/in^2)	T_a (^oF)
100	17	1.25	90	80.5
150	18	0.92	110	78.5
200	15	1.60	60	84.0
300	16	2.00	60	88.5
400	16.5	3.07	60	90.0

APPENDIX C: Experimental Data Used to Develop Relations for Heat Transfer Coefficients (Screw Configuration: 30F paddles)

Experimental run # 1

N = 250 RPM, $\dot{M}$ = 33 Kg/hr, T_w = 67, 71 ^oF

x (cm)	T (^oC)
44.45	22.1
50.80	31.8
57.47	42.2
61.91	48.2
67.94	57.2

Experimental run # 2

N = 350 RPM, $\dot{M}$ = 33 Kg/hr, T_w = 70, 78 ^oF

x (cm)	T (^oC)
44.45	21.2
50.80	37.0
57.47	46.9
61.91	51.5
67.94	67.8

Experimental run # 3

N = 350 RPM, $\dot{M}$ = 46 Kg/hr, T_w = 72, 79 ^oF

x (cm)	T (^oC)
44.45	24.3
50.80	39.3
57.47	46.3
61.91	50.5
67.94	63.3

Experimental run # 4

N = 450 RPM, M = 46 Kg/hr, T_w = 75, 89 ^oF

x (cm)	T (^oC)
44.45	22.6
50.80	37.7
57.47	50.9
61.91	57.9
67.94	71.7

Experimental run # 5

N = 250 RPM, M = 60 Kg/hr, T_w = 71, 74 ^oF

x (cm)	T (^oC)
44.45	21.7
50.80	38.9
57.47	41.1
61.91	43.3
67.94	55.0

Experimental run # 6

N = 350 RPM, M = 60 Kg/hr, T_w = 74, 81 ^oF

x (cm)	T (^oC)
44.45	22.3
50.80	41.7
57.47	47.4
61.91	50.7
67.94	61.1

Experimental run # 7

N = 350 RPM, $\dot{M}$ = 60 Kg/hr, T_w = 74, 81 ^oF

x (cm)	T (^oC)
44.45	22.3
50.80	41.7
57.47	47.4
61.91	50.7
67.94	61.1

Experimental run # 8

N = 450 RPM, $\dot{M}$ = 60 Kg/hr, T_w = 76, 84 ^oF

x (cm)	T (^oC)
44.45	22.6
50.80	41.3
57.47	49.7
61.91	54.0
67.94	66.7

1) T_w is the barrel temperature in zones z8 and z9 of the extruder which corresponds to the filled zone. The average values of the two was used as the barrel temperature.

2) x is the thermocouple position measured from the feed port (15 L/D).

3) T is the product temperature measured by a data acquisition system. The values reported are the average values of several steady state measurements over period of one minute.

APPENDIX D: Experimental Temperature Data Used to Validate The Heat Transfer Model For Three Screw Configurations

30F paddles, run # 1

N = 200 RPM, $\dot{M}$ = 33 Kg/hr, T_w = 79, 84 °F

x (cm)	T (°F)
44.45	81
50.80	99
57.47	100
61.91	117
67.94	140

30F paddles, run # 2

N = 200 RPM, $\dot{M}$ = 33 Kg/hr, T_w = 81, 89 °F

x (cm)	T (°F)
44.45	81
50.80	100
57.47	119
61.91	130
67.94	159

30F paddles, run # 3

N = 400 RPM, $\dot{M}$ = 46 Kg/hr, T_w = 81, 93 °F

x (cm)	T (°F)
44.45	81
50.80	98
57.47	127
61.91	142
67.94	175

30F paddles, run # 4

N = 400 RPM, M = 46 Kg/hr, T_w = 84, 97 ^oF

x (cm)	T (^oF)
44.45	85
50.80	102
57.47	126
61.91	141
67.94	172

30F paddles, run # 5

N = 300 RPM, M = 46 Kg/hr, T_w = 93, 93 ^oF

x (cm)	T (^oF)
44.45	85
50.80	103
57.47	119
61.91	130
67.94	158

30F paddles, run # 6

N = 200 RPM, M = 46 Kg/hr, T_w = 80, 84 ^oF

x (cm)	T (^oF)
44.45	87
50.80	102
57.47	111
61.91	117
67.94	141

30F paddles, run # 7

N = 200 RPM, M = 60 Kg/hr, T_w = 80, 84 ^{o}F

x (cm)	T (^{o}F)
44.45	90
50.80	102
57.47	108
61.91	114
67.94	135

30F paddles, run # 8

N = 400 RPM, M = 60 Kg/hr, T_w = 85, 94 ^{o}F

x (cm)	T (^{o}F)
44.45	87
50.80	106
57.47	125
61.91	136
67.94	164

30F paddles, run # 9

N = 300 RPM, M = 33 Kg/hr, T_w = 84, 92 ^{o}F

x (cm)	T (^{o}F)
44.45	90
50.80	101
57.47	113
61.91	125
67.94	156

Feed screws, run # 1

N = 200 RPM, M = 33 Kg/hr, T_w = 79 ^oF

x (cm)	T (^oF)
44.45	65
50.80	69
57.47	92
61.91	104
67.94	126

Feed screws, run # 2

N = 300 RPM, M = 33 Kg/hr, T_w = 85 ^oF

x (cm)	T (^oF)
44.45	66
50.80	70
57.47	99
61.91	121
67.94	144

Feed screws, run # 3

N = 400 RPM, M = 33 Kg/hr, T_w = 91 ^oF

x (cm)	T (^oF)
44.45	66
50.80	71
57.47	111
61.91	135
67.94	160

Feed screws, run # 4

N = 400 RPM, M = 46 Kg/hr, T_w = 92 °F

x (cm)	T (°F)
44.45	66
50.80	71
57.47	109
61.91	131
67.94	151

Feed screws, run # 5

N = 300 RPM, M = 46 Kg/hr, T_w = 89 °F

x (cm)	T (°F)
44.45	66
50.80	71
57.47	104
61.91	118
67.94	139

Feed screws, run # 6

N = 200 RPM, M = 46 Kg/hr, T_w = 84 °F

x (cm)	T (°F)
44.45	66
50.80	71
57.47	94
61.91	102
67.94	120

Feed screws, run # 7

N = 200 RPM, M = 60 Kg/hr, T_w = 80 °F

x (cm)	T (°F)
44.45	66
50.80	73
57.47	84
61.91	89
67.94	103

Feed screws, run # 8

N = 300 RPM, M = 60 Kg/hr, T_w = 80 °F

x (cm)	T (°F)
44.45	66
50.80	70
57.47	93
61.91	100
67.94	112

Feed screws, run # 9

N = 200 RPM, M = 46 Kg/hr, T_w = 83 °F

x (cm)	T (°F)
44.45	66
50.80	70
57.47	99
61.91	110
67.94	123

Single lead screws, run # 1

N = 200 RPM, $\dot{M}$ = 46 Kg/hr, T_w = 84 ^oF

x (cm)	T (^oF)
44.45	75
50.80	79
57.47	94
61.91	104
67.94	145

Single lead screws, run # 2

N = 300 RPM, $\dot{M}$ = 46 Kg/hr, T_w = 87 ^oF

x (cm)	T (^oF)
44.45	76
50.80	80
57.47	92
61.91	112
67.94	159

Single lead screws, run # 3

N = 400 RPM, $\dot{M}$ = 46 Kg/hr, T_w = 90 ^oF

x (cm)	T (^oF)
44.45	77
50.80	81
57.47	87
61.91	120
67.94	168

APPENDIX E: Computer Program For The Temperature Profile Simulation

```
C***********************************************************************
C
C  COMPUTER PROGRAM FOR THE SOLUTION OF THE TEMPERATURE PROFILE FOR
C                      THE 30 FORWARDING PADDLES
C
C************************************************************************
C
      DOUBLE PRECISION n,MO,K,K1,K2,K3,K4,KK,MD,Gz,Br,h,Cp,L,NN
      COMMON Gz,Br,h,TW
      OPEN(6,FILE='TEMP.OUT',STATUS='NEW')
C     WRITE(6,3)
C     WRITE(6,4)
3     FORMAT(1H '  FEED SCREW ' )
4     FORMAT(1H '  Run # 9.5 ')
C************************************************************************
C     RHEOLOGICAL & THERMAL PROPERTIES PARAMETERS
C************************************************************************
C     n  = FLOW BEHAVIOR INDEX
C     MO = REFERENCE CONSISTENCY COEFFICIENT, Pa s
C     DE = ACTIVATION ENERGY, CAL./g mole C
C     R  = GAS CONSTANT
C     Cp = SPECIFIC HEAT, BTU/LB-C
C     K  = THERMAL CONDUCTIVITY, W/M-C
      DATA n, MO,DE,R,CP,K /0.25,4647,4520,1.987,0.49,0.4983/
      DATA PI,TH,D,L,AI /3.14159,0.66323,0.05,0.23495,0.0015976/
C***********************************************************************
C     OPERATING CONDITIONS
C***********************************************************************
C     NN = R.P.M
C     MD = FLOW RATE (LB/HR)
C     TW = BARREL TEMPERATURE, C
C     TE = INLET TEMPPERATURE, C
C***********************************************************************
      NN = 300
      MD = 133.2
      TW = 31.11
      TE = 31.66
C***********************************************************************
C     ESTIMATION OF THE AVERAGE SHEAR RATE AND THE AVERAGE
C                  HEAT TRANSFER COEFFICIENT
C***********************************************************************
C
C     GAMA = AVERAGE SHEAR RATE
C      B1, B2 = AVERAGE SHEAR RATE CONSTANT
C      Gz = GREATZE NUMBER
C      Br = BRINKMAN NUMBER
C      h  = AVERAGE HEAT TRANSFER COEFFICIENT
C***********************************************************************
      DATA B1,B2,TO /42.7976,0.448,40/
      GAMA = B1*((NN/60)**B2)
      Gz = (Cp*MD)/(0.2879*0.77083)
      Br = (MO*L*L*((GAMA)**1.25)*EXP(-DE/(R*(TO+273))))/(K*(TO-TW))
      h = 0.0421*(Gz**1.406)*(Br**0.851)
C     WRITE(6,5) Gz,Br,h
```

```
5       FORMAT(1H '  Gz =  ',F10.5,4X,'  Br = ',f10.5,3x,' h = ',F10.5)
C       PRINT 10,Gz,Br,h
10      FORMAT(1H,3X,F12.5,4X,F12.5,4X,F12.5)
C
C**********************************************************************
C       BEGINNING OF THE SOLUTION FOR THE TEMPERATURE PROFILE
C**********************************************************************
        X0 = 0.0
        XF = 1.0
        X = X0
        IP = 4
        IIP = 4
        DH = (XF-X0)/100
        TT = (TE-TO)/(TW-TO)
C       WRITE(6,15)
15      FORMAT(1H '         X              TEMP. (C) ' )
20      I = I+1
        K1 = F(TT)
        K2 = F(TT+K1*DH/2)
        K3 = F(TT+K2*DH/2)
        K4 = F(TT+K3*DH/2)
        KK = (K1+2*(K2+K3)+K4)/6
        TT = TT+KK*DH
        X = X+DH
        T=TT*(TW-TO)+TO
C
C       PRINT OF THE TEMPERATURE PROFILE
C
        PRINT 30,X,T
        IIP = IIP+1
        IF((IIP/IP)*IP.NE.IIP) GO TO 25
        WRITE(6,30) X,T
25      CONTINUE
30      FORMAT (5X,F10.5,6X,F12.5)
        IF(X.LT.XF) GO TO 20
        END
C
C**********************************************************************
C       FUNCTION SUBROUTINE
C**********************************************************************
C
C       D = BARREL DIAMETER, m
C       TH = ANGLE DEFINED IN FIGURE 3.3
C       AI = NET FLOW AREA
C       L  = FILLED LENGTH, m
C**********************************************************************
        FUNCTION F(TM)
        DOUBLE PRECISION D,PI,TH,h,Gz,Br,AI,K,L,DE,R,TW,TO
        COMMON Gz,Br,h,TW
        DATA D,PI,TH,AI,K /0.05,3.14159,0.66323,0.0015976,0.4983/
        DATA L,DE,R,TO /0.23495,4520,1.987,40/
C       PRINT *, Gz,Br,h,TW
        F=((2*D*(PI-TH)*(TM-1)*h/K)-Br*(AI/(L*L))*EXP(DE/(R*(TM*(TW-TO)
     +  +TO+273))))/Gz
        RETURN
        END
```